The University Of Sheffield.

Department of Infection, Immunity and Cardiovascular Disease

Academic Unit of Radiology

THE STUDY OF SPERM ENERGY METABOLISM MEASURED USING ^{13}C MAGNETIC RESONANCE SPECTROSCOPY

By

Nurul Fadhlina binti Ismail

M.Sc.

This dissertation is submitted for the degree of

Doctor of Philosophy

January 2019

Declaration

This dissertation is my own work and contains nothing which is the outcome of work done in collaboration with others, except as specified in the text and acknowledgements.

Acknowledgement

As in all endeavours, thanks go to Allah without whose blessings nothing is possible.

I would like to thank my supervisors, Professor Martyn Paley and Professor Allan Pacey for giving me the opportunity to join the SpermNMR team and pursue a PhD at the University of Sheffield. Their suggestions and guidance are always very helpful and enlightening.

My great thanks also goes to Dr Steven Reynolds who has been tremendous supervisor for me. I am really appreciate him for lending a helpful hand, sharing his thoughts and knowledge especially on the MRS and DNP aspect, motivation and 'pushing' me beyond the limit.

Dr Sarah Calvert for her teaching on the sperm preparation and comment on the presentations arising from this thesis.

Dr Mari Herigstad for help in designing the oxygenation chamber, arranging the access on the hypoxic chamber and for comments on the thesis draft.

Professor Alison M Condliffe and Dr Benjamin Durham for granting access to use and an induction on the hypoxic chamber.

Staff of the Academic Unit of Reproductive and Development Medicine especially Dr Sarah Waite and Sarah Elliot for providing all the facilities I needed.

My acknowledgement to the Ministry of Education Malaysia and University of Sultan Zainal Abidin for funding my postgraduate study.

Last, but not least, I would like to express my special appreciation to my family especially my husband, Mohd Hafizi Abd Razab, for his endless support, understanding and patience throughout this journey.

Presentations arising from this thesis

Nurul Fadhlina bt Ismail, Steven Reynolds, Sarah J. Calvert, Allan A. Pacey & Martyn N.J. Paley. (2016) The effect of malonate on boar sperm metabolism using ^{13}C MRS. Proceedings for The British Chapter of ISMRM Annual Meeting (Poster and 3 minute oral).

Nurul Fadhlina bt Ismail, Steven Reynolds, Sarah J. Calvert, Allan A. Pacey & Martyn N.J. Paley. (2016) The effect of malonate, succinate, oxaloacetate and 2-deoxy-D-glucose on boar sperm metabolism using ^{13}C MRS. Proceedings for 25th Annual Meeting of International Society for Magnetic Resonance in Medicine (ISMRM) (Poster).

Nurul Fadhlina bt Ismail, Steven Reynolds, Sarah J. Calvert, Allan A. Pacey & Martyn N.J. Paley. (2016) The effect of oxaloacetate on boar sperm metabolism using ^{13}C MRS. Proceedings for the Academic Unit of Reproductive Medicine (AURDM) annual symposium (3 minute oral)

Nurul Fadhlina bt Ismail, Steven Reynolds, Sarah J. Calvert, Allan A. Pacey & Martyn N.J. Paley. (2017) The effect of hypoxia on sperm metabolism using ^{13}C MRS. Proceedings for The British Chapter of ISMRM Annual Meeting (Poster and 3 minute oral).

Nurul Fadhlina bt Ismail, Steven Reynolds, Sarah J. Calvert, Allan A. Pacey & Martyn N.J. Paley. (2017) The effect of malonate, succinate, and oxaloacetate on boar sperm metabolism using ^{13}C MRS. Proceedings for the 13th Annual Medical School Meeting (Poster).

Nurul Fadhlina bt Ismail, Steven Reynolds, Sarah J. Calvert, Allan A. Pacey & Martyn N.J. Paley. (2018) Sperm metabolism under a hypoxic atmosphere measured by ^{13}C MRS. Proceedings for Fertility Conference (Poster).

Nurul Fadhlina bt Ismail, Steven Reynolds, Sarah J. Calvert, Allan A. Pacey & Martyn N.J. Paley. (2018) Sperm energy metabolism in environmental hypoxia: Magnetic Resonance Spectroscopy study. Proceedings for the 14th Annual Medical School Meeting (Poster).

Nurul Fadhlina bt Ismail, Steven Reynolds, Sarah J. Calvert, Allan A. Pacey & Martyn N.J. Paley. (2018) ^{13}C Magnetic Resonance Spectroscopy: Study of sperm metabolism under a hypoxic atmosphere. Proceedings for 25th Annual Meeting of International Society for Magnetic Resonance in Medicine (ISMRM) (Poster).

Nurul Fadhlina bt Ismail, Steven Reynolds, Sarah J. Calvert, Allan A. Pacey & Martyn N.J. Paley. (2018) The study of sperm energy metabolism measured using ^{13}C MRS: The role of succinate. Medical School PhD student final year presentation (Oral).

Table of Contents

List of Figures

List of Tables

List of Abbreviations

AAA	ATPase associated
AI	Artificial insemination
ATP	Adenosine triphosphate
DGC	Double gradient centrifugation
dH_2O	Distilled water
DMSO	Dimethyl sulphoxide
DNP	Dynamic nuclear hyperpolarisation
EDTA	Ethylene-diamine-tetra- acetic acid
ETC	Electron transport chain
FID	Free induction decay
FT	Fourier transformed
ID	Inner diameter
IM	Immotile
LDH	Lactate dehydrogenase
LPM	Litre per minute
mDNA	Mitochondrial DNA
MPC	Mitochondrial pyruvate carrier
MR	Magnetic resonance
MRS	Magnetic resonance spectroscopy
NADH	Nicotinamide adenine dinucleotide
NMR	Nuclear magnetic resonance
NP	Non progressive
OD	Outer diameter
OXPHOS	Oxidative phosphorylation
PBS	Phosphate-buffered saline
PC	Pyruvate carboxylase
PDH	Pyruvate dehydrogenase
Pen/Strep	Penicillin/streptomycin
PEP	Phosphoenolpyruvate
PEPCK	Phosphoenolpyruvate carboxykinase

PM	Progressive motility
ppm	Parts per million
RF	Radio frequency
ROS	Reactive oxygen species
SGC	Single gradient centrifugation
SNR	Signal to noise ratio
WHO	World health organization

Summary

Studying energy metabolism in sperm may be helpful in understanding the relationship between poor sperm motility and infertility. Sperm motility is fuelled by Adenosine triphosphate (ATP). Main ATP related production pathways are anaerobic glycolysis and oxidative phosphorylation (OXPHOS). These pathways yield different metabolic products. By using a labelled substrate, ^{13}C, metabolic pathways for ATP production can be tracked by Magnetic Resonance Spectroscopy (MRS). In a previous ^{13}C MRS sperm study, only lactate and bicarbonate were detected. Lactate may represent anaerobic glycolysis but the origin of bicarbonate is unclear as it could be from OXPHOS associated with pyruvate dehydrogenase, pyruvate carboxylase, or the Krebs cycle. Thus, the main aim of this study was attempt to detect Krebs cycle intermediates using ^{13}C MRS. Several variables were investigated including Krebs cycle inhibitors, incubation temperature, U-^{13}C glucose and 2-^{13}C pyruvate labelled substrates, hyperpolarised 2-^{13}C pyruvate and manipulation of oxygen availability.

Inhibitor, succinate, significantly increased sperm vitality and decreased the MRS lactate integral from U-^{13}C glucose after 18 hours incubation. It suggested that inhibition did occur but the Krebs cycle intermediate concentration was below the detection level of ^{13}C MRS. By incubating sperm with 2-^{13}C pyruvate at 37^{o}C and 39^{o}C, lactate and bicarbonate were consistently detected and their concentrations were significantly higher than those derived from U-^{13}C glucose. Yet, no Krebs cycle intermediates were detected. However, disappearance of the bicarbonate signal from 2-^{13}C pyruvate metabolism by succinate suggests that bicarbonate was indeed produced in the Krebs cycle. Even though dissolution-DNP could overcome the sensitivity issue faced by MRS, presently it has limitations in detecting metabolites of interest in boar sperm due to the short half-life of the hyperpolarisation substrate. Consequently, the origin of the bicarbonate cannot yet be confirmed. The effect of oxygen on sperm metabolism showed that the energy producing pathway for boar sperm was dominated by anaerobic glycolysis rather than mitochondrial metabolism regardless of the oxygen concentration in the environment that they were incubated. Hence Krebs cycle intermediates were not observed even in an oxygen rich atmosphere.

Chapter 1: Introduction to spermatozoa and MRS

1.1 Spermatozoa and infertility

Semen analysis plays a crucial role in the diagnosis of male fertility. Infertility is "a disease of the reproductive system defined by the failure to achieve a clinical pregnancy after 12 months or more of regular unprotected sexual intercourse" (World Health Organization, 2010). Infertility can be found in one of six couples (Cates, Farley and Rowe, 1985; Drożdzik *et al.*, 2009).

While the cause of the infertility can be contributed to by various factors, poor semen quality, including low motility, is thought to contribute to 30-50% of cases of infertility in heterosexual couples (Peterson and Freund, 1974; Barratt, Kay and Oxenham, 2009; Pacey, 2009). Low sperm motility may be due to several causes, one of which is mitochondrial dysfunction that could reduce aerobic energy production which is the key source for sperm motility (Folgerø *et al.*, 1993). Some of the mitochondrial dysfunctions which relate to infertility are reduced activity of the mitochondrial enzyme and abnormal spermatogenesis (Folgerø *et al.*, 1993; Demain, Conway and Newman, 2017).

Studying energy metabolism in sperm plays an important role in understanding the relationship between motility and infertility. The assessment of male infertility has traditionally been based on the measurement of sperm morphology, motility, and concentration (Khatun, Rahman and Pang, 2018). Despite the availability of advanced diagnostic methods for the diagnosis and treatment of infertility, the exact cause of infertility is still unknown (Gupta *et al.*, 2013; Barratt, De Jonge and Sharpe, 2018). Therefore, there is a need for new signature biomarkers that offer a clearer understanding of every aspect of sperm behaviour for the diagnosis and treatment of infertility.

1.2 Male reproductive system

The male gametes (spermatozoa) are one of the most differentiated cell types (Freitas, Vijayaraghavan and Fardilha, 2016). The special features of spermatozoa include a mosaic plasma membrane, an acrosome containing several hydrolytic enzymes, a flattened pear shaped head containing a highly condensed nucleus, a helical assembly of mitochondria in the midpiece, and an elaborately constructed tail (Eddy *et al.*, 1985; Mortimer, 2018).

Spermatozoa are specifically designed to facilitate their function (Miki *et al.*, 2004), which is transferring male haploid DNA to female DNA through several processes. To achieve that goal, they must leave the male body where they are produced and navigate the female reproductive system (Suarez and Pacey, 2006).

1.3 Spermatozoa

Sperm are formed within the seminiferous tubules of the testes during spermatogenesis and constitute approximately 10% of the semen volume with the rest being seminal plasma (Boron and Boulpaep, 2009). During spermatogenesis, germ cells progress through three phases of development. The first is a spermatogoniogenesis in which spermatogonial cells divide mitotically, the second is the meiosis of primary and secondary spermatocyte development, and the third is spermiogenesis when the spermatids remodel into spermatozoa (Berruti and Paiardi, 2011). In general, the spermatozoa resulting from this process are composed of three distinct structures enclosed by a plasma membrane which are the head, midpiece and tail.

1.3.1 Sperm head

The head comprises of two main components which are the nucleus and the acrosome. The nucleus houses the paternal DNA to be delivered to the oocyte. It is highly condensed with proteins so that its volume is minimized for transport, and transcription is shut down (Alberts *et al* 2009). The acrosome is a unique membranous organelle wrapping the anterior part of the nucleus of the sperm head (Berruti and Paiardi, 2011). It contains several hydrolytic enzymes that are crucial for the spermatozoa to penetrate through the zona pellucida of the oocyte during fertilisation (Berruti and Paiardi, 2011).

1.3.2 Midpiece

From the connection point of the nucleus, the axoneme extends throughout the length of the midpiece to the tail. The exoneme is composed of 9 microtubule doublets and a central pair. The microtubule doublets connect to each other by nexin links and connect to the central pair by inward projections, the radial spokes (Turner, 2003). Projecting from the microtubule doublets are the inner and outer axonemal dynein arms (Freitas, Vijayaraghavan and Fardilha, 2016) (Figure 1.1). There are 9 outer dense fibers that lie outside each of the 9 outer axonemal microtubule doublets. It contains a sheath of mitochondria that encloses the outer dense fibers and the axoneme (Turner, 2003).

Mitochondria are sub-cellular organelles composed of four distinct sub-compartments. Starting from the outside, they have an outer mitochondrial membrane, an intermembrane space, an inner mitochondrial membrane and a matrix. The inner membrane and the matrix contain numerous proteins. 13 proteins are encoded by mitochondrial DNA (mtDNA) whilst most of the proteins are encoded by nuclear DNA in the head (Piomboni *et al.*, 2012).

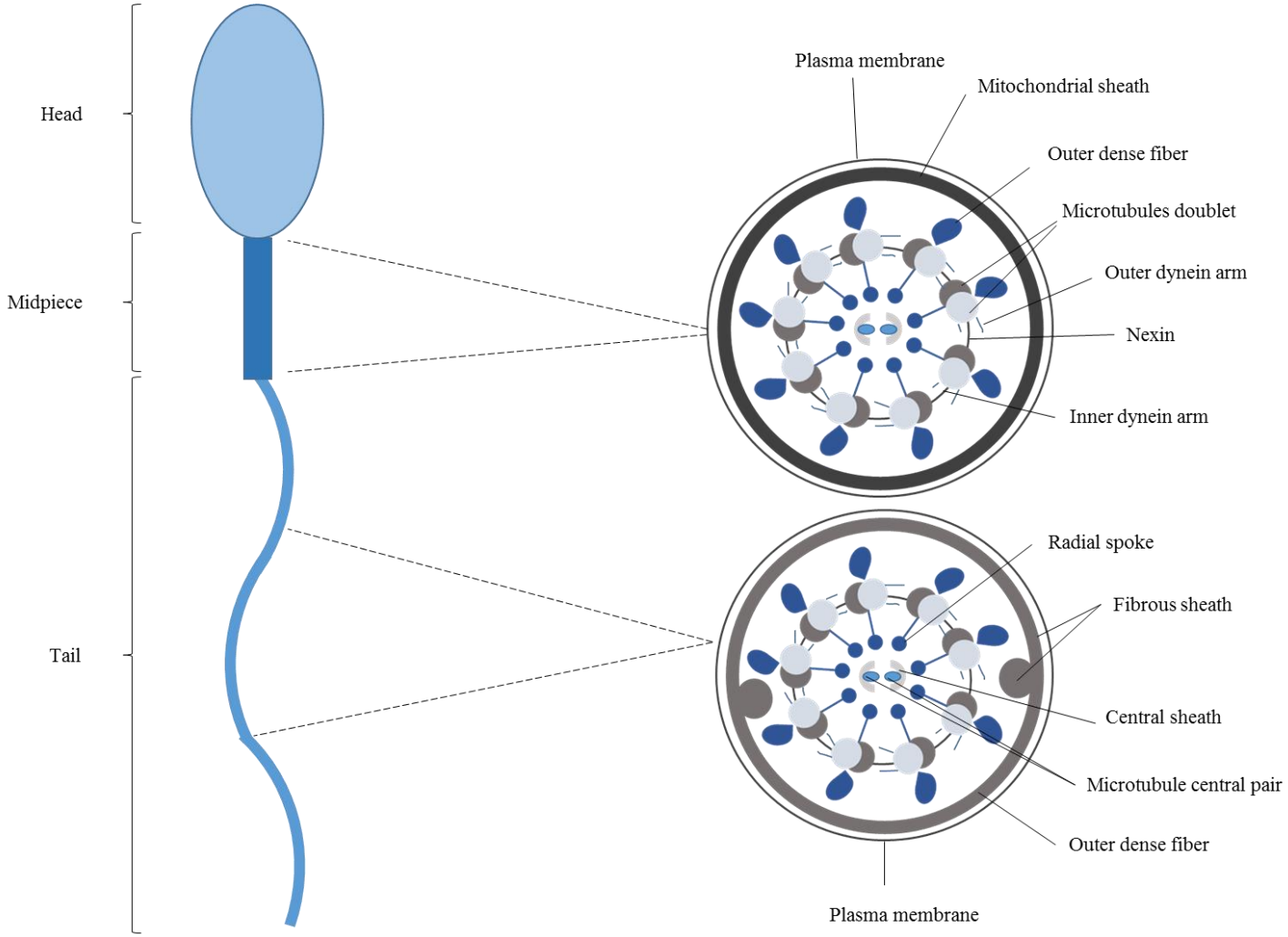

Figure 1.1: Schematic representation of spermatozoa. Spermatozoa are divided into head, midpiece and tail. A cross section demonstrates that the differences between the midpiece and tail.

All of the mtDNA is located in the inner mitochondrial membrane and forms part of the Oxidative phosphorylation (OXPHOS) machinery (Hüttemann *et al.*, 2007). Proteins that are synthesised outside of the mitochondria are transported into it by a transporter, which is referred to as mitochondrial import machinery (Wiedemann, Frazier and Pfanner, 2004).

Although the function of sperm mitochondria are similar to somatic mitochondria, they have a number of proteins or protein isoforms that are not found in the somatic mitochondria (Turner, 2003). One of which is an isoform of lactate dehydrogenase (LDH) (Storey, 2008).

Mitochondria are known as the 'power plant' because in here Adenosine triphosphate (ATP) is generated by OXPHOS. However, there are many other metabolic pathways which occur inside the mitochondria, such as the Krebs cycle, the oxidative decarboxphosoxylation of α-ketoacids, the β-oxidation of fatty acids, many reactions of amino acid metabolism and of pyrimidine synthesis (Piomboni *et al.*, 2012).

1.3.3 Tail

The tail is surrounded by outer dense fibers and a fibrous sheath around the axenome. It consists of principal piece and end piece. The principal piece makes up about two-thirds of the length of the tail and consists two longitudinal dense columns connected by circumferential ribs (Turner, 2003). The fibrous sheath provides a rigid support to the tail and may determine its movement, which is known as flagellar beat (Eddy *et al.*, 1985). Though it is devoid of mitochondria, it is enriched in glycolytic enzymes (Eddy *et al.*, 1985). The end piece is composed of only axoneme surrounded by the plasma membrane.

1.4 Energy needs of spermatozoa and fertilization

Mammalian fertilization consists of several complex processes. This is due to the location of semen deposition and the fact that fertilization occurs in the upper reproductive tract (Fallopian tube) (Suarez and Pacey, 2006). Hence, cellular processes such as motility, capacitation, hyperactivation and the acrosome reaction must occur in a synchronized fashion (du Plessis *et al.*, 2015). All these processes require energy. Bohnensack *et al* (1986) have studied the relation between motility and respiration in sperm. The sperm motility was calculated as the percentage of sperm moving per minute from the bottom of the cuvette into the light path. Respiration was measured using the Clark electrode. The relationship between them was calculated based on the changes in ATP/ADP that were produced from respiration (difference between before and after adding an inhibitor) and motility. They found that most

of the ATP was consumed by the motility process, which is 75% of the total produced energy and at least 10% of ATP was used by other cellular processes.

The energy is used to fuel sperm motility toward the Fallopian tube and to reach the ovum (Suarez and Pacey, 2006). Sperm motility is generated by altering the shape of the dynein molecule. Dynein consists of several heavy chains, intermediate chains, and light chains. The core component of the dynein is the heavy chain. The heavy chain has all motor domain elements that are needed to convert energy from the ATP hydrolysis into sperm motility. It consists of three major parts: the ATPase associated (AAA) ring (head), the stalk and the stem (Burgess *et al.*, 2003) (Figure 1.2).

The AAA ring consists of six AAA (AAA 1-6) domains, four of which (AAA1-4) contain nucleotide binding Walker A and B (P-loop) signature. Walker A is responsible for binding with the phosphate groups of the nucleotide and Walker B is responsible for polarizing H_2O for an inline attack on the γ-phosphate of ATP hydrolysis. AAA1 is mainly the ATPase site (that hydrolyses ATP) (Cho and Vale, 2012). The function of the remaining AAA domains are unknown but are thought to act in regulatory and structural roles (Burgess *et al.*, 2003; Cho and Vale, 2012).

The stalk protrudes out of the head and has a microtubule binding domain at its tip (Cho and Vale, 2012). Both the stalk and head are formed by two-thirds of the heavy chain. The stem binds the intermediate and light chains, and is formed by the aminoterminal region (Cho and Vale, 2012).

Microtubules have an intrinsic polarity, with a plus and minus end. The dynein motor domain moves toward the minus end of the microtubule. Absence of the nucleotide on the AAA1 ATPase site, results in the motor domain attaching tightly to the microtubule. However, during the ATP hydrolysis cycle, bonded nucleotide at the ATPase site induces dissociation of the motor domain from the microtubule (Roberts *et al.*, 2013).

After converting the ATP to ADP and inorganic phosphate (Pi), the dynein components rebind to the forward binding site on the microtubule, by a weak binding state. Strong binding to the microtubule accelerates the release of Pi from AAA1 (Bhabha *et al.*, 2016). This transition is suggested to represent the powerstroke. Energy, from the ATP hydrolysis, is transmitted to the attached ADP and releases the ADP from the AAA1 site.

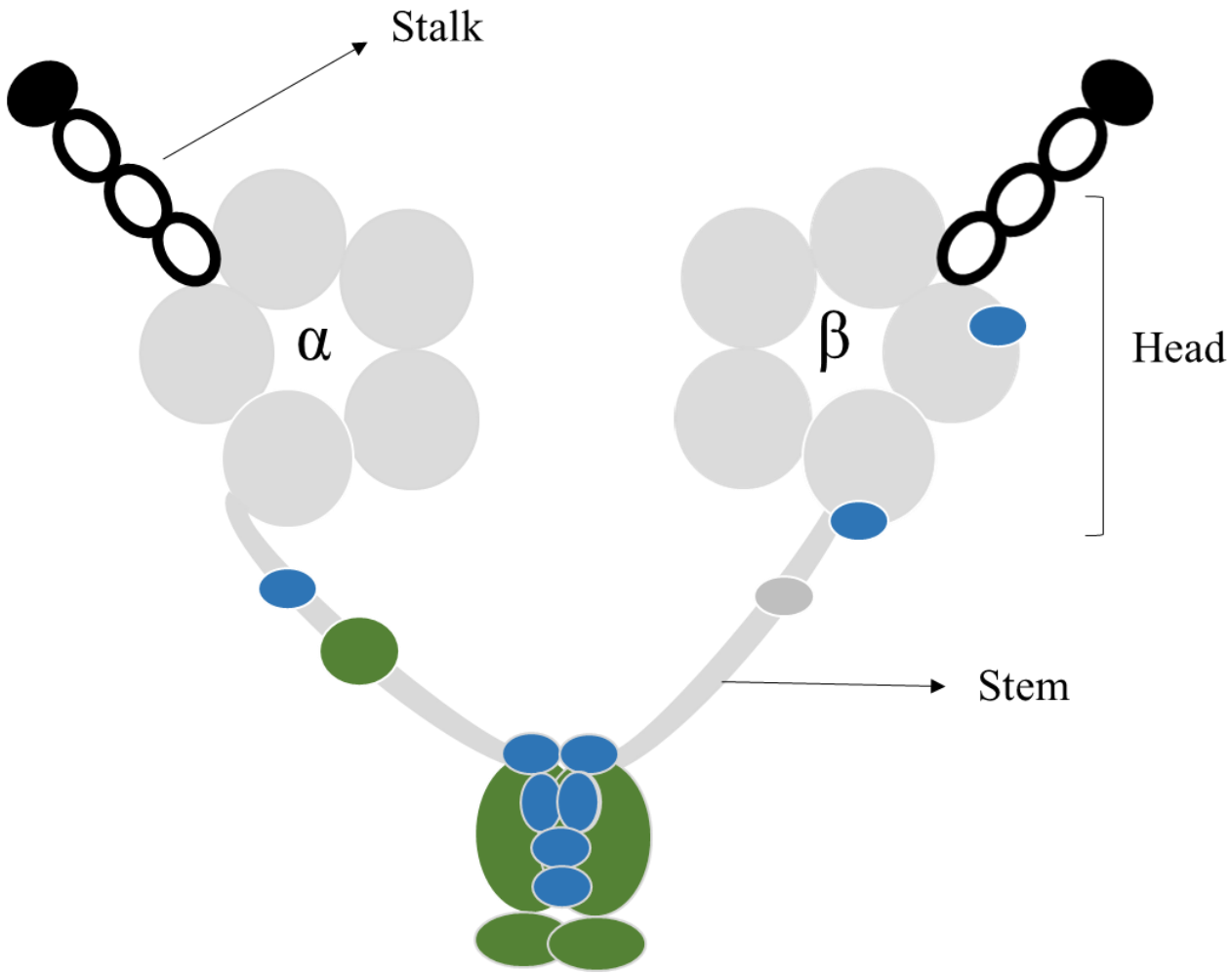

Figure 1.2: Structure of outer arm dynein. Schematic subunit structure of outer arm dynein from *Ciona* sperm flagella. The dynein is divided into three parts; head, stalk and stem. Outer arm dynein is composed of two heavy chains (α and β), five intermediate chains (green) and six light chains (blue). Redrawn from (Mohri *et al.*, 2012).

Electron microscopy has enabled visualization of the conformation changes in dynein due to the sperm motility mechanism (Mohri *et al.*, 2012). The comparison of dynein between, during and post-power stroke has showed several conformation differences. One of which is during the power stroke, the head is roughly circular whereas during post-power stroke, it has an obviously different shape (Burgess *et al.*, 2003). Moreover, the stem and stalk are closer together for the post-power stroke than during the power stroke (Burgess *et al.*, 2003). Besides that, the stalks during the power stroke are curved when flexed and straight when extended whereas post-power stroke the stalks are always straight (Burgess *et al.*, 2003).

These conformations consequently cause the microtubule doublets to shift to one upon another (Cho and Vale, 2012) converting them into bending deformations that transmit along the axoneme. This enables the sperm to move through seminal plasma (Roberts *et al.*, 2013).

Although sperm motility is dependent on ATP, how it is generated metabolically is still unclear. A major issue in deciding the metabolic pathway responsible for the ATP production for sperm motility is the availability of substrate. Therefore, glycolysis substrate, OXPHOS substrate or both should be available for sperm in adequate concentration. Pyruvate, lactate, glucose and oxygen are present along the female reproductive tract and hence they are commonly used as energy substrates by mammalian sperm (Ruiz-Pesini *et al.*, 2007).

Pyruvate, lactate and glucose concentrations in the human Fallopian tube have been measured by Dickens *et al*. (1995) using a vascular perfusion technique. The Fallopian tubes were obtained from women in the follicular phase of their ovarian cycle. They found that the glucose, lactate and pyruvate concentrations in the tubal fluid were 0.53, 8.58 and 0.17 mM respectively. In the seminal plasma, glucose and lactate concentration found in pig were 5 - 8 and 0.1 mM respectively (Prendergast and Veneziale, 1975). Oxygen concentration in the cervix was 15 - 35 mmHg (Hill *et al.*, 2005), 35 - 76 mmHg in Fallopian tube (Maas *et al*., 1976; Mastroianni and Jones, 2008; García-Martínez *et al.*, 2018) and 6.4 - 32 mmHg in uterus (Ottosen *et al.*, 2006).

Although the metabolic substrates used for ATP generation by sperm vary among species, it has been reported that boar sperm could metabolise lactate, pyruvate, citrate, glycerol, and acetate, obtained from media (Jones and Bubb, 2000). In contrast, dog sperm was able to survive when it was incubated in the media without any substrate. (Fernández-Novell *et al.*, 2011). To understand the peculiar functional and anatomical characteristics of sperm between boar and dog sperm, the metabolism of glucose was studied (Rodriguez-gil, 2006). Boar sperm is characterized by low average motility and a long tail (40 µm (Liebich, 1990)) and dog sperm is characterised by fast average motility and a shorter tail (6.8 µm

(Dahlbom *et al.*, 1997)). The results obtained from this study suggested that glycolysis plays an important role as an energy source in boar sperm, while the dog sperm shows an active anabolic metabolism and even an active pentose phosphate cycle pathway.

1.5 Boar and human sperm: Dominant pathway in producing ATP.

In spite of a long-standing debate on the metabolic pathway responsible for sperm motility, current understanding is that the major pathways involved are either anaerobic glycolysis, OXPHOS, or both (Rodrigues and Cerdán, 2005; Piomboni *et al.*, 2012; du Plessis *et al.*, 2015). For boar sperm, most of the studies have suggested that glycolysis (Marin *et al.*, 2003; Medrano *et al.*, 2006; Ferramosca and Zara, 2014) is the main metabolic pathway. Marin *et al* (2003) have reported that the glycolysis rate in boar sperm was higher than mitochondrial metabolism in producing ATP. They assessed the glycolysis rate by monitoring lactate production while the Krebs cycle was evaluated by monitoring carbon dioxide (CO_2) production. Both lactate and CO_2 production was calculated after 1 hour incubation with glucose. They found that, most of the glucose was converted into lactate while 5.7% of glucose was converted into CO_2. They added that all of the lactate was formed through glycolysis because no lactate isotope was detected in other lactate producing pathways.

Human sperm has also been reported to favour glycolysis over OXPHOS in producing ATP. The report was from Hereng *et al* (2011) in which they suggested that ATP production was produced by glycolysis as they did not detect OXPHOS metabolism from human sperm. They also commented that, exogenous pyruvate is able to stimulate glycolysis through the lactate fermentation reaction because pyruvate is able to regenerate NAD^+ following its conversion to lactate without involvement in mitochondria metabolism.

There are differences between boar and human sperm both morphologically and metabolically. However, since both boar and human sperm prefer glycolysis over OXPHOS and especially the high sperm concentration from boar, it was reasoned that boar sperm could be used as a model for comparison with human sperm.

1.6 Glycolysis

Glycolysis is the process by which six carbons of a single glucose molecule are converted into two molecules of a three-carbon pyruvate. It consists of 10 steps divided into 3 stages: (1) glucose is trapped and destabilized; (2) two interconvertible three-carbon molecules are generated by cleavage of six-carbon fructose; and (3) ATP is generated (Berg, Tymoczko and Stryer, 2002a). It is well reported that all the enzymes for this process are found in the sperm tail (Ford 2006; Piomboni *et a*l. 2012a). Some

of which are hexokinase, glyceraldehyde 3-phosphate dehydrogenase and aldolase (Piomboni *et al.*, 2012). These enzymes are tightly bound to the fibrous sheath (Storey and Keyhani, 1974). During this process, glucose is oxidized to pyruvate as the end product. The energy is released in the form of ATP and Nicotinamide adenine dinucleotide (NADH), with a rate of 2 ATP molecules per glucose (**Error! Reference source not found.**).

1.7 Major fate of pyruvate

1.7.1 Lactate fermentation or anaerobic glycolysis

This reaction normally takes place in anaerobic conditions. Pyruvate is used to regenerate Nicotinamide adenine dinucleotide (NAD^+) from NADH in the reduction into lactate by a bi-directional enzyme LDH. LDH is a tetrameric enzyme and there are four LDH genes: LDH-A, LDH-B, LDH-C or LDH-X and LDH-D (Lawrence R. Gray, Tompkins and Taylor, 2014). They are enzymatically similar but have a slightly different structure and are found in different concentrations in different tissues (Quistorff and Grunnet, 2011). LDH-A is predominantly located in skeletal muscle, LDH-B is mainly found in heart, LDH-X is found mostly in testes and sperm, and LDH-D is a yeast specific protein (Lawrence R. Gray, Tompkins and Taylor, 2014).

As the NADH formed in glycolysis is consumed in this reaction, there is no net oxidative reduction. However this reaction is vital for continuing glycolysis.

1.7.2 Pyruvate carboxylation

This reaction is used for the generation and replenishment of Krebs cycle intermediates, such as oxaloacetate. The oxaloacetate produced by PC could condense with the acetyl-coenzyme A (acetyl-CoA) formed by PDH to initiate the Krebs cycle. This is to ensure that the concentration of substrates in the Krebs cycle remains sufficient so that the cycle remains unperturbed (Mccommis and Finck, 2016). Moreover, oxaloacetate which is generated could be both decarboxylated and simultaneously phosphorylated by Phosphoenolpyruvate carboxykinase (PEPCK), either in the cytosol or in the mitochondria to produce Phosphoenolpyruvate (PEP) and CO_2 (Berg, Tymoczko and Stryer, 2002b).

1.7.3 Krebs cycle

In order to extract more energy from pyruvate, pyruvate must undergo the Krebs cycle. This reaction normally takes place when the concentration of the oxygen is available (aerobic condition). The conversion of pyruvate to acetyl-CoA removes the carboxyl group while producing ATP. For this to

happen, pyruvate is transported into the mitochondria through a specific protein transporter. Once in the mitochondrial matrix, it is oxidized to Acetyl-CoA and CO_2 by a Pyruvate dehydrogenase (PDH). This reaction is irreversible and tightly regulated.

Acetyl-CoA then enters the Krebs cycle. The Krebs cycle is composed of eight reactions. The first reaction is to form citrate. This happens by condensing the acetyl-CoA, which contain acetic acid, with oxaloacetate to form citrate. Acetyl CoA transports acetic acid from one enzyme to another enzyme. After that, it is combined with another acetic acid molecule and begins the first reaction again. The second reaction is isomerization of citrate in the presence of aconitate hydratase, which creates isocitrate and releases water (H_2O). Then oxidation of isocitrate to α-ketoglutarate and α-ketoglutarate to succinyl-CoA are performed by the NAD^+ and NAD^+ with CoASH molecules respectively. During these reactions, NADH, H^+ and CO_2 are released. The next reaction is conversion of succinyl-CoA into succinate. A GTP, an energy carrying molecule equivalent to ATP, is released during this stage. After that, succinate is oxidized by a molecule of Flavin adenine dinucleotide (FAD) to become fumarate. Next, water combines with the fumarate to become malate. Lastly, an NAD molecule oxidizes malate and produces oxaloacetate. The reduced compounds, 3 NADH and 1 FADH2 (in the single turn of the cycle), are used in the OXPHOS process taking place, also in the mitochondria.

1.8 Oxidative phosphorylation

Oxidative phosphorylation (OXPHOS) is an important functional process in the inner mitochondrial membrane. It is a combination of Electron transport chain (ETC) processes and ATP synthesis. The ETC consists of four proteins complexes, NADH-dehydrogenase (complex I), succinate dehydrogenase (complex II), ubiquinone, bc_1 complex (complex III), cytochrome *c* (Cyt *c*), and cytochrome *c* oxidase (CcO; complex IV) (Hüttemann *et al.*, 2007). Most of the electrons transferred by the ETC are from NADH. The electrons enter the ETC via complex I. As the electrons are transported across a membrane, they translate from a higher to lower energy state and release energy. This energy results in pumping of H+ out of the mitochondrial matrix to the inter membrane space. At the end of the chain, oxygen accepts the electrons, then splits in half and combines with H^+ to form H_2O (Berg, Tymoczko and Stryer, 2002b). ATP is synthesized when protons flow back to the mitochondrial matrix through an ATP synthase. 26 of the 30 ATP molecules are formed through OXPHOS when glucose is completely oxidized to CO_2 and H_2O (Berg, Tymoczko and Stryer, 2002b).

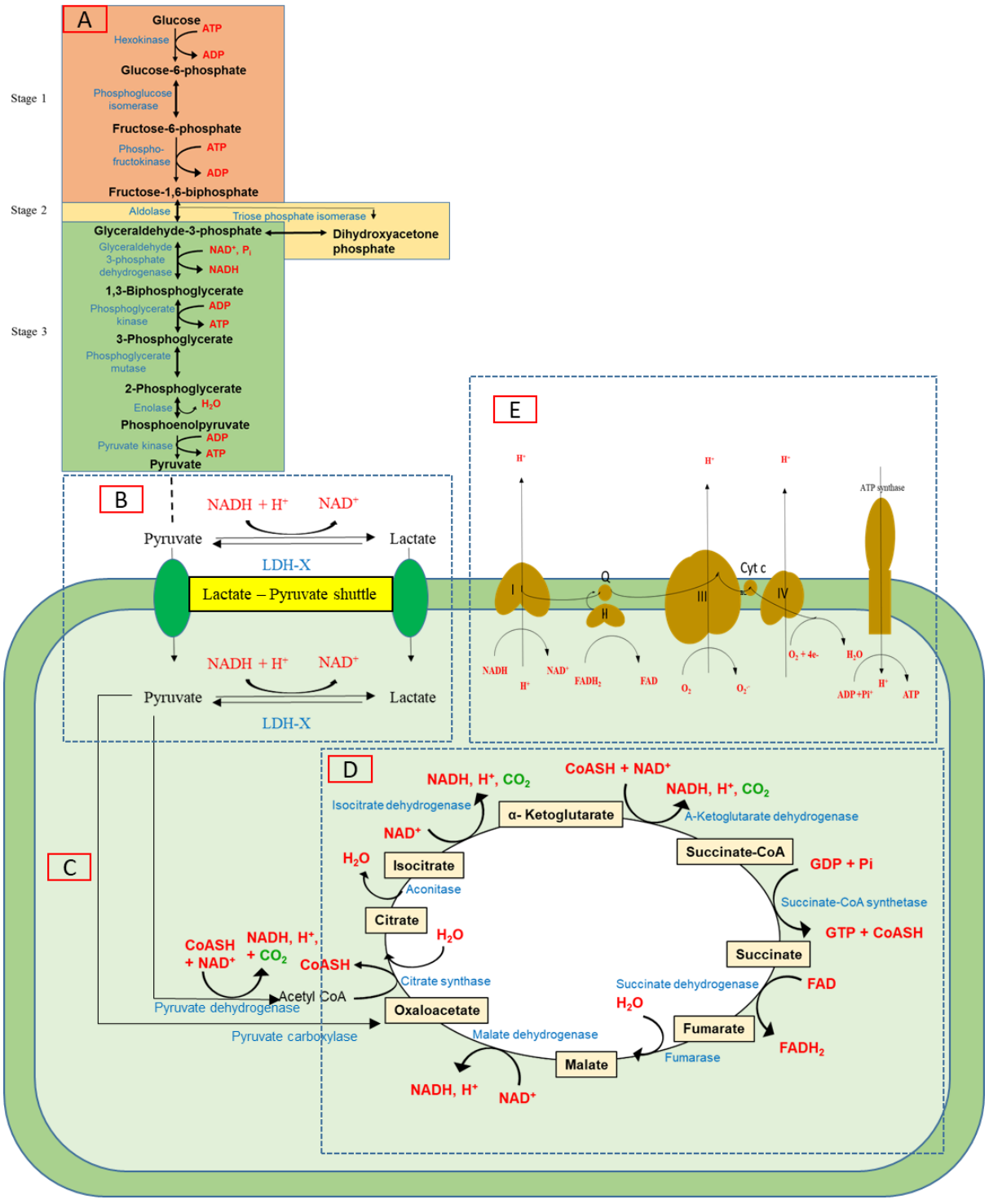

Figure 1.3: (A) A glucose molecule is converted into two molecules of pyruvate in ten steps of glycolysis. (B) Pyruvate could be converted into (i) lactate in which this reaction is mediated by LDH-X, isoenzyme X of lactate dehydrogenase (cytosolic and mitochondrial isoenzymes), (C) oxaloacetate by pyruvate carboxylase or (D) Acetyl CoA by pyruvate dehydrogenase and continue the conversion in the Krebs cycle. (D) Produced NADH and FADH from the Krebs cycle initiates the electron transport mechanism in OXPHOS. OXPHOS comprises five multimeric enzyme complexes (I–V). Complex V is the ATP synthase complex. Electrons from NADH go down the mitochondrial electron transport chain (ETC) and finally reduce O_2. Energy is released during each redox reaction creating a proton gradient resulting in a proton being dumped into ATP synthase which produces ATP.

1.9 Magnetic resonance spectroscopy

Magnetic resonance spectroscopy (MRS) has emerged as an important diagnostic methodology in addressing many diseases using different biological fluids and tissue extracts. Apart from identifying the constituents of sample cells, it can also provide qualitative and quantitative metabolic information, such as metabolite concentrations (Balci, 2005). Primarily, the information acquired can be used towards a better understanding of the underlying biological causes of infertility due to sperm.

MRS is able to obtain signal that is proportional to the concentration of a particular metabolite or chemical compound with the use of radiofrequency irradiation and external magnetic fields. The chemical compound(s) that can be detected depends on the nucleus being studied. The most common nucleus used in MRS is the proton, ^{1}H. Some of the other observable nuclei are ^{13}C, ^{15}N, ^{19}F, ^{31}P. Proton spectroscopy is widely used because it gives higher signal to noise ratio (SNR) compared to other nuclei due to it has higher natural abundance and precession frequency (Balci, 2005). However, MRS using ^{13}C is ideally suited to the study of metabolism due to the extensive range of metabolites that can be detected and the ability to attribute signals to the different carbon atoms within an individual metabolite.

^{13}C MRS enables detection of magnetic resonance from ^{13}C which is the only stable carbon isotope that can produce an MRS signal. The natural abundance for ^{13}C is appropriately 1.1% of the total carbon present and its gyromagnetic ratio is roughly ¼ of that of the proton. These two factors cause ^{13}C MRS to be less sensitive than proton MRS (Hore, 1989). The sensitivity problem can be partially overcome by using ^{13}C labelled substrates (Chance *et al.*, 1983). Utilization of ^{13}C MRS detection and selectively labelled ^{13}C substrates has allowed monitoring of the metabolism of various metabolic pathways in cells, animals, and humans (Rodrigues and Cerdán, 2005). These include glycolysis, Krebs cycle, OXPHOS and others (Beckmann, 1995).

1.9.1 Basic principle of MRS

Matter is composed of atoms. Combination of several atoms creates molecules. Atoms can be bound together with other atoms by sharing their electrons. An atom consists of three main elements: protons, positively charged particles, neutral neutrons and negatively charged electrons (Hendee and Ritenour, 2003). Neutrons and protons are located at the centre of an atom in the nucleus. The electrons are located in shells, which surround the nucleus. Atoms can be categorized based on their atomic number and atomic weight. The atomic number describes the number of protons in the atom. The atomic weight is related to the total number of protons and neutrons. Atoms with the same atomic number but a different atomic weight are called isotopes (Brown, Kincaid and Ugurbil, 1982).

Nuclei can be characterized based on their spin quantum number, I (Claridge, 2016). The value of I can be greater than or equal to zero. Only nuclei that have I greater than zero are MRS active (Balci, 2005). Such nuclei have odd atomic number, or odd atomic mass, or both. Nuclei whose atomic number and atomic mass are both even have I = 0 and are not MRS active.

MRS active nuclei possess the quantum property of "spin". Classically, spin can be described as rotation about an axis at a constant velocity. They possess a property known as angular momentum which can be represented as a vector with a definite direction and momentum (Brown, Kincaid and Ugurbil, 1982).

The spin of a nucleus combined with its positive charge produces a magnetic field known as the local magnetic field or magnetic moment, μ. It is parallel to the axis of rotation. The ratio of its magnetic moment to its angular momentum, P, is known as the gyromagnetic ratio, γ. This relationship can be described by Equation 1.1.

$$\mu = \gamma P \qquad \text{Equation 1.1}$$

In an external magnetic field, the magnetic moment of nuclei becomes oriented in the direction of the external field, and determined by I. For instance, for ^{13}C, I = ½, the number of orientations of ^{13}C magnetic moments in the external magnetic field is $(2 \times ½ + 1) = 2$. The orientation of μ depends on γ. If $\gamma > 0$, spin and μ point in the same direction, or parallel. If γ is negative, they will lie in opposite directions, or anti-parallel (Posse *et al.*, 2013). The orientations are distinguished by two different energy levels in which the nuclei in the parallel orientation have a lower energy than those in the anti-parallel orientation. The difference of energy, ΔE, depends on the external field strength, B_0, as given in equation shown in Figure 1.4, where h is Planck's constant.

ΔE also relates to polarisation, P. A higher polarisation level provides a better MRS signal. Polarisation can be increased by increasing the magnetic field strength, B_0. When an external magnetic field is applied, at a temperature, T, the spins reach thermal equilibrium and distribute based on spin orientation and the Boltzmann distribution (Equation 1.2) (Barskiy *et al.*, 2017).

$$P = \frac{h\gamma B_0}{2k_B T} \qquad \text{Equation 1.2}$$

Where k_B is the Boltzmann constant $\approx 1{:}38\text{x}10^{-23}\ m^2\ kg\ s^{-2}\ K^{-1}$.

In the lower temperature regime, sample nuclei spins will relax to a new equilibrium condition increasing the polarisation (Barskiy *et al.*, 2017). Higher MRS signal could also be achieved by

increasing the number of nuclei in the sample (Ardenkjaer-Larsen *et al.*, 2003), for instance, by raising the sperm concentration of the sperm sample

In addition to the nuclear spin re-orientation, if the nuclei are in the influence of an external magnetic field, they begin to rotate or precess at a specific rate. The rate of precession is proportional to the strength of the magnetic field and influenced by the gyromagnetic ratio of the particular nucleus (Brown and Semelka, 2003) as expressed by the Larmor equation (Equation 1.3).

$$\omega_0 = \frac{\gamma \beta_0}{2\pi} \qquad \text{Equation 1.3}$$

Where:

ω_0 = Larmor frequency (MHz),

B_0 = magnetic field strength (T), and

γ = gyromagnetic ratio, (MHz T^{-1})

Nuclei from different elements have different precession rates (James, 2012) and precess at widely different frequencies in the same external magnetic field. The precession rate is also not always uniform for all nuclei with the same nominal gyromagnetic ratio. This is because of the influence from internal magnetic fields which are produced by neighbouring nuclei, meaning nuclei from the same element can also precess at slightly different frequencies.

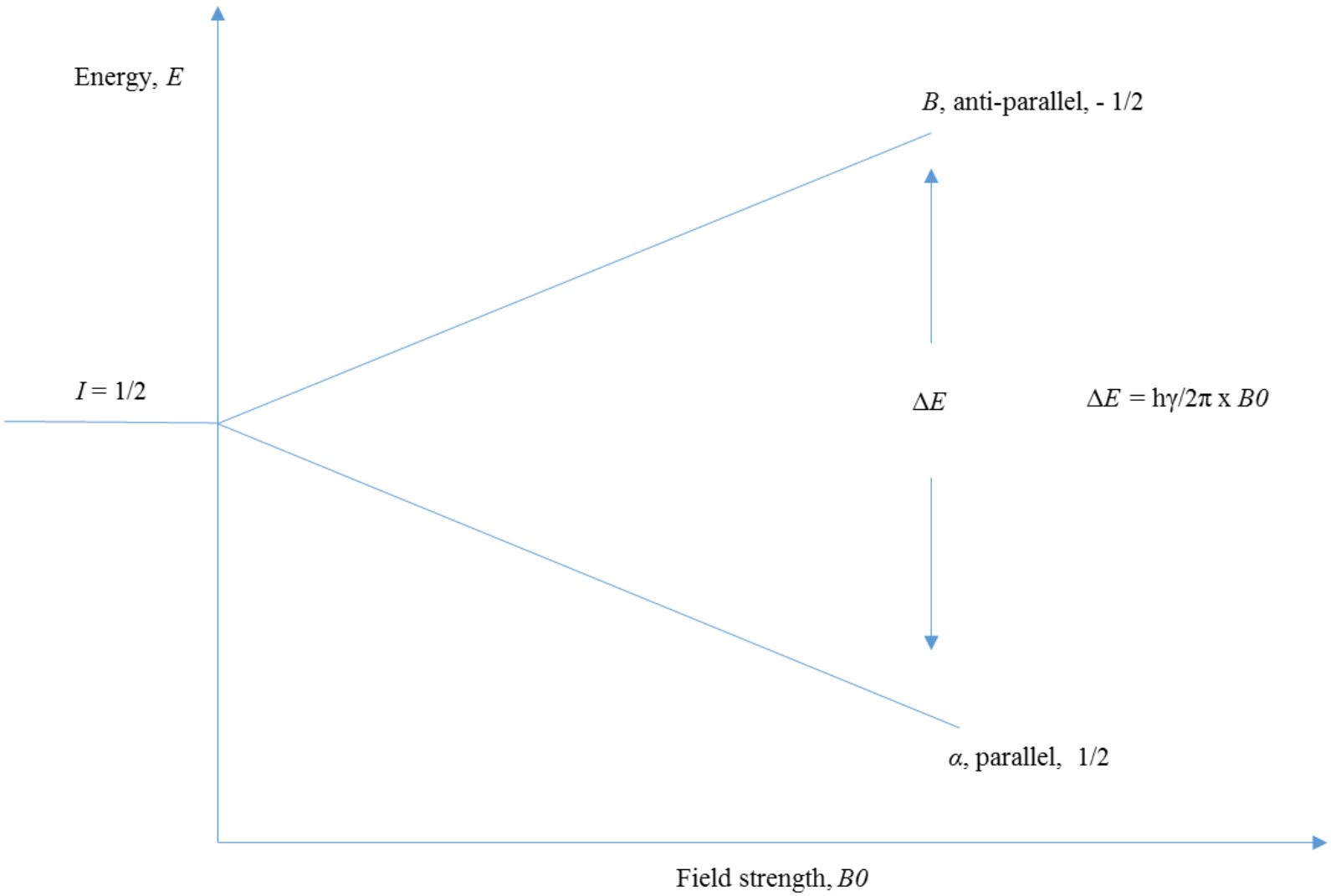

Figure 1.4: Energy level depicted for a I=1/2 spin nuclei.

1.9.2 Magnetization

In an MRS experiment, a very large number of nuclei align to produce a macroscopic magnetic moment. In the absence of the external magnetic field, the spins are distributed randomly and there will be no net magnetisation effect. However, in the presence of an external magnetic field, as explained before, the magnetic moments align parallel or anti-parallel to the external magnetic field. Normally, there are more nuclei in the parallel than in the anti-parallel direction. Therefore, there is a net magnetic moment when the effect of all the spins are added up, proportional to the difference in the number of spins in each level. Without a radio frequency pulse being applied and after sufficient time for alignment with the magnetic field, the net magnetization is said to be at equilibrium magnetization, $M_{0,}$ aligned with the direction of the external magnetic field, B_0. B_0 is assumed to point along the z direction. M_Z is referred to as the longitudinal magnetization. No components of transverse magnetization, M_Y and M_X, are observed at equilibrium (Figure 1.5).

1.9.3 Data acquisition

To obtain information about nuclei in atoms, radio waves (rf), with a frequency which matches the Larmor frequency, ω_0 are transmitted. The absorption of a photon of radio frequency will move nuclei between different energy states. To create this resonant absorption of energy, E, the photon must have exactly the energy difference, ΔE, between the nuclear spin levels. Since $\Delta E = h\nu$, it follows that ω_0 is proportional to the magnetic field, $B_{0.}$

The nucleus absorbs energy from the photon and is excited. After the absorption of the photon, the nucleus has extra energy and moves from the lower energy state into the higher energy state (parallel to antiparallel) resulting in a reduction in the $M_{Z.}$ In addition, the nuclear magnetic vectors align with each other in phase coherence, which results in the generation of transverse magnetisation, M_{XY} (James, 2012).

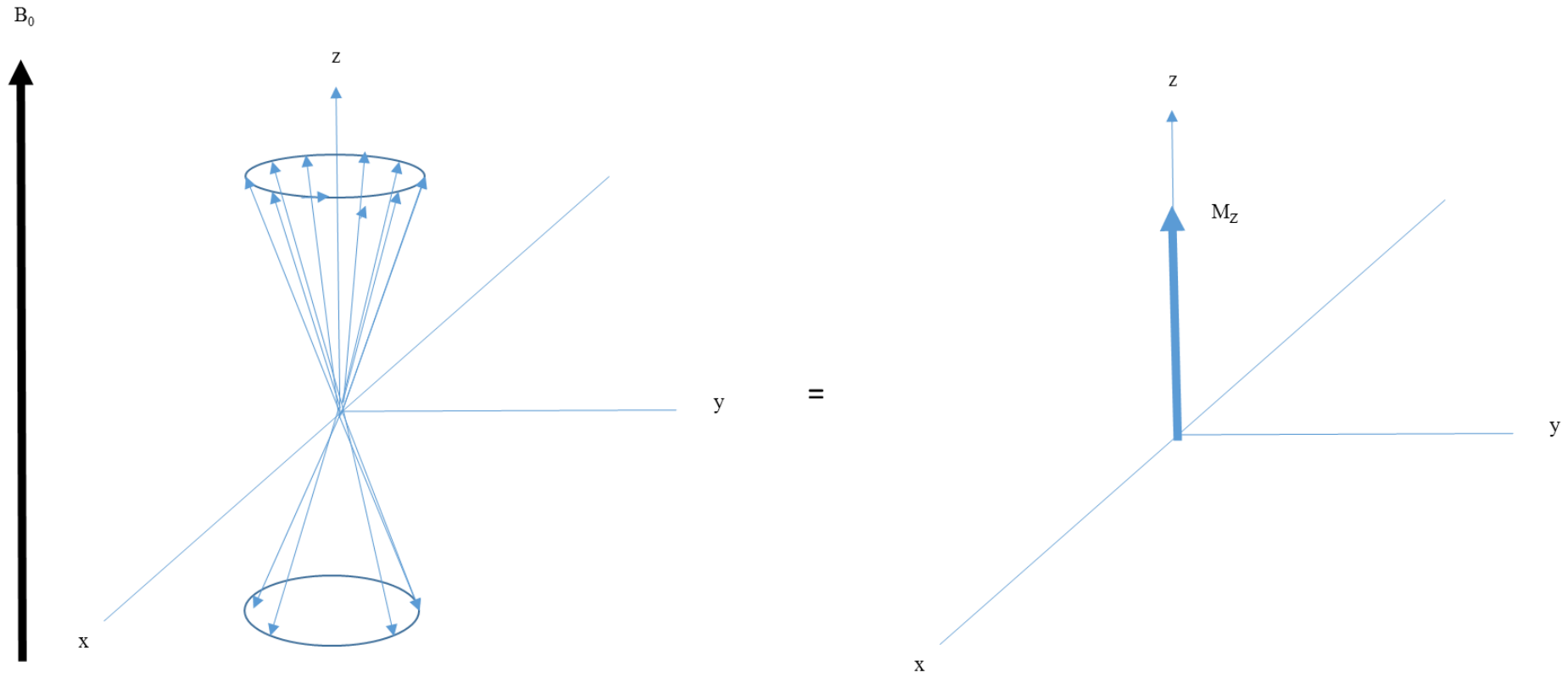

Figure 1.5: (Right) Parallel and anti-parallel alignment of the nuclear spins in the magnetic field, B_0. (Left) Longitudinal magnetization, M_Z in numerous nuclei produced by the population difference in the number of spins.

1.9.4 Relaxation times

Nuclei cannot hold this extra energy for a long time due to motional interactions with their magnetic neighbours and are said to be in an unstable state. To become stable, they have to release energy in the form of photons and return to the lower energy state again. The result is a re-generation of the longitudinal magnetisation, M_Z (Figure 1.6). The period of time required for M_Z to return to its equilibrium value is known as the T1 relaxation time. Besides that, a cumulative loss of phase coherence results in in transverse magnetisation, M_{XY} decay. This is known as T2 relaxation.

The photon energy emitted by the nuclei after the RF is turned off, is received as a signal by an inductive resonant coil surrounding the sample. This signal is measured as an induced voltage, known as a free induction decay (FID) (Brown and Semelka, 2003). The FID is in the time domain but can be transformed into the frequency domain by using a Fourier transform (FT) (Figure 1.7). The spectrum produced contains information on the different resonance frequencies of metabolites within a biological sample (Belkic and Belkic, 2010). The same metabolite may have more than one signal peak. This is due to the J-coupling and chemical shift effect.

1.9.5 Chemical shift

In an external magnetic field, $B_{0,}$ the applied magnetic field induces the electron cloud around the nucleus to circulate. The electron's magnetic moment orients anti-parallel to B_0 and decreases the net magnetic moment. Therefore, this results in a decrease in the external magnetic field around the nucleus which is called shielding (Balci, 2005) and results in the frequency of that nucleus being shifted “up field”. To compensate for this effect, the strength of the external magnetic field can be increased. The opposite of shielding is called deshielding in which the nucleus feels a stronger magnetic field, and its frequency is shifted “downfield” (Balci, 2005). Metabolites may experience different shielding effects if the electron density and chemical environment are different and hence resonate at slightly different frequencies (Figure 1.8). It is this which makes it possible to distinguish signals from different nuclear spins.

On the horizontal axis the chemical shift is calibrated to a single peak in the spectrum,, e.g. a deuterated solvent peak or other identified molecule, with a known reference value measured in parts per million (ppm). Molecules such as Tetramethylsilane (TMS) has been assigned a chemical shift of 0 ppm as a reference peak. The difference between the position of the signal of interest and that of the reference compound is termed the chemical shift. The purpose of measuring chemical shift in ppm is that it is invariant to the applied magnetic field, unlike the use of frequency in Hz which increases with the applied magnetic field.

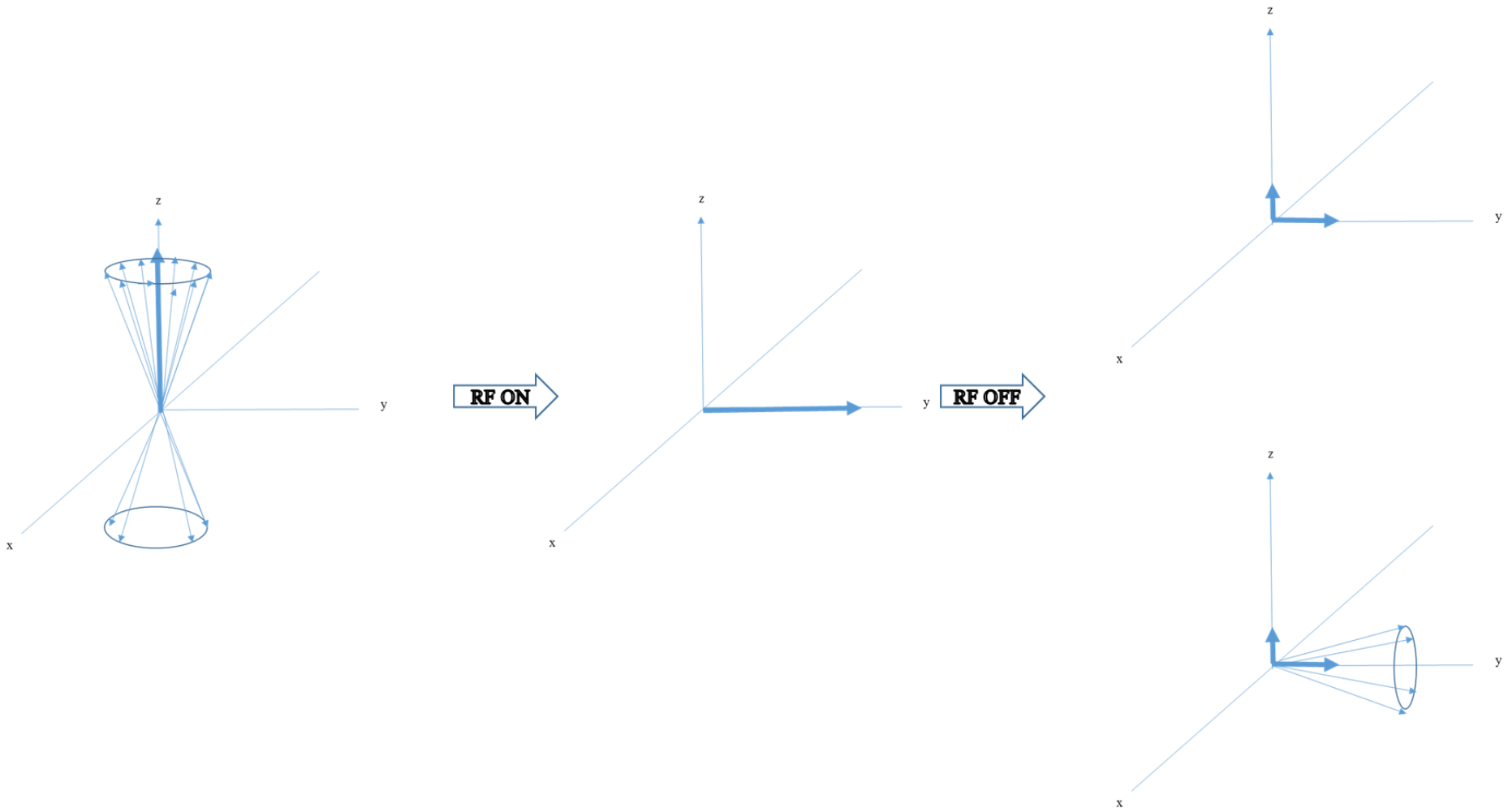

Figure 1.6: Tipping of the magnetization vector M_Z towards the y-axis under the influence of the radiofrequency (RF) field. After RF is switched off, M_{XY} decreases due to T1 (upper) or T2 (bottom) relaxation.

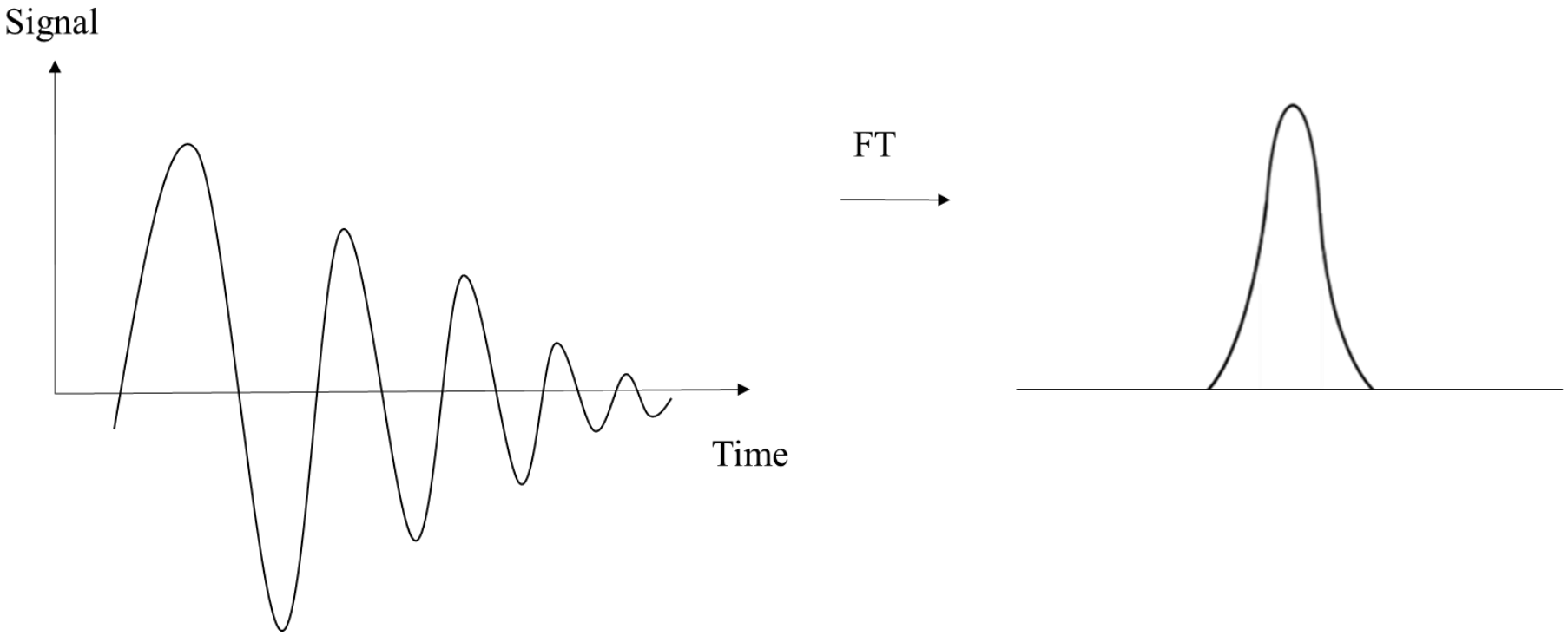

Figure 1.7: Free induction decay signal (FID) in the time domain is converted using Fourier transform into frequency domain

Reference peaks can also be utilised as an internal standard for concentration determination for the MRS signal (Mo and Raftery, 2008). Since the FID is an emission spectrum, the linear relationship between MRS signal integration and known concentration from the reference peak can potentially allow any detected signal concentration to be calculated. The reference solvent is suited for this purpose because of its known chemical shift which eases its observation in the spectrum and the concentration can be accurately pre-determined (Shimizu *et al*., 1994) .

1.9.6 J-coupling or Spin-spin splitting

The MRS signal produces a spectrum of resonances that correspond to different molecular arrangements of the isotope being excited. One metabolite may have several peaks. This is called spin-spin splitting (Figure 1.8). Between adjacent nuclei, there is an electron-coupled nuclear spin-spin interaction. The spin-coupling can pass through this interaction in both directions. The orientation of the neighbouring spin influences the local magnetic field of the observed spin (Brown and Semelka, 2003).

Spin-spin coupling can split the MRS spectrum into multiplets. Patterns of peak splitting can be predicted using the 2nI + 1 formula (Brown and Semelka, 2003). I is the spin quantum number, n is the number of other nuclei interacting with the nucleus. For example, for a given nucleus, I=1/2, there are three neighbouring methyl protons, then the line will be a quartet. The line separation is always constant within a given multiplet and is called the coupling constant, J. The magnitude of J, typically in units of Hz, is magnetic field independent (James, 2012). Moreover, the external magnetic field strength does affect the chemical shift but not the spin-spin splitting. The spin-spin splitting pattern can be predicted by Pascal's triangle.

Generally, this circumstance could explain why some metabolites have doublet peaks and some metabolites have triplet peaks in the spectra. For instance, lactate has three split peaks when using ^{13}C. There is a doublet at 183.5 ppm from the carboxylate proton, a quartet at 69.5 ppm from the CH carbon, and a doublet at 22 ppm from the CH_3 carbon (Lloyd *et al.*, 2004).

1.10 ^{13}C MRS, metabolic pathways' biomarker and fertility

Currently, only one study has been complete in human sperm using ^{13}C MRS. This work was carried out by Calvert *et al* (2018). They reported that, lactate was always detected when incubating the human sperm with U-^{13}C glucose, U-^{13}C fructose, and 1-^{13}C pyruvate while bicarbonate was occasionally detected after incubation with 3-^{13}C lactate, 2, 4-^{13}C D-3-hydroxybutyrate, 1-^{13}C butyrate, 5-^{13}C glutamate and 2-^{13}C glycine.. Pyruvate and acetate, acetoacetate, and glutamate were also detected in the spectra using 3-^{13}C lactate, 2, 4-^{13}C D-3-hydroxybutyrate, 1-^{13}C butyrate, and 5-^{13}C glutamate

respectively. They also reported that the conversion rate of 1-^{13}C pyruvate to lactate was three times faster than that of U-^{13}C glucose and U-^{13}C fructose.

Typically in this ^{13}C MRS study, observed lactate was suggested to represent lactate fermentation, bicarbonate represented OXPHOS, and acetate may have emerged from acetyl-CoA (Calvert *et al.*, 2018). However, from glycolysis to OXPHOS, there are several reactions that generate bicarbonate, some of which are reactions in the Krebs cycle, PDH and PC. Biochemical functions of these pathways are different. PDH yields acetyl-CoA for oxidation in the Krebs cycle, PC produces oxaloacetate to replenish intermediates of the Krebs cycle and the Krebs cycle produces NADH for further re-oxidation in OXPHOS. The relative relationship of these pathways and fertility have been studied previously (Matzuk, Brown and Kumar, 2001; Panneerdoss *et al.*, 2012; Siva *et al.*, 2014).

In mammalian sperm energy metabolism, the role of PDH in the fertilization process is thought to be regulation of intracellular lactate, pH and calcium during the process of capacitation and the acrosome reaction (Panneerdoss *et al.*, 2012). Moreover, Siva et al. (2014) have reported that by inhibiting PDH, the successful fertilization rate in the hamster decreased by about 90%. PC is usually associated with a decline in the fertility rate due to diabetes mellitus (Gray *et al*. 2014; Temidayo & Stefan 2018). For the Krebs cycle, reduction of aconitase, which is a Krebs cycle enzyme, has shown an effect on human sperm motility and in contrast, incubation of human sperm with isocitrate has improved sperm motility (Tang *et al.*, 2014).

1.11 Problem statement

Sperm functional tests are typically destructive to sperm. Thus, there is a need for a sperm test that is not detrimental to sperm which could also provide diverse information on sperm function. MRS has been used in many metabolomic studies, including sperm (Aaronson *et al*. 2010; Bonechi *et al*. 2015; Paiva *et al*. 2015; Bone *et al*. 2000; Calvert *et al*. 2018). Some of these studies used ^{13}C MRS to estimate glycolysis turnover in the presence of a glycolysis inhibitor (Bone *et al.*, 2000) and measured the glycolysis and OXPHOS rate (Calvert *et al.*, 2018). Moreover, Calvert *et al* (2018) have reported that human sperm which were incubated with ^{13}C labelled substrate, generated a detectable lactate and bicarbonate peak but no intermediates of the Krebs cycle.

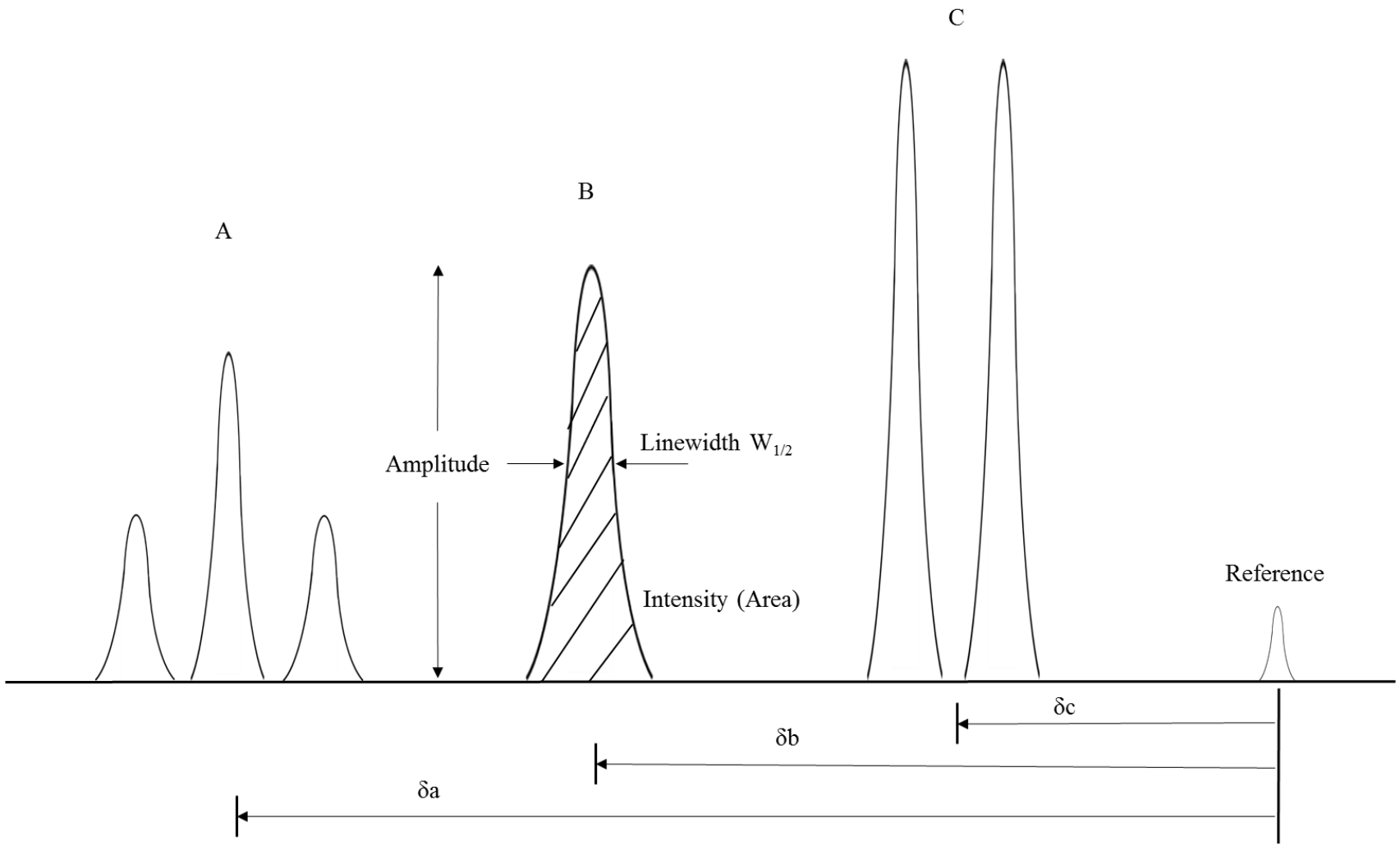

Figure 1.8: Schematic figure of the spectrum metabolite X which has three carbons; A, B, and C, nuclei in different molecular environments. This results in metabolite X having three peaks at chemical shift of δa, δb and δc. Peak A splits into a triplet peak and C splits into a doublet peak due to spin-spin coupling. Amplitude, linewidth $W_{1/2}$ and intensity are the general parameters for MR spectra. Redrawn from (James, 2012).

Krebs cycle intermediates, measured using ^{13}C MRS has been discovered in several cell types such as in the myocardium and brain (Lewandowski *et al.*, 1996; Wijnen *et al.*, 2010) but none of these have so far been discovered in sperm. However, their presence in sperm metabolism have been found using other methodologies such as mass spectroscopy (Marin *et al.*, 2003), Western blot analyses (Medrano *et al.*, 2006) and fluorimetry (Peterson and Freund, 1974). Since MRS is not detrimental to sperm (Reynolds *et al.*, 2017), it would be useful if it could detect Krebs cycle intermediates.

It is hypothesized that ^{13}C MRS will be able to detect Krebs cycle intermediates if their concentrations are above the detection level. Thus, to enable detection of Krebs cycle intermediates by ^{13}C MRS, a range of variables including various inhibitors, incubation temperature, labelled substrates and oxygen availability were investigated. A powerful tool, Dynamic nuclear hyperpolarization (DNP), was used to overcome the sensitivity issue of ^{13}C MRS.

1.12 Aim and Questions

Though an exact cause of infertility remains unknown (Gupta *et al.*, 2013; Barratt, De Jonge and Sharpe, 2018), poor sperm motility was reported as one of the causes of infertility (Pacey, 2009). For a successful fertilization, sperm undergo several cellular processes in the female reproduction tract such as capacitation and hyperactivation. This raises the biological question as to how sperm manage energy metabolism production in order to sustain motility during these processes.

Since sperm can metabolise several substrates including glucose and pyruvate, concentration of the produced metabolite, such as lactate, bicarbonate and possibly Krebs cycle intermediates, depends on the oxidation of these substrates by sperm. Therefore, the metabolism pattern between sperm from the healthy and infertile subjects may be different. As the Krebs cycle is the key source for ATP production, bicarbonate is thought to be generated by the Krebs cycle. Detection of the Krebs cycle could prove its involvement in bicarbonate production. Ultimately, the relationship between the Krebs cycle, the ratio of bicarbonate from the Krebs cycle or other pathways and lactate production with sperm motility from the target group sample can be investigated. In addition, due to its specificity, it has a potential to contribute to medicine new methods to improve sperm motility.

Therefore, this thesis is aimed at answering the following questions:

General question

1. Can Krebs cycle intermediates be detected using ^{13}C MRS?

Specific questions

1. What is the ideal sperm washing techniques that can yield the optimum sperm quality for experimentation? (see Chapter 3)
2. What is the ideal sperm incubation time and the volume of the labelled substrate which will give an optimum MRS signal? (see Chapter 3)
3. Could addition of inhibitors increase the concentration of Krebs cycle intermediates in sperm metabolism to enable their detection by ^{13}C MRS? (see Chapter 4)
4. Would the effect of an inhibitor on sperm vitality influence the detected metabolite peaks measured by ^{13}C MRS? (see Chapter 4)
5. Could incubation of sperm at body temperature with strategically selected ^{13}C labelled substrates increase the Krebs cycle intermediate concentration? (see Chapter 5)
6. What is the metabolic rate of the selected ^{13}C labelled substrate? (see Chapter 5)
7. Could hyperpolarized ^{13}C dissolution-DNP be used to detect intermediates of the Krebs cycle in the sperm? (see Chapter 6)
8. Could manipulating oxygen concentration affect sperm metabolism process particularly on the Krebs cycle? (see Chapter 7)

Chapter 2: Materials and methods

This chapter describes the samples, sperm washing techniques and centrifugation, sample preparation for MR scanning and quality assessments, ^{13}C MR scanning, data analysis, and statistical analysis. The exact methodology used for each study is specified within individual chapters.

2.1 Sample: Boar spermatozoa

Sperm rich samples of semen were provided from an artificial insemination (AI) company (JSR Genetic, Thorpe Willoughby, UK). The ejaculate was freshly obtained from the same breed of boar and mixed with an extender; Beltsville Thawing Solution (BTS) or Duragen extender (Gadea, 2003), Figure 2.1 (a), prior to dispatch. Components in the extender such as glucose, sodium citrate and potassium, enable sperm quality to be preserved for up to three days (Kaeoket *et al.*, 2010). Immediately after arrival, semen samples were placed in an incubator oven (INB200, Memmert GmbH + Co. KG, Germany) at 17°C, which is the recommended storage temperature for boar sperm. The motility of the spermatozoa was pre-screened upon arrival in the laboratory by using a microscope (Olympus BH2 Microscope, London, UK) to make sure that the samples contained motile sperm and that they were used before the expiry date.

2.2 Sperm washing techniques

On the day of the experiment, the boar semen (see Section 2.1) was washed through a double gradient centrifugation (DGC) process. This decision was based on findings presented later in Section 3.1. Briefly, as the boar sperm supplied was a mixture of semen and extender (semen and extender later will be referred to as a supporting fluid), it needed to be processed first for MRS. This is because, non-sperm cells could be present in the supporting fluid which would consume and metabolise the labelled substrate just like sperm does. Therefore, they needed to be removed from the sperm sample so that, the metabolite signal detected by MRS was genuinely from the metabolism of the sperm. To isolate the sperm from supporting fluid, three techniques were employed: (1) simple washing, (2) single gradient centrifugation (SGC), and (3) DGC.

2.2.1 Simple washing

3 ml of the boar semen (with extender), as described in Section 2.1, was pipetted and was placed in a clean conical tube (Biologix, Dutscher Scientific Ltd, Brentwood, UK) (Figure 2.1 (b)). This method centrifuged the sperm (as stated in Section 2.3) without using any colloid reagent for the density gradient.

2.2.2 Single gradient centrifugation

For separation using SGC, 2 ml of 70% (v/v) Percoll (see section 2.2.3) was added to a conical tube and then 3 ml of the semen (see Section 2.1) was carefully placed on top of the Percoll (Figure 2.1 (c)).

2.2.3 Double gradient centrifugation

Boar semen was washed through a gradient of 70% and 30% (v/v) isotonic Percoll (GE Healthcare Life Sciences, Little Chalfont, UK) in PBS (Figure 2.1 (d)). To prepare 30% Percoll, 2.7 mL Percoll was mixed with 1 mL of 10 x PBS and 6.3 ml of distilled water (dH_2O); to prepare 70% Percoll, 6.3 mL Percoll was mixed with 1 mL of 10 x PBS and 2.7 ml of dH_2O.

For separation using DGC, 2 ml of 70% (v/v) Percoll was added to a conical tube and then overlaid with 2 ml of 30% (v/v) Percoll (Harrison, 1976). The semen (3 mL) was then placed on top of the Percoll. This step was done carefully by keeping the tip of the pipette against the wall of the tube just above the surface of the Percoll to avoid a splash and mixing between the layers. The formation of a meniscus between the interfaces represents a sharp change in density between the gradient layers.

2.3 Centrifugation and recovered sperm

For all washing techniques listed above, the semen in the conical tube was centrifuged at 200 g for 15 minutes in a Sigma 3–16 K (SciQuip Ltd, Wem, UK), followed by a second centrifugation for 15 minutes at 1000 g at room temperature. After centrifugation, without disturbing the pellet, the waste supernatant which contains Percoll and/or supporting fluid, was gently aspirated and the pellet formed in the high density gradient for DGC or at the bottom of the tube for SGC and simple washing, was placed into a new, clean snap cap polystyrene round-bottom tube (Falcon, Corning, UK) before it was re-suspended with 1 ml of PBS (Figure 2.2). It was necessary to gently re-suspend the pellet so that mechanical stress on the sperm was minimized. Sperm remained in the isotonic media to reduce osmotic stress.

2.4 Sample preparation for incubation and fresh sample scanning

To prevent any bacterial growth in the recovered sperm sample after the centrifugation process, 12 µl penicillin\streptomycin (Pen/Strep), an antibiotic (10000 units/ml penicillin and 10 mg/ml streptomycin diluted to 1/3 with PBS, so that in tube concentrations were 90 units/ml penicillin and 90 µg/ml streptomycin, Sigma Aldrich) was added to a 100 µl aliquot of sperm.

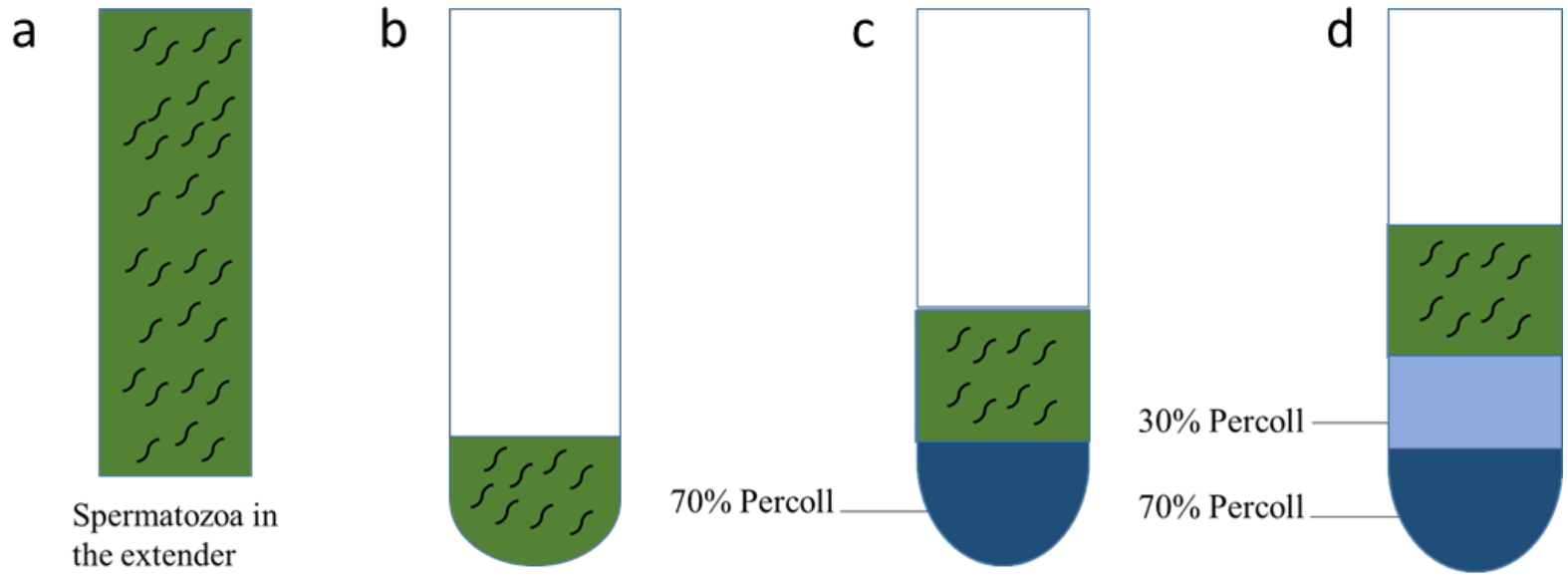

Figure 2.1: (a) sperm in the extender was placed in the conical tube for (b) simple washing, (c) SGC (above the single layer of 70% Percoll) and (d) DGC (above the layer of 30% and 70% Percoll) gradients before centrifugation process techniques.

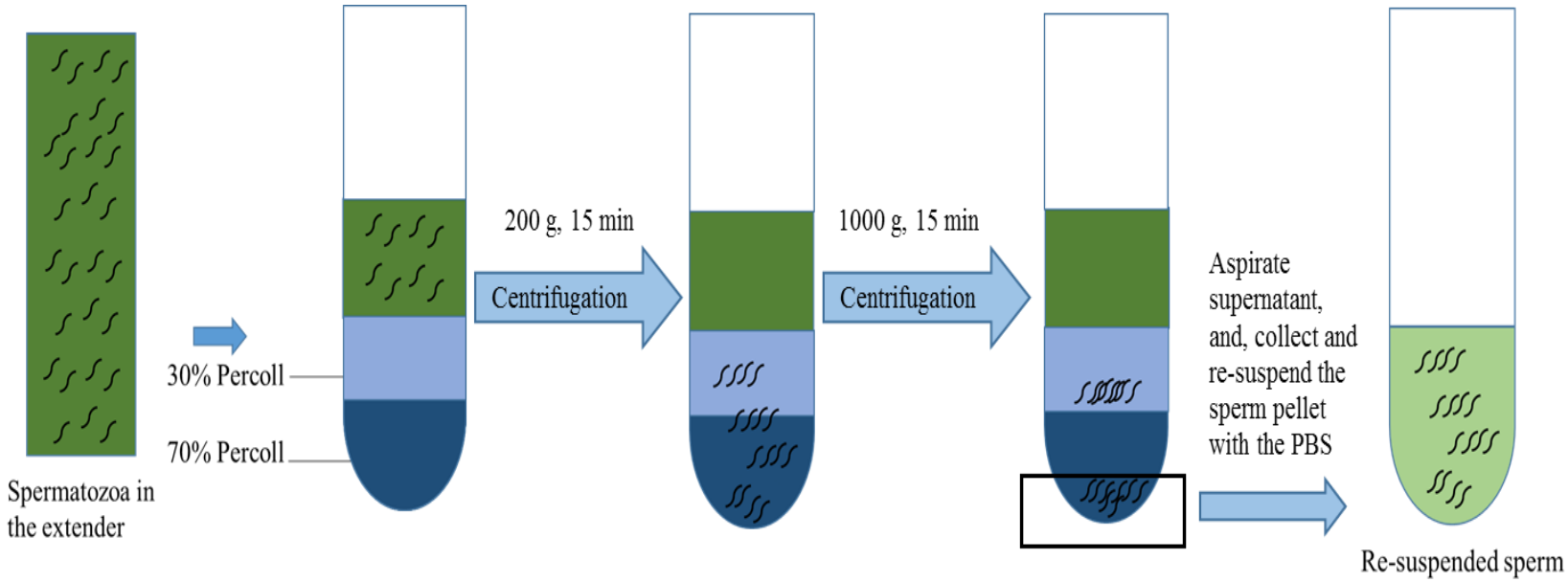

Figure 2.2: After the sperm sample was centrifuged using the DGC technique, the pelleted sperm at the bottom of the conical tube was collected and gently re-suspended with the PBS.

Phosphate buffered saline (PBS) was added to maintain a final volume of the sample (570 µl) for MRS experiments. Typical sample volumes for a 5 mm MRS probe are 450 to 600 µl (Aitken and Roman, 2008). The correct concentration is necessary to acquire an MRS spectrum from sperm with sufficient signal to noise ratio (SNR) and resolution for data acquisition in a reasonable amount of time. Since the MRS signal is proportional to the metabolite concentration, which is likely to be a function of the sperm concentration. Therefore, concentrated samples are obviously desirable. However, samples that are too concentrated can lead to problems with sample shimming and yield spectra with poor resolution.

Sperm samples had 60 µl of 100 mM U-^{13}C labelled glucose (Cambridge Isotopes Laboratories, Tewksbury, MA, USA) or 2-^{13}C pyruvate (Sigma Aldrich, Missouri, USA) added depending on which metabolic pathway was being studied. The sample was either incubated at 37°C for 18 h for experiments with metabolic inhibitors (see Chapter 4), or 4h for the oxygenation experiments (see Chapter 7). For the experiments in Chapter 5 and 6, the sample was either incubated or scanned continuously in the MRS, at 37°C and 39°C, for 18 h. All incubated samples were incubated in snap cap tubes with the cap closed half way to allow gas changing. The incubation time and volume of 100 mM U-^{13}C glucose were decided on based upon the preliminary experiments described in Section 3.2). After the incubation period, the sample was removed and frozen at -80°C (InnovaR, SoCal BioMed, Canada) prior to scanning in the MRS, without preservation.

2.5 Sperm quality assessments

Sperm quality plays an important role in MRS experiments. This is because, to achieve a reasonable high quality of the metabolite signal, a sufficient number of live sperm with an acceptable motility range are needed. The guideline for the reference range of vitality for human sperm is 55 - 63% (World Health Organization, 2010) and the minimum total motility of fresh boar sperm for AI is set at 70% (Lopez Rodriguez *et al.*, 2017). For this study, the cut-off limit for vitality and motility in the initial unprocessed sample was 60% since quality declines over the delivery time from the AI Company to the time that the boar sperm is stored in the laboratory fridge. The assessed sperm quality included: sperm concentration, motility and vitality.

2.5.1 Concentration

Sperm concentration was assessed for each sample by following WHO guidelines (World Health Organization, 2010). For sperm concentration using 1:20 dilution, re-suspended samples were diluted with formalin. Two 10 µl replicates were placed on the Neubauer haemocytometer (Hawksley, Lancing, UK) and left for ~ 5 minutes allowed for sperm to settle onto the surface of the chamber. Sperm were then counted within the central grid of 25 large squares area using a microscope (Olympus BH2

Microscope, London, UK) set to 20 × magnification with at least 200 spermatozoa in each replicate (see Figure 2.3). Only sperm heads touching the bottom and left lines of the small square were included in the count, while those touching the top or right lines were not counted. Sperm counts with acceptable difference between replicates, were used to calculate the sperm concentration using Equation 2.1.

$$Concentration = \frac{N}{n} \times \frac{1}{20} \times Dilution factor \qquad \text{Equation 2.1}$$

Where:

- *N*: number of counts
- *n*: number of rows in which they were found

2.5.2 Motility

Sperm motility was measured in accordance with WHO guidelines (World Health Organization, 2010). Re-suspended sperm was added to extender in a 1:1 dilution. Two aliquots of 10 µl of diluted semen were placed on the glass slide with a (22 x 22 mm) cover slip. They were then placed on a preheated stage at 37°C and graded using a phase-contrast microscope at 20 × magnification (Olympus BH2 Microscope, London, UK). Progressive motility (PM), non-progressive (NP) motility and immotile (IM) sperm were counted for at least 200 spermatozoa in each replicate. Average percentage motility was calculated. The sperm motility was graded according to the WHO definitions below:

- PR: spermatozoa moving actively, either linearly or in a large circle, regardless of speed.
- NP: all other patterns of motility with an absence of progression, e.g. swimming in small circles, the flagellar force hardly displacing the head, or when only a flagellar beat can be observed.
- IM: no movement.

2.5.3 Vitality

The viability of the samples were assessed and determined using Propidium Iodide (PI) and SYBR 14 (SYBR) dye (Live/Dead Sperm Viability Kit (L-7011): Molecular Probes, Eugene, Oregon, USA). One microliter of SYBR and 2 µl of PI were added to 50 µl of diluted sperm pellet. Samples were mixed and incubated for 10 minutes at room temperature. Two replicates (10 µl each) of semen sample were placed on a microscope slide and observed under 20 x magnification using an Olympus CKX41 fluorescence microscope (Olympus, London, UK). Theoretically, viable cells have an intact cell membrane which excludes the red dye, whereas for non-viable cells, the dye can infuse into the cell membrane and they are stained. Therefore, the green fluorescent spermatozoa were classified as viable and red fluorescent spermatozoa were classified as non-viable. A minimum of 200 spermatozoa were counted for each replicate. Average percentage vitality was calculated.

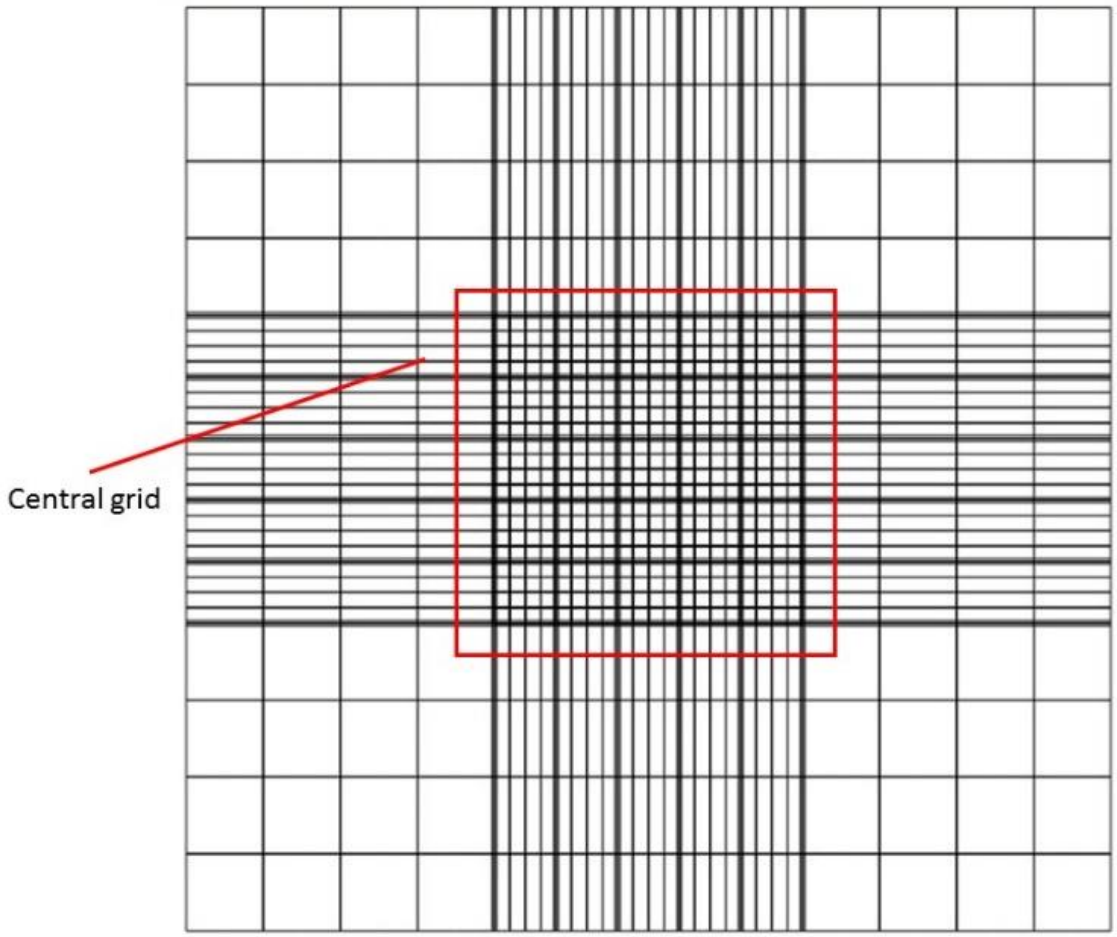

Figure 2.3: Illustrated image of the grid on the haemocytometer. Sperm were calculated if they were located within the central grid only (marked within the red line).

2.6 ^{13}C MR scanning

Both thawed or fresh sample scanning (with the final volume of 570 µl) , had 10 µl of 200 mM ^{13}C urea added as a concentration and chemical shift reference, and 10 µl of deuterium oxide (D_2O), used as a field/frequency lock solvent. The sample was then transferred to a 5 mm MRS tube (Norell, Marion, NC). ^{13}C urea was used because theoretically the labelled carbon of urea will not be consumed by sperm, thus any changes of urea integral would be as a result of inconsistency during data acquisition.

A 9.4 T, Avance III, Bruker (Bruker BioSpin GmbH, Karlsruhe, Germany) scanner, with 5 mm broadband observe probe was used for all experiments. The probe coil can be tuned "broadband" to measure nuclei such as ^{13}C and ^{1}H. The probe head resonance frequency and match were optimized by manually tuning the probe capacitors to the frequency of the corresponding nucleus and matching to the standard impedance of the system (50 Ohms). For the ^{13}C study, the ^{13}C probehead was tuned before the ^{1}H probehead.

In order to acquire a high resolution spectrum, the magnetic field has to be stable and homogeneous. To make sure that the magnetic field was stable during the spectral acquisition, a lock mechanism, which uses the resonance signal from the deuterium in D_2O to measure the magnetic field, was applied. As the D_2O signal frequency changes due to any change in the field, an electric current is applied to a coil in the magnet to increase or decrease the field strength to ensure the overall magnetic field remains constant.

Once the frequency is locked, the magnetic field homogeneity over the whole sample was improved by the shimming process. This involves applying different electrical currents to shim coils located around the probe to compensate for deficiencies in the B_0 field homogeneity. The value of the lock signal was maximized by increasing or decreasing the X, Y and Z as well as higher order shim components. A single pulse ^{1}H acquisition sequence was acquired to check for ’good’ shimming by calculating the full line width at half-height (FWHM). The shim was accepted when the FWHM for water resonance was between 10 to 15 Hz.

^{13}C spectra were then acquired using a 1 dimensional ^{13}C {^{1}H} inverse-gated pulse sequence. The acquisition parameters were spectral width = 239 ppm, number of acquisition = 4096, acquisition time = 0.5 s, delay time = 2 s, time domain point = 24036 and flip angle = 16° (for Chapter 4) or 90° (for Chapter 3, 5, 6, and 7). The spectral acquisition was performed at room temperature (21°C) for frozen-thawed samples and 37°C and 39°C for fresh sample scanning.

2.7 Data analysis

Data was acquired and processed using the Bruker Topspin 2.1.6 software. Spectra were Fourier transformed with automatic phasing and baseline correction to help remove broad baseline signals and signal offset. No exponential line broadening function was applied. Chemical shifts were referenced by setting the ^{13}C urea peak to 165.5 ppm.

2.7.1 Peak assignment

Identified metabolite signals were integrated if the SNR was more that 3:1. The metabolite peak was assigned by matching its chemical shift to the pre-defined chemical shift database (HMDB, 2010) and supported with the previous literature. Both database and literature provided the exact chemical shift where a metabolite should be detected in the spectra. The predefined integral ranges for substrate molecules are:

- 2-^{13}C pyruvate: 207.4 – 207.7 ppm
- 1-^{13}C lactate : 184.9 – 185.7 ppm
- 1-^{13}C Pyruvate : 173.5-172.5 ppm
- ^{13}C urea: 163.5-162.7 ppm
- ^{13}C Bicarbonate : 162.9 – 163.0 ppm
- ^{13}C glucose: 102 - 99.6 ppm,
- 2-^{13}C Lactate : 71.0 – 71.2 ppm

2.7.2 Quantification of metabolite

Relative concentrations of metabolites in the sperm sample were calculated by direct integration of the spectral region. The peak area, which is proportional to metabolite concentration, was integrated from the far left side of the peak until the far right side of the peak (Figure 2.4). Integral region was decided on the control sample spectrum and then copied to other related spectra.

2.7.3 Normalisation

Normalisation is an integral part of MRS data processing as it scales the spectra to the same overall concentration accounting for sample variations and inconsistency during the MRS data acquisition process (Dieterle *et al.*, 2006). Sample to sample variation results from differences in sperm concentration, motility and vitality between samples.

These parameters were not adjusted to any specific range so as to achieve as optimum as possible SNR. Therefore, to eliminate this variation and inconsistency, the following assumptions were made. First, spectral inconsistency can be predicted by urea integral changes. Second, concentration of the detected metabolite product depends on the concentration of sperm present in the sample where sperm samples with different concentration consume different amounts of ^{13}C substrate. Consequently, to correct spectral inconsistency, ^{13}C substrate integrals were divided by the ^{13}C urea integral. To correct sample to sample variation, metabolite product integrals were divided by the respective sperm concentration.

2.8 Statistical analysis

All statistical analysis was performed using GraphPad PRISM 7 (GraphPad Software, Inc). Values are quoted as mean ± SD unless otherwise stated. The significance value for all tests was $p < 0.05$.

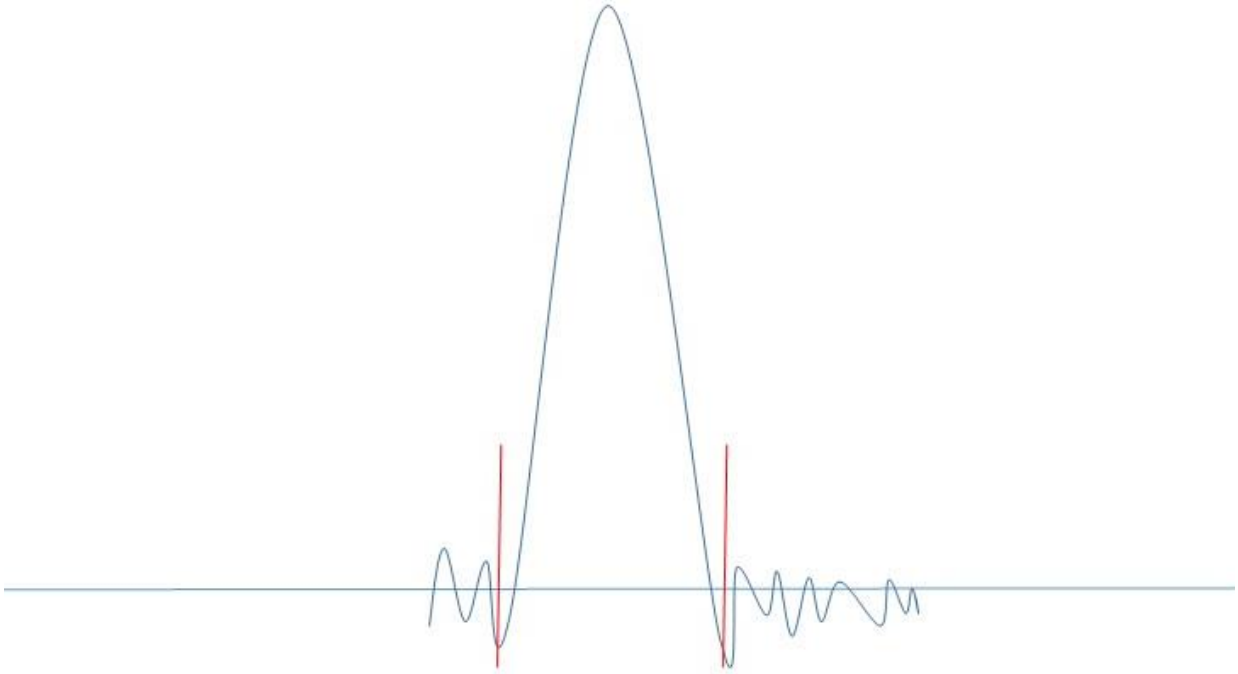

Figure 2.4: Integration area for detected peak in the spectra was assigned (marked with red lines).

Chapter 3: Preliminary experiments

This chapter describes two sets of experiments that were performed to optimise the protocols for subsequent chapters. These are to define the preparation of the sperm to remove the media in which they are supplied and, secondly, to determine the conditions required for incubation of sperm with ^{13}C-labelled substrates.

3.1 Sperm motility and vitality between simple, SGC and DGC

3.1.1 Introduction

For an MRS study, it is important to use a separation method that will not be deleterious to the sperm, as this will reduce the detected signal and efficiently isolate the sperm from the supporting fluid and other media. Separation methods for boar sperm include swim-up (Berger and Horton, 1988), gradient centrifugation (Lessley and Garner, 1983; Grant, Long and Parkinson, 1994; Matás *et al.*, 2010, 2011; Kruse, Dutta and Morrell, 2011) or glass wool filtration (Berger and Horton, 1988; Bussalleu *et al.*, 2009). Among these, density gradient centrifugation is the method most frequently used in separating or washing semen (Morrell and Wallgren, 2010). This is because it is not a time-consuming procedure, is able to separate a lot of motile spermatozoa, is not deleterious to the sperm, excludes dead sperm and other cells and can process a large volume of semen (Tahir Beydola, Sharma and Agarwa, 2014).

Density gradient centrifugation involves a rotation about a fixed axis to produce a centrifugal (g) force. This centrifugal force forces sperm down through a density gradient medium and physically separate the sperm according to size, shape, density, viscosity of the medium and rotor speed. There are two types of centrifugation separations which are separation by density and by the size. Separation by density or Isopycnic will separate the particle based on the differences in density, irrespective of size while separation by size or Rate Zonal Centrifugation (RZC) will separate the particle according to density and the particle size. In Isopycnic, the density gradient is continuous which means the density will linearly increase towards the bottom of the tube. In the RZC, the density gradient is discontinuous.

The discontinuous gradient is accomplished by adding layers of the gradient medium with different densities into the tube. The top layer of the tube will have the lowest gradient density and the bottom layer will have higher gradient density. A mature morphologically normal sperm has a higher density of 1.10 g/mL whereas an immature and morphologically abnormal sperm has a lower density between 1.06 and 1.09 g/mL (Malvezzi *et al.*, 2014). At the end of centrifugation, the highly motile sperm

migrate to the bottom of the tube. Poorly motile sperm situated at the interphase between low and high density gradient regions while dead spermatozoa, leukocytes, bacteria and debris float at the interphase between the low density gradient and seminal plasma (and other supporting fluid) (Figure 3.1). This is the preferred technique to select the greater number of motile spermatozoa (Natali, 2011). The most applied discontinuous density-gradient method is a double density-gradient (DGC), formed by a top layer of 40% (v/v) and a lower layer of 80% (v/v) silane-coated silica colloids. Centrifugal force and time should be kept at the lowest possible values (Gardner, 2004) to minimise the mechanical stress on sperm. However, this study use 30% and 70% for the gradient density, a centrifugal force of 200 g and 1000 g for 15 minutes each cycle, following the standard protocol for boar sperm for this laboratory.

The recently developed single density gradient (SGC) utilises only one layer of the gradient centrifugation. Usually the colloid medium for gradient density is a species-specific formulation. After the centrifugation, the seminal plasma or other media float on top of the medium whilst sperm move down through the medium, with the motile, vital spermatozoa pelleting in the bottom of the tube (Morrell and Wallgren, 2011) (Figure 3.1).

A density gradient can be prepared using various reagents. However, for this study, Percoll was used to prepare the gradient following the method that was outlined by Calvert *et al*. (2018). In boar sperm, Percoll density gradients have been used in numerous studies, including boar sperm preparation for a reactive oxygen species (ROS) study (Guthrie and Welch, 2006) and the study of the components of cytoplasmic droplets (Fischer *et al.*, 2005). One of the characteristics which is advantageous for the sperm study, are that it will not penetrate into sperm membranes hence making it non-toxic to sperm (Hernandez-Lopez *et al.*, 2005).

Washing of sperm without using any colloid medium is known as the simple washing technique. The principle is quite similar to SGC however, the amount of the pelleted sperm at the bottom of the tube might be less compared to sperm which is washed using the colloid medium.

Most previous studies have investigated the effect of motility after centrifugation (Lessley and Garner, 1983; Grant, Long and Parkinson, 1994; Matás *et al.*, 2010; Morrell and Wallgren, 2011; Reynolds *et al.*, 2017) but the effect of different washing techniques, between simple, SGC and DGC, on sperm vitality and different types of motility, has not previously been reported in the literature. Moreover, it would be a time and cost saving if the simple washing technique could produce similar sperm quality to SGC or DGC.

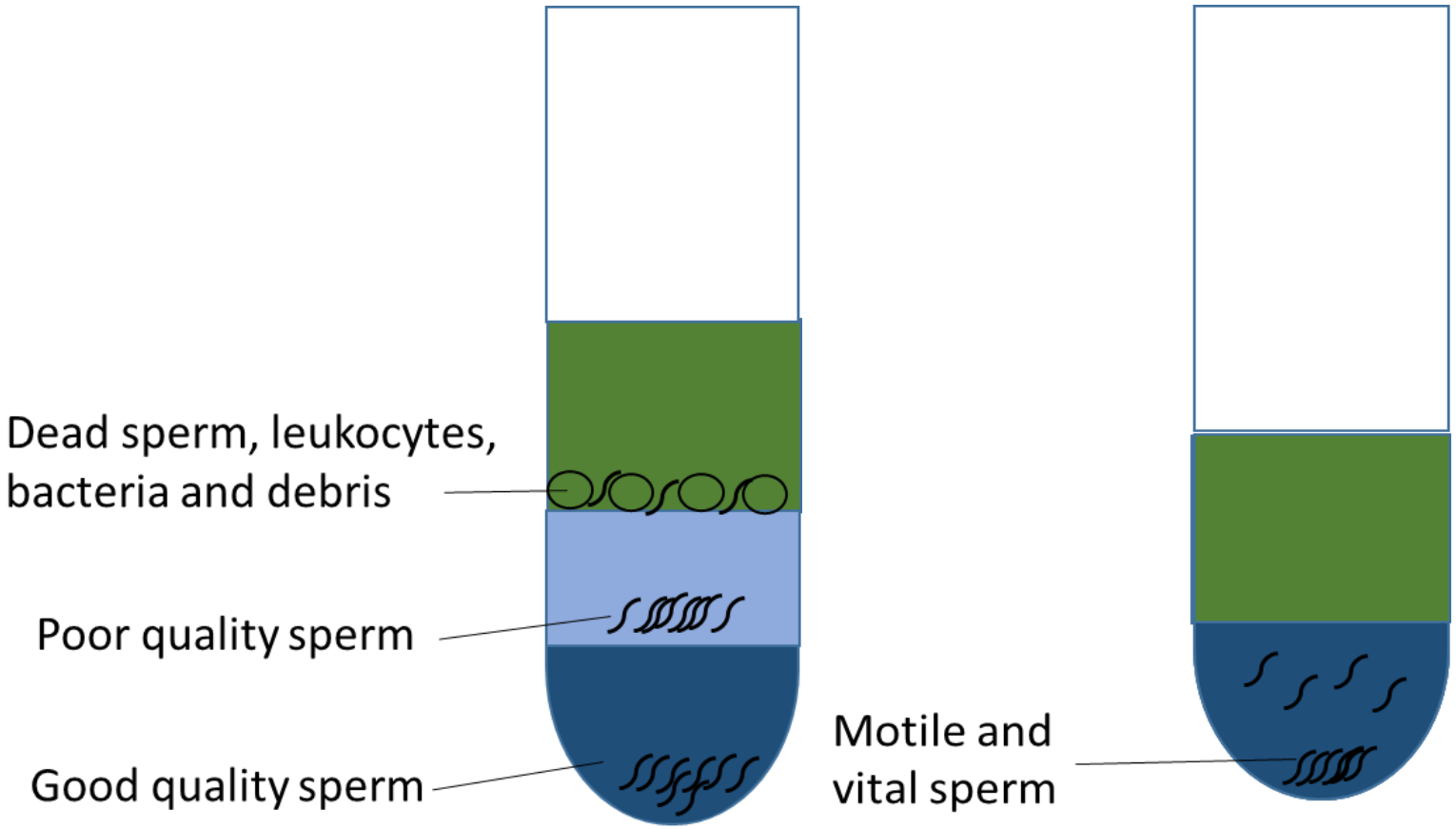

Figure 3.1: Post-centrifugation diagram for: DGC (Left), the top layer of the centrifuge tube will have the lowest density molecule, and the bottom layer will have higher density. For the SGC (Right), sperm move down through the medium, with the motile, vital sperm pelleting in the bottom of the tube.

Therefore, this preliminary experiment sought to investigate two aims. First to evaluate the effect of centrifugation on sperm motility and vitality. Secondly, to choose the best technique from the simple, SGC and DGC methods based on the best sperm motility and vitality yielded.

3.1.2 Methodology

Boar sperm from different animals, n = 5 (Section 2.1) was grouped according to the respective washing technique. The washing techniques were, as discussed above, simple centrifugation, SGC and DGC. The procedure was applied based on the methods outlined in Section 2.2 (Figure 3.2). A control group, which was an aliquot of the sperm in the extender, which had not undergone any washing procedure, was also prepared. Before centrifugation assessment, the motility and vitality assessments (Section 2.5.2 and 2.5.3) were performed (time, t = 0 min) for the control group only. After centrifugation and dilution of the sperm pellet, the assessment of motility and vitality was performed (t = 45 min) for all groups (control, simple, SGC and DGC). During 0 to 45 minutes, the control group was stored at room temperature. Average percentage motility and vitality of each group was calculated and compared.

3.1.3 Statistical analysis

One way ANOVA with Tukey's multiple comparison test was performed to compare differences between mean ± SD of PM, NP, IM, motile and vital sperm for simple, SGC and DGC washing methods and the control group, t = 45 min. A paired Student's T-test was used for comparing motility and vitality for the control group at 0 min and 45 min.

3.1.4 Results

The PM, NP, TMmotility (the sum of PM and NP) and vitality of sperm decreased after 45 minutes but were not statistically different for any type of motility (

Table 3.1).

To assess the effect of the different sperm washing techniques on sperm quality, the motility and vitality comparisons were made between those in the control group, at 45 minutes, and simple centrifugation, SGC and DGC).

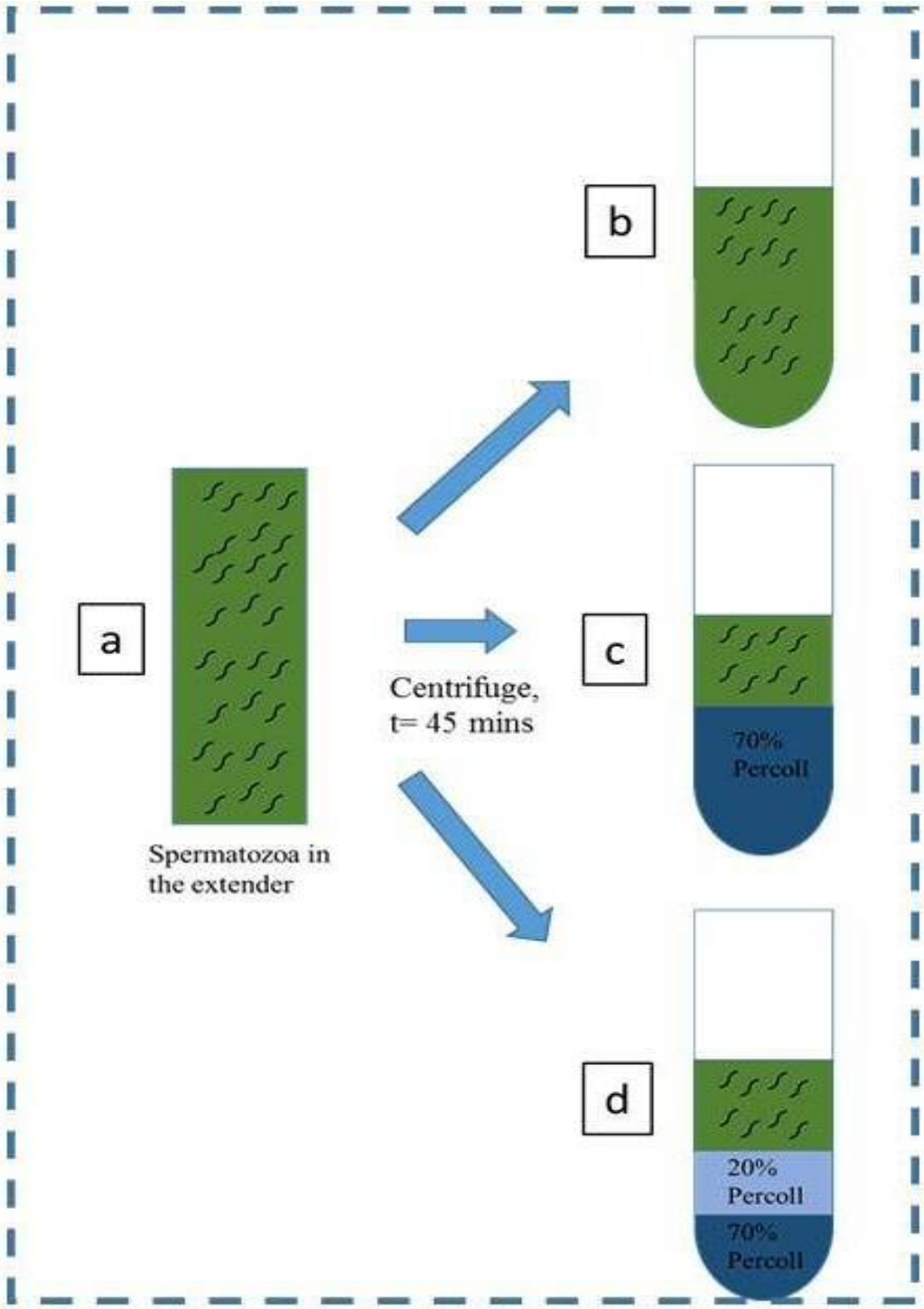

Figure 3.2: Paired boar sperm samples were prepared for motility and vitality assessment using (a) unwashed control sample (at t = 0 s) and those washed (at t = 45 mins) using (b) simple centrifugation (c) SGC and (d) DGC.

Table 3.1: Mean percentage ± SD vitality and motility including motile, PM, NP, and IM. Comparison between control 0 min and 45 min was made using a Paired t-test.

Sample	Motile, %	PM, %	NP, %	IM, %	Vitality, %
*C*ontrol, t =0 min	76 ± 5	2 ± 2	74 ± 6	24 ± 6	64 ± 1
*C*ontrol, t =45 min	63 ± 2	1 ± 1	63 ± 2	36 ± 2	62 ± 8
Paired T test	NS, 0.21	NS, 0.12	NS, 0.23	NS, 0.21	NS, 0.36

The percentage of motile sperm decreased after the washing procedure regardless of the technique. This was significantly different compared to the control group after washing with the simple technique. Among the washed groups, the DGC method retained the highest sperm motility (Figure 3.3 (a)).

The DGC also had the highest PM compared to the other washed groups. The PM of the sperm was increased numerically after washing with DGC and SGC. There was a significant difference between PM from the DGC technique compared to the control group. The mean difference between the SGC and DGC methods was quite similar at 2%. No PM sperm were detected in all the samples from the simple washing technique (Figure 3.3 (b)).

Generally NP numbers decreased after sperm were washed with any of the washing techniques. The decline was the lowest when washed with DGC, followed by SGC and then the simple washing method. The mean number of NP sperm was significantly different using the simple washing technique (Figure 3.3 (c)).

Conversely, IM of sperm was higher after washing. The highest IM was from washing the sperm with the simple technique, followed by DGC and then SGC. (Figure 3.3 (d)).

The vitality of sperm increased slightly after washing with DGC. Otherwise, vitality was decreased when washing with other techniques with a small change of ~ 1% between before and after washing with SGC (Figure 3.3 (e)). None of these differences were significantly different.

3.1.5 Discussion

In this preliminary experiment, the goal was to determine which washing technique would produce the highest or best sperm motility and vitality for subsequent experiments.

Boar sperm can retain vitality and motility for a few hours after ejaculation without extender (Lopez Rodriguez *et al.*, 2017) and several days when diluted with the extender (Kaeoket *et al.*, 2010). Special attention must be given to the duration of the sperm preparation so that the quality of the sperm does not degrade. This then means that an improved SNR can be obtained for the MRS study.

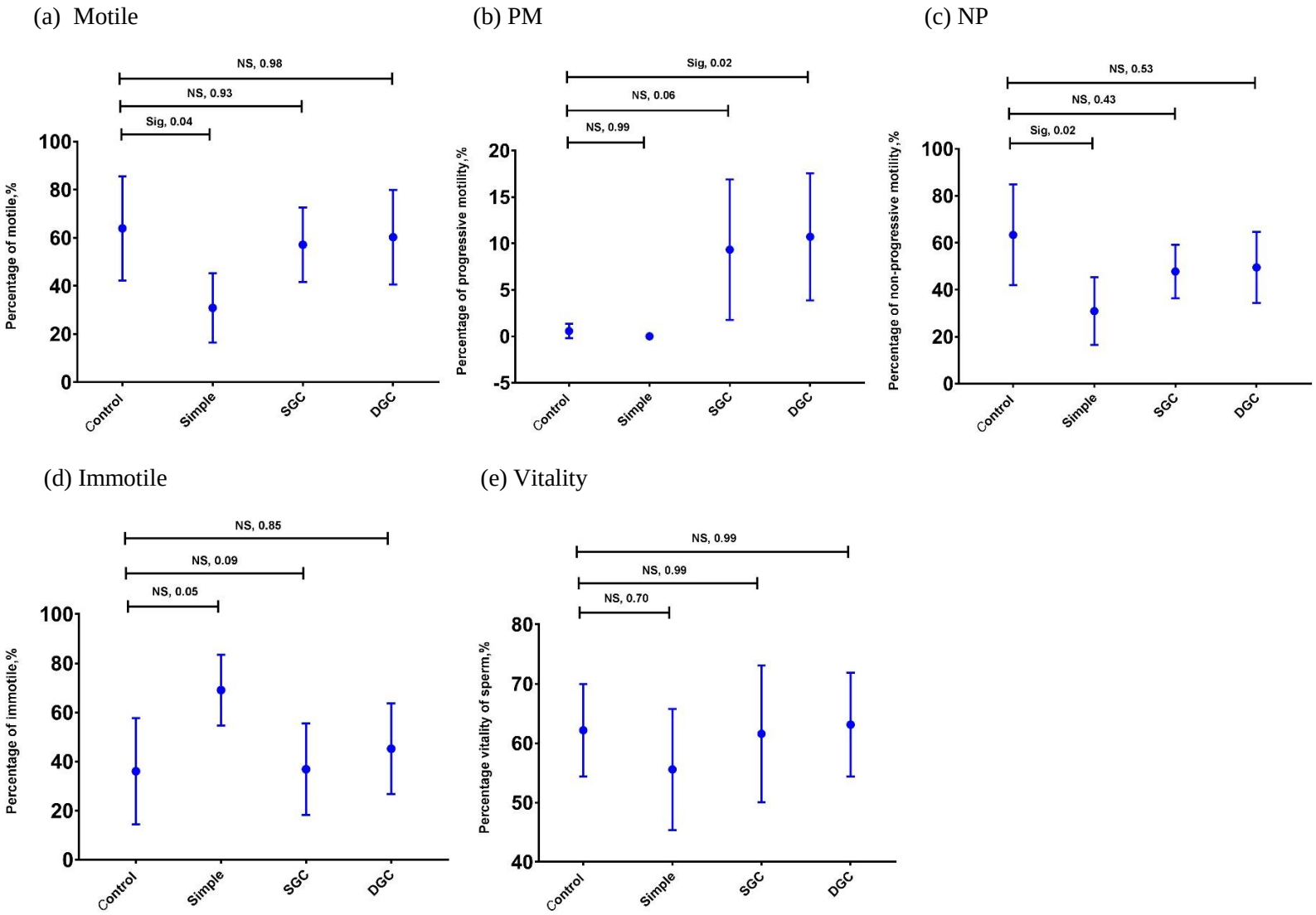

Figure 3.3: Mean percentage ± SD of (a) Motile, (b) PM, (c) NP, (d) IM and (e) vitality, with statistical analysis from One Way ANOVA with Tukey's test for the sperm washed with simple, SGC and DGC techniques.

Depending on which washing process is used, a typical centrifugation technique takes 20 minutes to 1 h. However, all sperm washing methods used in this study required ~ 45 minutes for a two step centrifugation process. Results from the comparison between the control group at 0 and 45 minutes suggests that the duration needed for sperm washing is safe and acceptable. Boar sperm are sensitive to temperature (Lopez Rodriguez *et al.*, 2017), thus this result might have been different if different temperature had been used to store the sperm sample. This could also explain why sperm motility decreased after 45 minutes as the recommended storage temperature for AI sperm is at 17°C.

As mentioned previously, the role of the extender is to inhibit sperm motility. This study did not calculate or measure the amount of extender or Percoll in the prepared sperm after centrifugation. However, high percentages of IM and zero PM of the sperm when washed using the simple washing technique suggests that the extender and other supporting fluids were still present in the recovered sperm even after washing. However, contamination of the semen by non-sperm cells, could produces a detectable metabolite signal. This could cause spectral misinterpretation if those molecules match with metabolites produced from sperm ^{13}C metabolism. High sperm vitality when washed using the simple washing technique may suggest that the sperm washed using that technique are more susceptible to the effect of the mechanical stress compared to other washing techniques. Therefore, from these results, it can be concluded that the simple washing technique was ineffective for washing the sperm without interfering with the sperm quality and contamination.

In contrast, the significant increase of PM in the DGC group may indicate an efficient separation of high quality sperm from the low quality sperm from recovered sperm in the high density gradient. Indeed, for this study, DGC was thought to be a better technique than SGC. This was because, (i) DGC produced higher PM by ~ 2%, NP by ~ 2%, and ~ 1% for vitality than SGC, (ii) DGC produced the highest motility and PM of the sperm out of the other washed groups and (iii) DGC was also able to retain motile sperm between 89 - 94% of the control value. Lastly, sperm vitality improved when sperm were washed using DGC.

In short, the findings showed that sperm washing by DGC was effective and the best method to retain sperm motility and vitality.

3.2 Optimization of MRS spectra: Function of the labelled substrate volume and incubation time

3.2.1 Introduction

The relatively low sensitivity of ^{13}C MRS has limited its application in metabolomics studies owing to the low SNR. The sensitivity issue can be improved by using an optimized technique. This includes using a ^{13}C labelled substrate. An aspect to be considered when using labelling studies is the integration of a sufficient quantity of labelled substrate into the sample to enable detection by MRS. This can be calculated by applying a mathematical model to analysis of the metabolic flux of the ^{13}C glucose (Buescher *et al.*, 2015).

A simpler method, which might give similar findings, can be achieved by comparing the detected signal from ^{13}C spectra between different ^{13}C substrate concentrations. The concentrations must be high enough so that substrate availability will not be the limitation for sperm metabolism. Since the concentration of the substrate can influence the rate of metabolism where a higher concentration of substrate will stimulate the metabolism flux. The goal was to provide the sperm with an unlimited but not excessive, supply of labelled substrate so that they can undergo the metabolism process needed.

SNR can also be increased by signal averaging over a longer acquisition time. Instead of continuously acquiring the metabolite signal from the sperm, this study allowed a period of time for U-^{13}C glucose to be metabolised by the sperm outside of the scanner. It was expected that, as long the sperm were still alive, there will be a need for energy which can be provided by ^{13}C glucose metabolism. Therefore ^{13}C glucose will be consumed and catabolised over this time period. Accumulation of the U-^{13}C glucose end product will increase the signal and enhance the SNR (Barratt, Kay and Oxenham, 2009; Buescher *et al.*, 2015).

Therefore, the aims in this preliminary experiment were to determine the sperm sample incubation time and the volume, 40 µl and 80 µl, of 100 mM U-^{13}C glucose which will give an optimum MRS signal.

3.2.2 Methodology

Boar sperm (n = 5 ejaculates) were washed using DGC (Section 2.2.3) and then had either 40 µl or 80 µl of 100 mM of U-^{13}C glucose added. Samples were then incubated in a water bath at 37°C for incubation periods of 1, 2, 4, 16, 18 and 21 hours, and subsequently frozen. Thawed samples were scanned in the MR scanner and spectra were analysed (see Section 2.6 and 2.7).

3.2.3 Statistical analysis

The relationship between metabolite integral, and incubation time for 40 and 80 µl of 100 mM of U-^{13}C glucose were analysed using Pearson correlation respectively. Two way ANOVA with Sidak's test was carried out to analyse the integral difference between 40 and 80 µl. Commonly Sidak or Bonferroni methods are used for comparison between one set of means with another. Sidak assumes that each comparison is independent of the others thus family wise error rate could be controlled (Lee, 2018). Therefore, it was selected for statistical analysis in this study.

3.2.4 Results

Two metabolites were detected, which were lactate and bicarbonate. Lactate and bicarbonate integrals were normalised by their respective sperm concentration. Statistical analysis was performed on the lactate integral only as its SNR was higher than the bicarbonate (which was below the detection limit) and was constantly produced by all samples, (lactate, N = 5; bicarbonate, N = 2).

The lactate signals for 40 µl and 80 µl of 100 mM U-^{13}C glucose were significantly increased with the incubation time (40 µl, $r^2 = 0.79$, 80 µl, $r^2 = 0.90$).

Generally, the lactate signal from 40 µl and 80 µl reached the maximum level at 18 h and decreased beyond that point. Lactate signal from the short incubation periods (1, 2 and 4 h) was not significantly different from control. Statistical comparison showed significant differences for the longer incubation times of lactate levels at 16 and 21 h (Figure 3.4). It was found that, there was a significant different between lactate signal for 40 µl and 80 µl at 16 h. and 21 h (Table 3.2).

3.2.5 Discussion

The goal of these experiments were to determine sperm sample incubation time and the volume of 100 mM U-^{13}C glucose which will give an optimum MRS signal.

U-^{13}C glucose, the labelled substrate, was fed to, consumed and metabolised by sperm through several metabolic pathways. Since all carbons in the glucose were labelled, the carbon will incorporate into all carbon positions of the glucose metabolism products through the glycolysis process and this reaction can be tracked using MRS. As described in the Section 1.9, lactate might represent a metabolic product from pyruvate, which is the end product of glycolysis. The bicarbonate might represent Krebs cycle, PDH or PC.

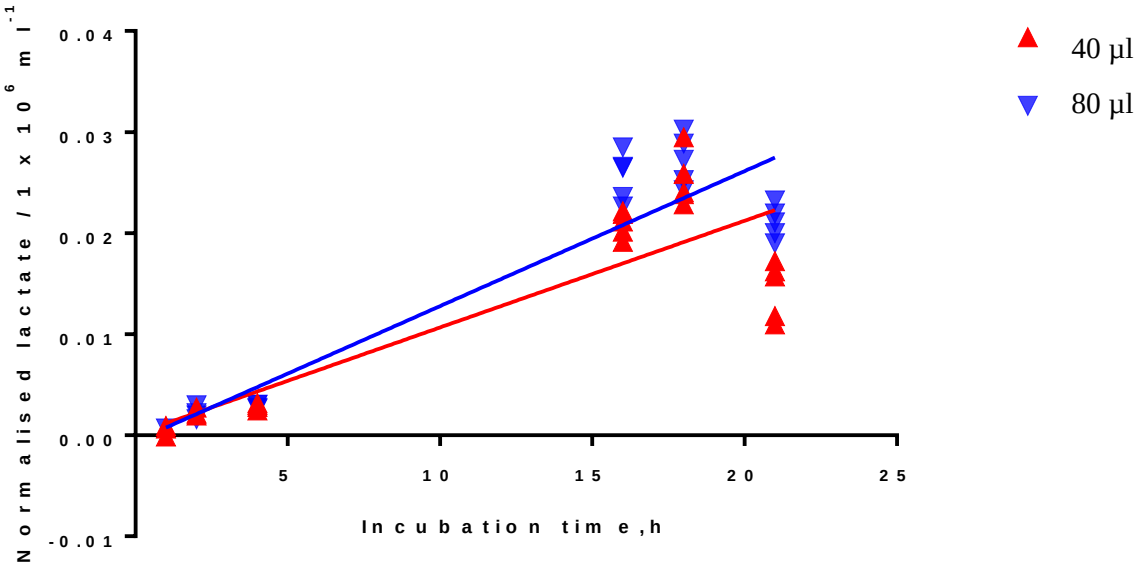

Figure 3.4: Lactate integral normalised by sperm concentration at different incubation times (1, 2, 4, 16, 18, and 21 h).

	1 h	2 h	4 h	16 h	18 h	21 h
40 µl	$0.001 \pm 0.002 \times 10^{-5}$	$0.02 \pm 0.322 \times 10^{-5}$	$0.03 \pm 0.416 \times 10^{-5}$	0.021 ± 0.001	0.024 ± 0.002	0.015 ± 0.003
80 µl	$0.001 \pm 0.003 \times 10^{-5}$	0.002 ± 0.001	$0.003 \pm 0.005 \times 10^{-5}$	0.026 ± 0.002	0.027 ± 0.003	0.021 ± 0.002
P value	NS, > 0.999	NS, > 0.999	NS, > 0.999	Sig, $p < 0.001$	NS, $p = 0.145$	Sig, $p < 0.001$

Table 3.2: Comparison between mean lactate integrals normalised by sperm concentration for 40 and 80 µl of 100 mm ^{13}C glucose after incubated in the sperm for several time points.

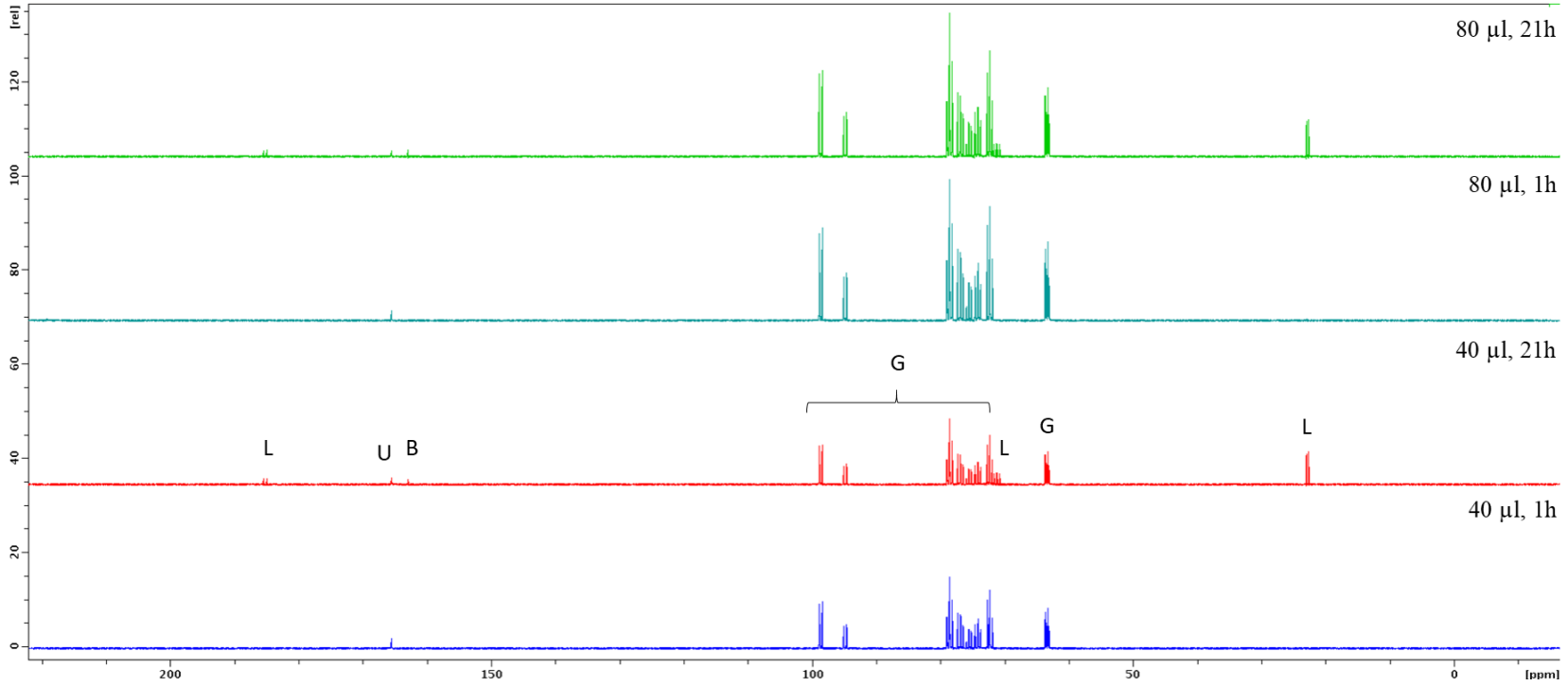

Figure 3.5: Stack of spectra acquired from incubating sperm with the 40 µl, 80 µl at 1 h and 21 h. L is lactate peak, G is glucose peaks, B is the bicarbonate peak and U is the urea peak.

By adding 80 µl of U-^{13}C glucose into 100 µl of the re-suspended sperm, the sample will contain a higher molarity of dissolved ^{13}C glucose than using 40 µl. Higher availability of ^{13}C might increase metabolism rate (Berg, Tymoczko and Stryer, 2002b). As expected 80 µl yielded higher integral for lactate than 40 µl. Lower lactate signal for 40 µl could also indicate limited availability of the substrate that restricted the metabolism process. If there is not enough substrate to be consumed by the sperm, catabolism of the substrate cannot be activated. However, the difference between lactate signal for 40 µl and 80 µl was not significantly different at 18 h. The results suggest that lactate slowly accumulated and reached a peak at 18 h for both 40 µl and 80 µl of the U-^{13}C glucose. Therefore, a U-^{13}C glucose volume in between 40 µl and 80 µl, i.e. 60 µl was used for subsequent experiments.

Decrease of lactate signal from 18 h to 21 h may suggest an altered lactate concentration, possibly by conversion by another reaction. This includes that lactate was being converted back to pyruvate possibly through gluconeogenesis. However, no pyruvate (or other related metabolite) signal was observed in the spectra. This might indicate that the concentration of the labelled pyruvate was below the detection level of MRS. Pyruvate concentration can be roughly predicted by comparison with the lactate integral. If half of the lactate been reconverted into pyruvate, the pyruvate peak would be half of the lactate peak. However, since ^{13}C glucose was observed in the spectrum at 21 h for both 40 µl and 80 µl, it suggests that there is an excess supply of glucose and therefore gluconeogenesis may not activated (Figure 3.5). Furthermore, glucose concentration after 1 hour and 12 hours incubation spectrum were hardly differentiate suggesting that its starting concentration was abundant. Therefore, not much information could be obtained from the glucose concentration analysis. Although the rate of glucose depletion could be calculated and compared to the rate of lactate production, it was not carry out because little contribution to this chapter's aim.

Conversely, for low incubation times, the lactate signal could be low because of little conversion of U-^{13}C glucose to lactate. In the condition where the sperm metabolism rate can be stimulated, a short incubation period might produce a signal which is comparable to that measured at long incubation times. Therefore, a shorter 4 h incubation time was used for oxygenation experiments where such an increase in rate could be expected. Also, if an 18 hour incubation time were to be employed for the oxygenation study, a high volume of gas would be needed with a probability of gas running out during incubation.

Ideally, for all incubation times, (1, 2, 4, 16, 18, and 21 h) sperm samples should be from the same ejaculate so that a paired comparison can be carried out. However, by using a different ejaculate for each sample allows higher sperm concentration and hence higher MRS signal. To eliminate variance between samples quality (see Figure 3.3 for example), all detected metabolites were normalised by sperm concentration respective to each ejaculate.

In conclusion, 18 h was an optimum incubation period except for the oxygenation experiment, where the shorter incubation time (4 h) was more practical. For the concentration of the ^{13}C glucose (or other substrate), 60 µl of 100 mM was considered as an optimum volume.

3.3 Conclusion

DGC will be used in subsequent experiments to prepare sperm samples for MRS experiments. Diluted sperm will have 60 µl of 100 mM ^{13}C labelled substrate added and incubated at 4 h for oxygenation experiments or 18 h for investigation of the effects of labelled substrates, inhibitors and temperature.

Chapter 4: The effect of metabolic inhibitors on sperm metabolism and vitality

4.1 Introduction

Several factors affect the rate of enzymatic cell metabolism. These include the temperature, pH, enzyme concentration, substrate concentration and the presence of any inhibitors or activators (Harrow and Mazur, 1958). This chapter will focus on use of inhibitors to regulate the metabolism reaction of sperm.

An inhibitor is a molecule that decreases activity of an enzyme (Berg, 2008). An enzyme is a molecule that can accelerate the catabolic reaction of a substrate into product. It possesses a region called the active site, where it binds substrates and also has other binding areas called allosteric sites, which are located away from the active site. An allosteric site does not bind a substrate, but instead binds another molecule such as an inhibitor (Cox and Nelson, 2008). Decrease of reaction activity due to inhibitors can be reversible, where activity may be restored by the removal of the inhibitor or irreversible, where activity can be restored by synthesis of a new enzyme (Berg, 2008). Most studies report that inhibitor's effects are reversible (Bhagavan and Ha, 2011). There are two common types of reversible inhibition: competitive and non-competitive.

A competitive inhibitor binds to the enzyme's active site where it competes with the substrate for the active site of an enzyme, depending on concentration. If the inhibitor occupies the active site, it prevents binding of the substrate to the enzyme. The reaction does not proceed since the inhibitor has a different structure compared to the substrate. Even short term inhibitor-enzyme binding could lower the efficiency of the enzyme (Devlin, 2006). It can disturb substrate catabolism by slowing or stopping the reaction when the substrate concentration is low. However, if the concentration of substrate is high, the inhibition reaction can be out-competed. This happens when almost all the enzyme active site is occupied by the substrate rather than the inhibitor (Engelking, 2015) (Figure 4.1 (a)).

A non-competitive inhibitor binds with an enzyme at an allosteric site. When inhibitor-enzyme binding happens, it alters the enzyme's shape and changes how the enzyme functions. The substrate may still bind with the enzyme at the active site but it will not be converted into a product. Therefore, even though substrate-enzyme binding continues, the reaction will never reach its normal maximum rate unless the inhibitor is removed from the allosteric site (Figure 4.1 (b)).

Reversible inhibition will result in either accumulation of the substrate or decrease of the product generation.

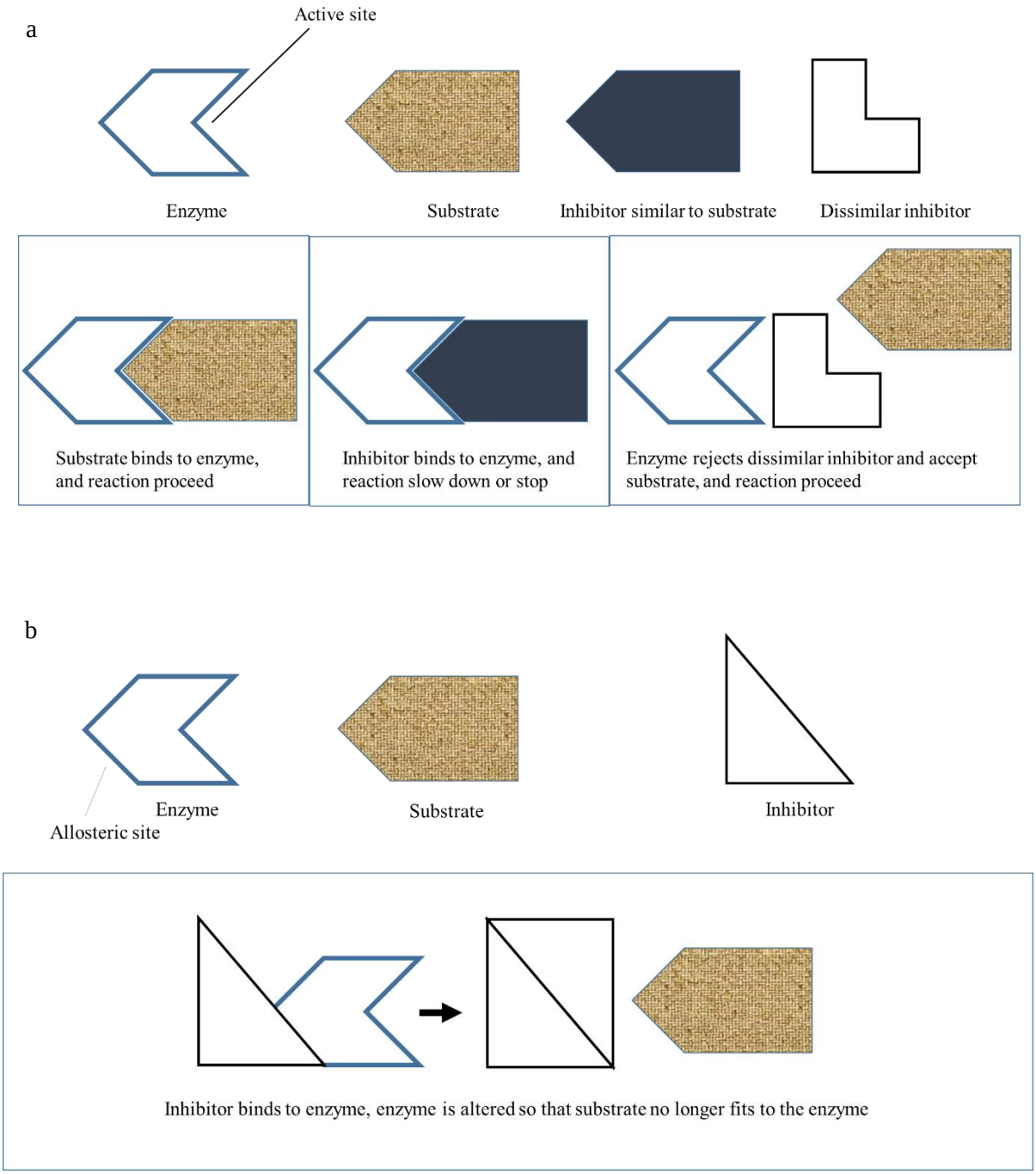

Figure 4.1: Competitive inhibitor: (a) the substrate binds with the enzyme and the reaction proceeds. However, when an inhibitor which resembles the substrate is present, it will compete with the substrate for the active site in the enzyme. When the inhibitor occupies an active site, it binds with the enzyme but stops the reaction at that site proceeding. Hence, the overall observed reaction is slowed down because some of the available enzyme sites are occupied by the inhibitor. If a dissimilar substance which does not fit the active site is present, the enzyme rejects it, accepts the substrate and the reaction proceeds normally. Non-competitive inhibitor: (b) the inhibitor binds to an enzyme at the allosteric site and altered the enzyme shape and function. Consequently, the substrate is unable to bind with the enzyme.

The rationale for using an inhibitor to increase Krebs cycle intermediates was taken from an earlier finding in a non-sperm cell study by Peter (1953) when he observed the accumulation of citrate after addition of oxaloacetate (Krebs, 1953) and succinate accumulation by adding malonate (Quastel and Wheatley, 1931; Krebs and Johnson, 1937). In most cases, the substrate acts as a competitive inhibitor when it is added at high concentration into the sample. The same effect was found in a rat study of the impact of a high concentration of malonate on succinate (Smith *et al*., 1974). However, there were studies which reported the ability of an inhibitor to decrease the respiration process (Macleod, 1943), concentration of malate and fumarate (Smith *et al*., 2007), and α-ketoglutarate (Selak *et al.*, 2005). These finding all suggest that there might be a possibility to detect Krebs cycle intermediates in sperm by utilizing an inhibitor.

Indeed, a previous fluorimetric study has succeeded in detecting Krebs cycle metabolites in human sperm using an inhibitor in which citrate level increased three to fourfold after addition of a very high concentration of succinate (Peterson and Freund, 1974). For this study, the chosen competitive inhibitors were malonate and oxaloacetate, which are inhibitors for succinate dehydrogenase (Pardee and Potter, 1948; Valls-Lacalle *et al.*, 2016) and succinate, the inhibitor of *α*-ketoglutarate dehydrogenase complex (Smith *et al*., 2007) (Figure 4.2). The hypothesis was that the presence of these inhibitors would slow down or stop the related reaction in the Krebs cycle and result in an accumulation of succinate when using malonate or oxaloacetate, and *α*-ketoglutarate when using succinate or produce a reduction of the intermediate/metabolite product at the point in the Krebs cycle after the inhibition site.

This raises the biological question as to how boar sperm utilise U-^{13}C glucose, as an energy source, in the presence of a Krebs cycle inhibitor: either by activation of the Krebs cycle or by the entry of glucose in metabolic pathways other than glycolysis or the Krebs cycle. This is a crucial biological question, since a better understanding of energy metabolism could improve the strategies used to increase the motile lifetime of sperm in the female reproduction tract.

As inhibition of the Krebs cycle could reduce oxygen uptake and induce toxicity to sperm (Lardy and Phillips 1940) there is a need to examine the sperm vitality after being subjected to the inhibitor for a period of time. Therefore, this study aimed to: (i) increase the Krebs cycle intermediate concentration by using Krebs cycle inhibitors to enable detection by ^{13}C MRS, and (ii) assess sperm vitality after incubation with inhibitor for 18 hours.

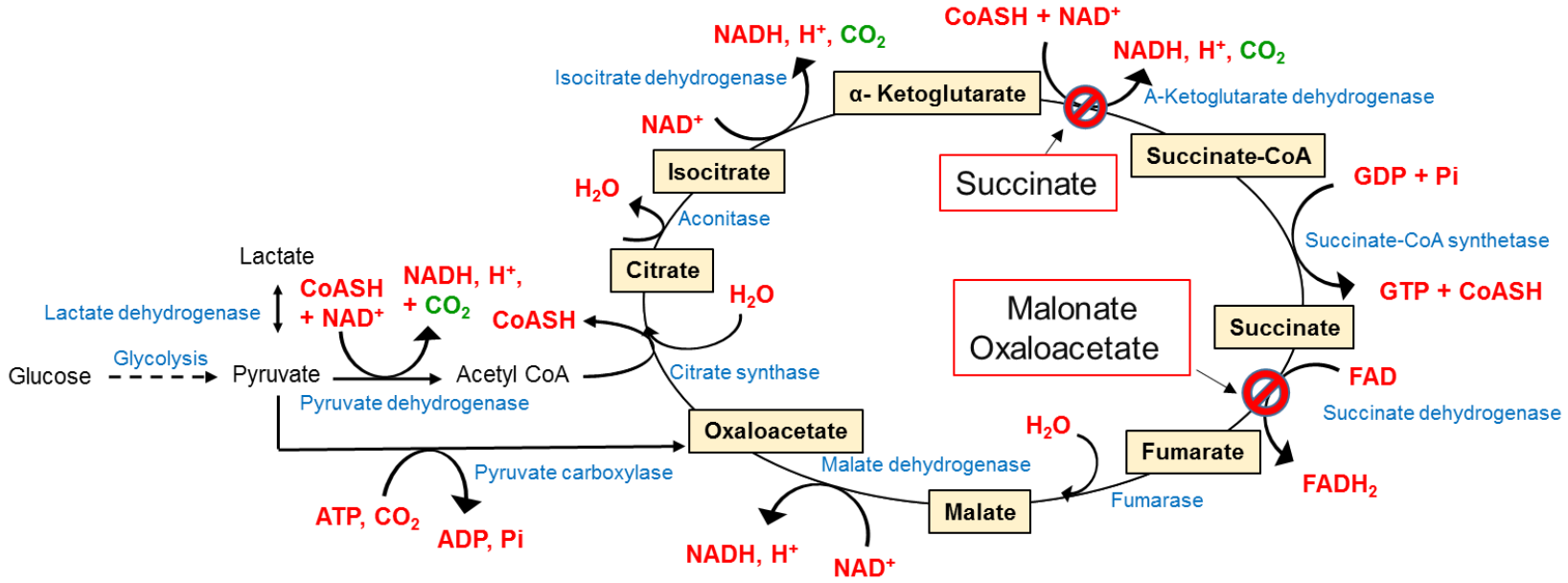

Figure 4.2: Overview of glucose catabolism. Through glycolysis, glucose undergoes several reactions (dashed arrow represents more than one chemical reactions) before converted into pyruvate. Pyruvate is subsequently converted either into lactate, Acetyl CoA, before entering the Krebs cycle, or oxaloacetate. CO_2 (which has a chemical equilibrium with bicarbonate) is produced in several reactions including with pyruvate dehydrogenase, isocitrate dehydrogenase and α-ketoglutarate dehydrogenase. The 'Ø'symbol represents inhibition sites in the Krebs cycle for succinate, malonate and oxaloacetate respectively

4.2 Methods

4.2.1 Preparing the inhibitors

Prior to experiments, inhibitors: malonic acid (Supelco, Bellefonte, USA), succinic acid (Acros Organics, Ceel, Belgium) and oxaloacetic acid (Sigma Aldrich, MA, USA), were transferred into a Eppendorf tube and weighed using a balance (Scientific Laboratory Supplies, UK) to obtain their mass respectively. The mass was used to calculate the volume of diluent needed for the desired final concentration using Equation 4.1. As the inhibitors were in acidic form, they needed to be neutralised. The neutralisation process was done by adding 2 M NaOH (Fisher Scientific, UK) into the inhibitors and the pH was monitored using a pH meter (IQ150, with an ISFET NMR tube microprobe. Hach, Manchester, UK). The solution was stirred well using a mixer (Stuart, Scientific Laboratories Supplies, UK) before the pH reading was taken. The process of adding NaOH was repeated until the mixture was between pH 7.2 to 7.6. Once they were neutralised, stock inhibitor solutions were prepared by diluting the inhibitor with PBS to give a final concentration of 1 M. The stock inhibitors were then aliquoted into several clean tubes with a smaller volume and stored at the recommended conditions.

$$C = \frac{m}{v} \qquad \text{Equation 4.1}$$

Where,

C = concentration
m = mass
v = volume

4.2.2 Sample preparation for MRS and vitality study

Boar sperm, (see Section 2.1) was prepared by washing using Percoll/PBS DGC (Process (a) in Figure 4.3) (see Section 2.2.3). The MRS sample for aim (i), (Process (b) in Figure 4.3) was prepared from each ejaculate using 100 µl of aliquot from re-suspended sperm sample to which was added 60 µl of 100 mM U-^{13}C labelled glucose, 12 µl of Pen/Strep and the inhibitor with a range of final concentrations: 3, 7, 15, 31, 62, 125, 250 and 500 mM.

To investigate the findings from aim (i) further, a separate vitality experiment was carried out, (aim (ii). The sample for this experiment (Process (c) in Figure 4.3), was prepared from different ejaculates using 100 µl of aliquot from re-suspended sperm samples to which was added 60 µl of 100 mM of unlabelled glucose (BDH Laboratory Supplies, England), 12 µl of Pen/Strep and a set of inhibitor concentrations:

7, 31, 125 and 500 mM. The final concentration was prepared by diluting the 1 M stock inhibitor solution, using Equation 4.2, with PBS so that the final sample volume was 570 µl.

For both MRS and vitality test samples, control sperm samples with no inhibitor added, were also prepared. A total of 30 samples from different ejaculates were used for both MRS and vitality experiments (Figure 4.4). Samples with the inhibitor were then incubated in a water bath at 37°C for 18 hours (Process (d) in Figure 4.3) and, where possible, more than one inhibitor incubation was conducted in parallel.

For MRS samples, an aliquot from a re-suspended sperm sample was pipetted (Process (e) in Figure 4.3) for sperm concentration measurement (see Section 2.5.1) and motility assessment (see Section 2.5.2) while an aliquot of re-suspended sample was pipetted for vitality assessment (see Section 2.5.3). All sperm concentration measurements, motility and vitality assessments were conducted before incubation.

After 18 hours incubation, MRS samples were frozen at - 80° C until MR scanning (see Section 2.6) (Process (f) in Figure 4.3) while vitality assessment was conducted immediately.

$$V_1 C_1 = V_2 C_2 \qquad \text{Equation 4.2}$$

Where

V_1 = stock inhibitor volume

C_1 = stock inhibitor concentration

V_2 = final sample volume

C_2 = final sample concentration

4.3 Data analysis

Visual inspection was performed to compare the control sample MR spectra with the inhibitor sample spectra to detect any changes in the detected metabolite peaks and the presence of any new peaks. Chemical shift reference was achieved by comparing the detected peaks from the control sample spectra to those from 500 mM of inhibitor, which did not have any labelled substrate or sperm sample added (Figure 4.5, Figure 4.6). For the succinate peak, the chemical shift value was obtained from an existing database (HMDB, 2010). Detected peaks were analysed as described in Section 2.7.

Calculated sperm vitality and metabolite integrals were relative to their respective control vitality or metabolite integral for each sample. The correlation between metabolite integral or vitality, and

inhibitor concentration was determined by Pearson correlation based on the r^2 value and significance of the correlation.

Ordinary Two way ANOVA with Dunnett's test was performed to compare differences between metabolite integral and vitality for control samples versus each inhibitor concentration. The Dunnet test is an analogue to the Tukey test. Both are multiple comparison tests and assume a Gaussian distribution of the sample mean (Lee, 2018). If the comparison is between each mean with every other mean, Prism will perform a Tukey test. In this chapter the comparison was tested between each mean with the control, therefore Dunnet test was performed.

Values are quoted as $\log_{10}$ (for inhibitor concentration) and mean ± SD for vitality and metabolite integral.

4.4 Results

4.4.1 Aim (i): Effect of inhibitor on the detected ^{13}C metabolites

The sperm concentration for 15 ejaculates used for MRS experiments was 73 to 188 x 10^6/ml with a progressive motility from 3% to 17% and motility from 66% to 74% (post-preparation calculation).

Two sets of peaks were detected from ^{13}C glucose metabolism in control sample spectra, which were from 1, 2 and 3-^{13}C lactate and ^{13}C bicarbonate (Figure 4.7). The conversion into lactate was always observed (especially 3-^{13}C lactate peak) in the control sample and in some samples with a low concentration of inhibitor (Figure 4.8, Figure 4.9, and Figure 4.10). The lactate integral, normalised to sperm concentration, decreased for all inhibitor concentrations and from Pearson correlation analysis, there was a significant negative correlation between normalised lactate integral and concentration for all inhibitors (Figure 4.11 (a)). The inhibitor concentration which resulted in significant change of lactate integral, varied amongst inhibitors. For oxaloacetate, a low concentration resulted in significant changes in lactate while for other inhibitors, a higher concentration was needed to produce similar changes (Table 4.1).

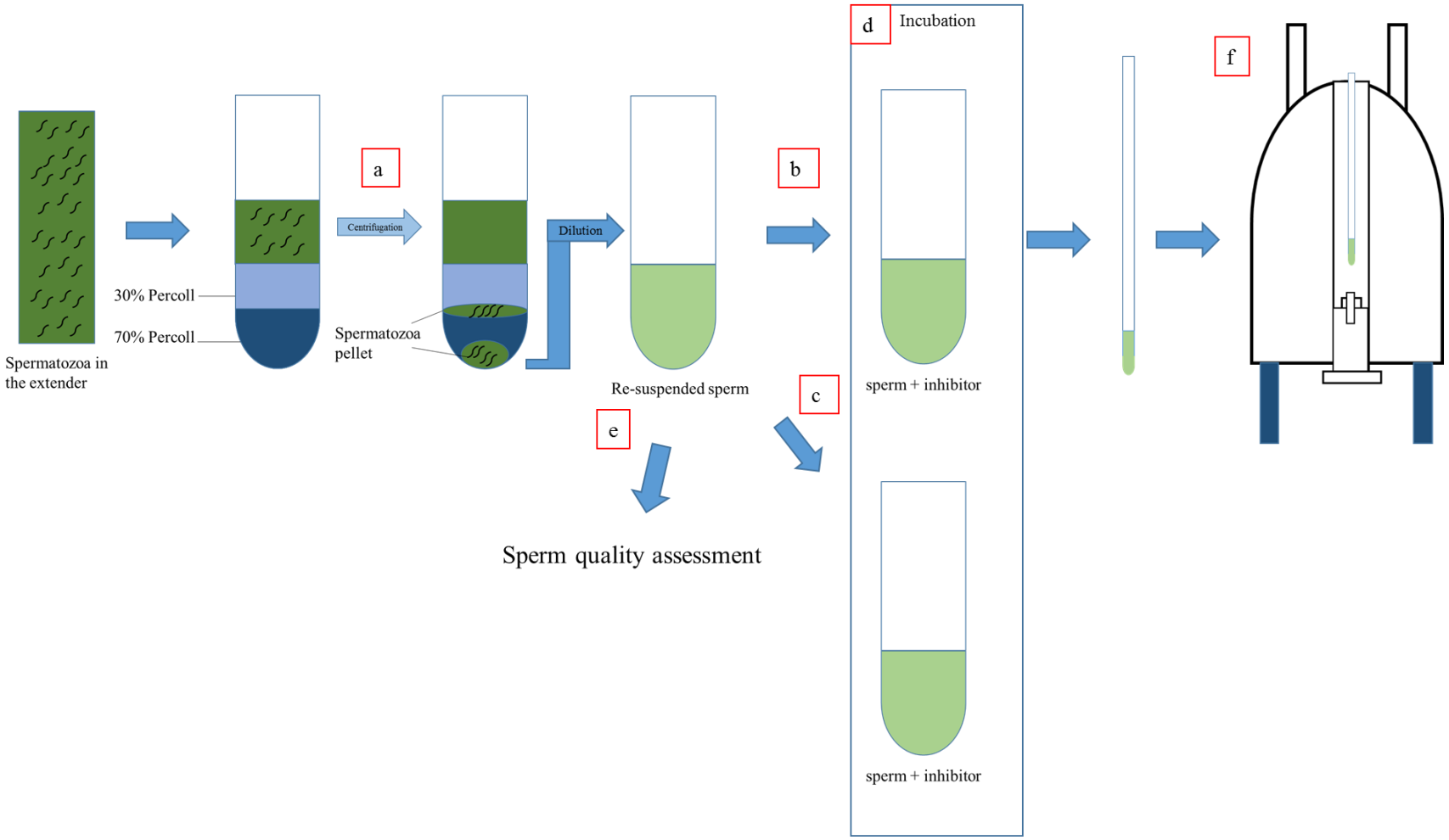

Figure 4.3: Overall schematic diagram of sperm sample preparation for MRS and vitality experiments. a is the centrifugation process. b is the process for MRS sample while c is for vitality sample. d, e and f represent the process for incubation, sperm quality assessments and MR scanning respectively.

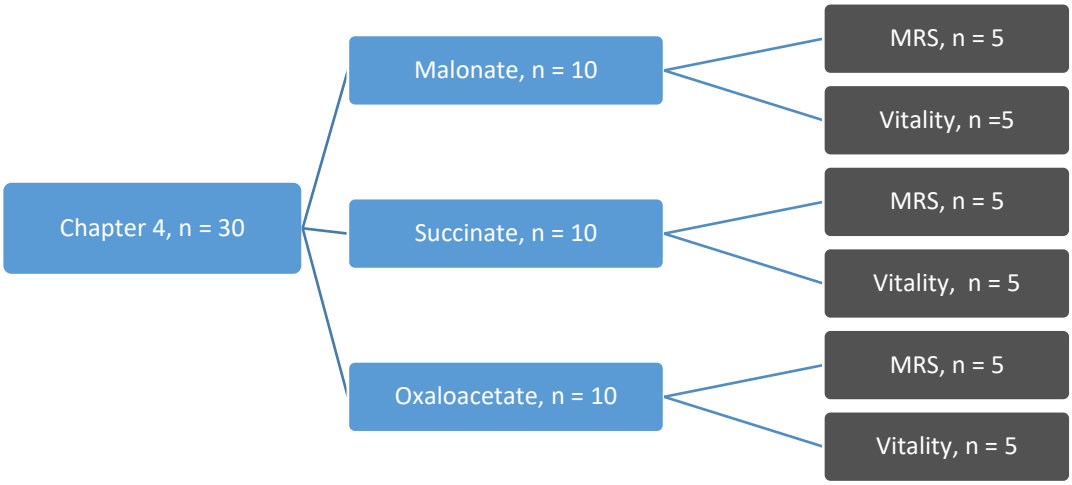

Figure 4.4: Summary of sperm sample usage. MRS and Vitality measurements were performed on separate samples from different ejaculates.

Compared to lactate, bicarbonate was rarely detected in spectra, even in control sample spectra. Bicarbonate was observed only twice in samples which were incubated with malonate and their respective control samples. There was no significant correlation between normalised bicarbonate integral and malonate concentration (Figure 4.11 (b)) and also no significant difference between bicarbonate integral for each concentration compared to control samples (Table 4.1).

4.4.2 Aim (ii): Effect of inhibitors on sperm vitality

To investigate whether the pattern of decreasing lactate was due to an inhibition reaction or sperm death, a sperm vitality assessment was conducted. It was found that, after 18 hours, on average, 39 ± 3% of the sperm were still alive in the samples that had inhibitors added (malonate, 37 ± 5%; succinate, 41 ± 5%; oxaloacetate, 39 ± 5%). The vitality of the sperm samples increased with increasing concentration of inhibitor, however no significant correlation was found (Figure 4.11 (c)). A comparison of sperm vitality between samples which had inhibitors added and their respective controls showed that only a sample that was incubated with 500 mM of succinate resulted in a significant higher vitality (Table 4.1).

4.5 Discussion

The aim of these experiments was to detect Krebs cycle intermediates using ^{13}C MRS by subjecting sperm samples to Krebs cycle inhibitors and also to investigate the impact of the inhibitors on sperm vitality. The results showed that, with an increasing concentration of all the inhibitors, lactate integral significantly decreased and only addition of 500 mM of succinate significantly influenced the sperm vitality.

Initial concentration, C_i, for all inhibitors were calculated based on the literature reported by Lahnsteiner *et al* (1999) in which they found significant effects of the inhibitor on fish sperm motility. However, in the present experiment, no Krebs cycle intermediates were observed when a concentration of C_i was applied. Thus, for this study, the concentration was adjusted several times but the results remained the same. Since C_i varied among inhibitors (malonate = 10 - 50 mM, succinate = 100 -300 mM and oxaloacetate = 0 – 10 mM), a final new range of concentration (3 – 500 mM) was developed for all inhibitors to ease subsequent statistical analysis.

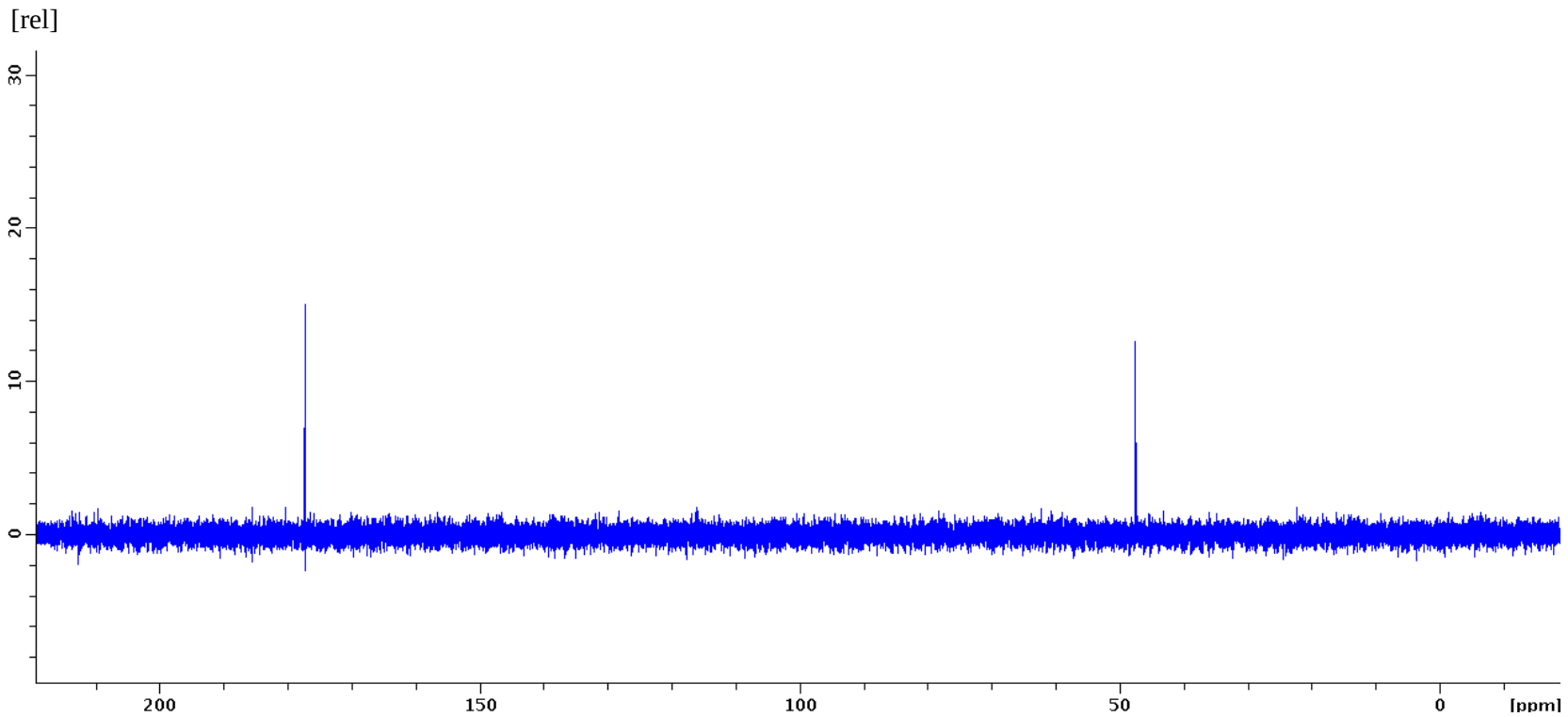

Figure 4.5: ^{13}C Spectrum of un-labelled malonate where two peaks were detected. This spectrum was set as the reference spectrum when inspecting any new peak arising in the ^{13}C spectra of sperm samples incubated with different concentrations of malonate (Figure 4.8).

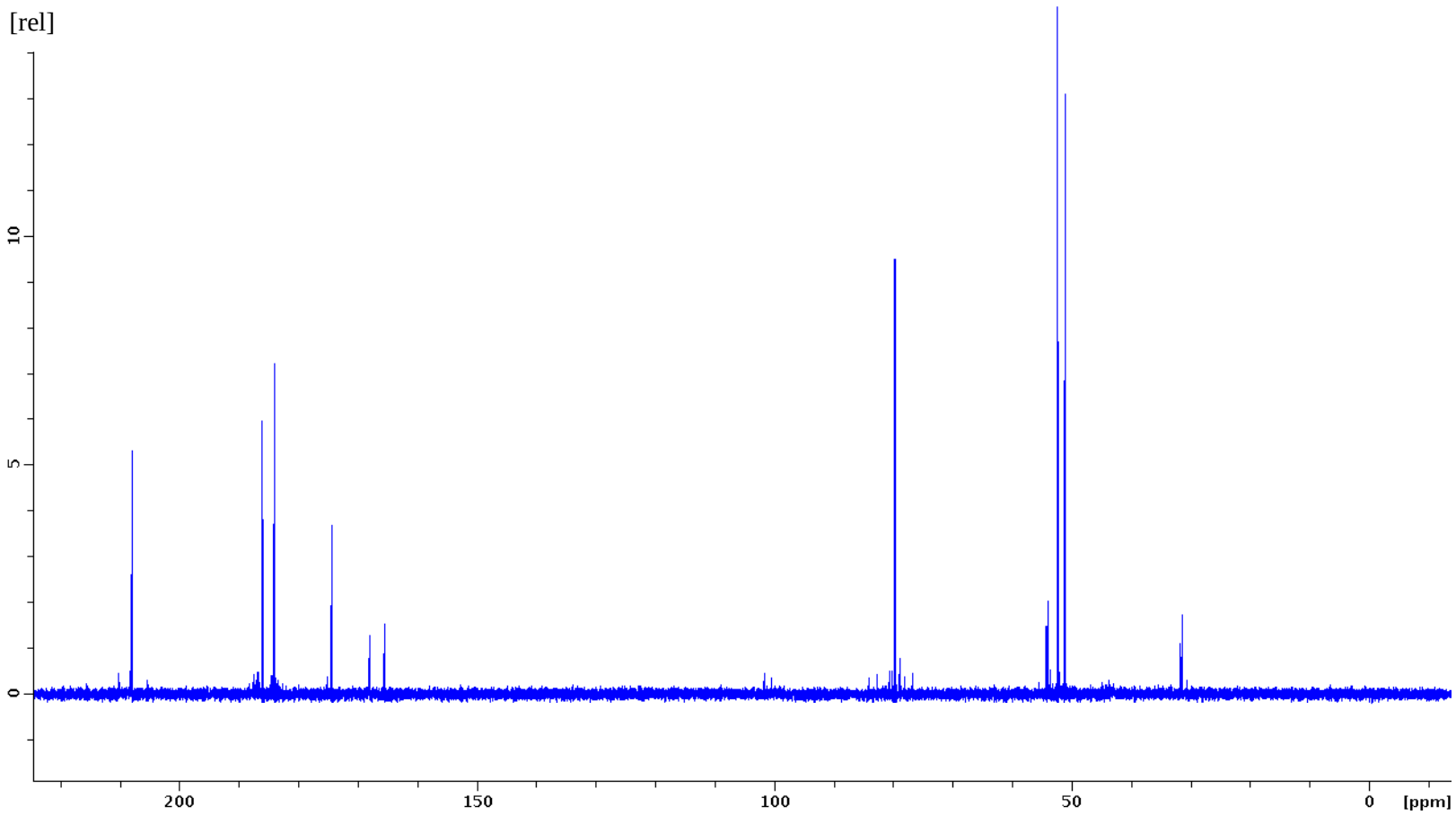

Figure 4.6: ^{13}C Spectra of un-labelled oxaloacetate where several peaks were detected. This spectrum was set as the reference spectrum when inspecting for any new peaks arising in the ^{13}C spectra of sperm samples incubated with different concentrations of oxaloacetate (Figure 4.10). Theoretically, four peaks should be visualised from oxaloacetate acid (C1 = 168.1, C2 = 199.8, C3 = 49.1 and C4 = 174.8 ppm (Kurz, Ackerman and Drysdale, 1985)). Other peaks were detected in the spectra in this experiment suggesting oxaloacetate decarboxylates spontaneously in PBS to form pyruvate (Tsai, 1967).

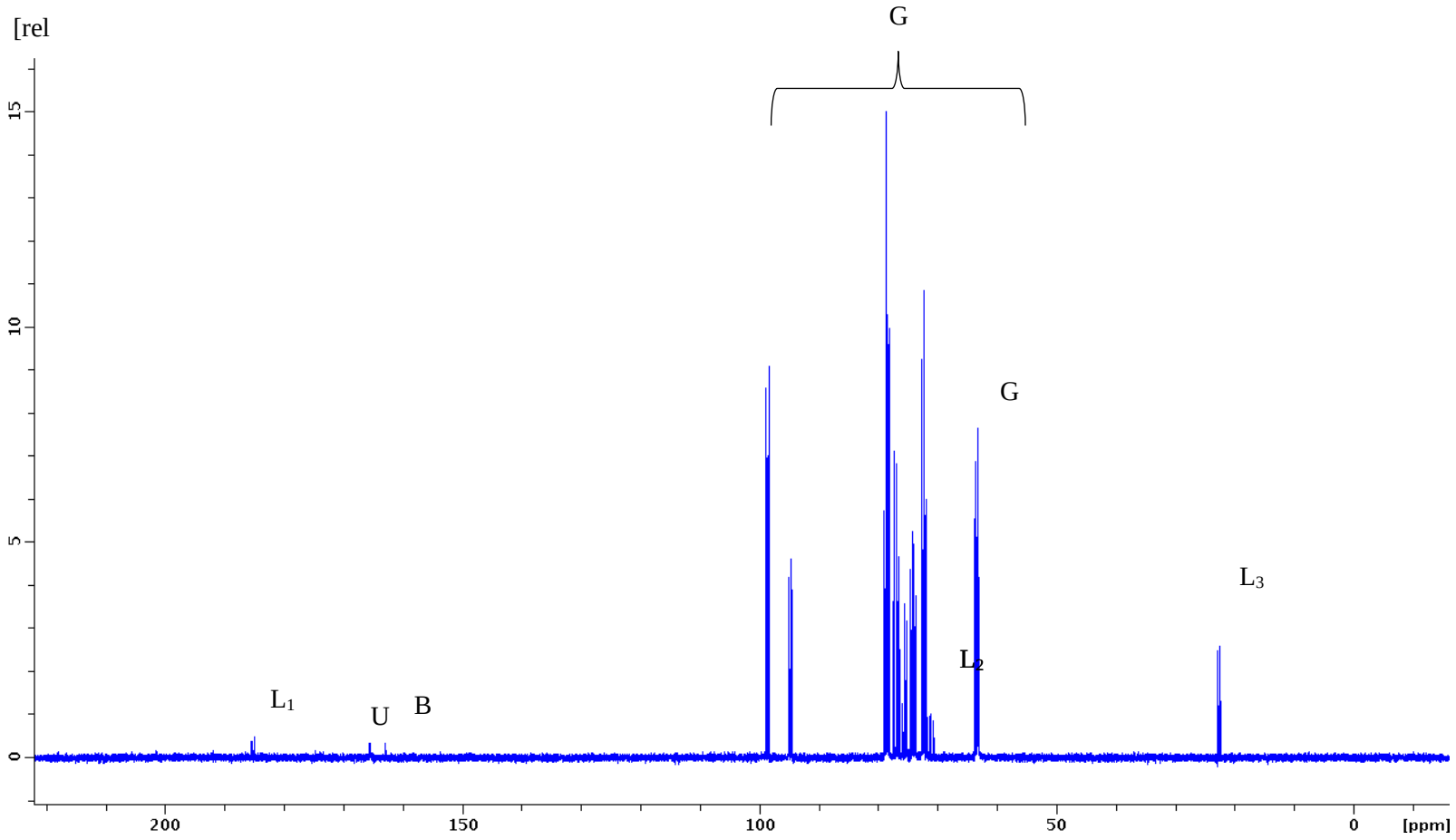

Figure 4.7: Representative ^{13}C spectrum of the control sample after incubation with U-^{13}C glucose. The spectrum was phased and based line corrected and referenced to the (U) ^{13}C urea chemical shift. (L_1, L_2, L_3) Lactate, where number indicates the carbon position, and (B) bicarbonate were detected as the metabolite products from (G) U-^{13}C glucose metabolism.

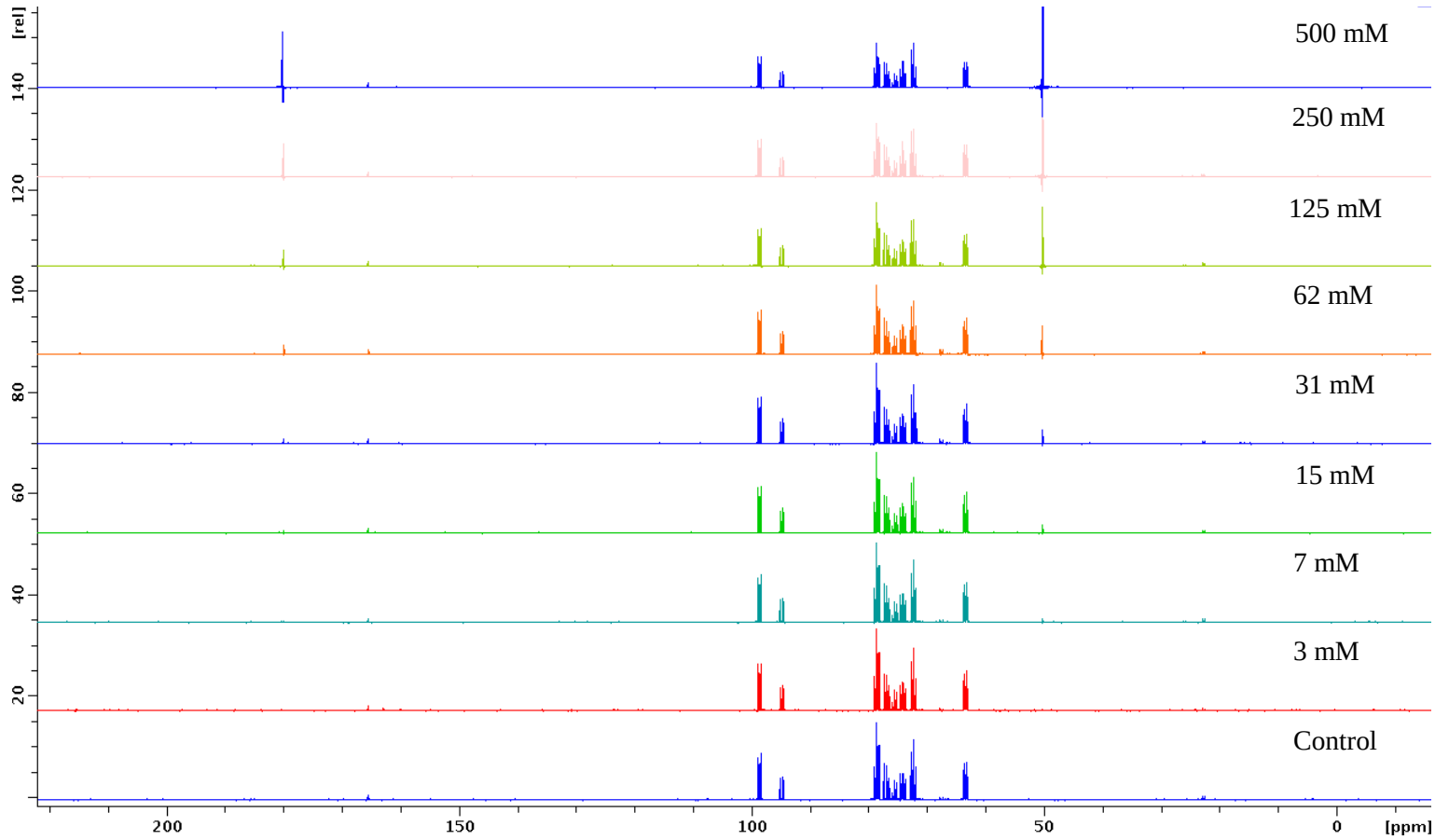

Figure 4.8: ^{13}C spectra of sperm samples incubated with different concentrations of malonate.

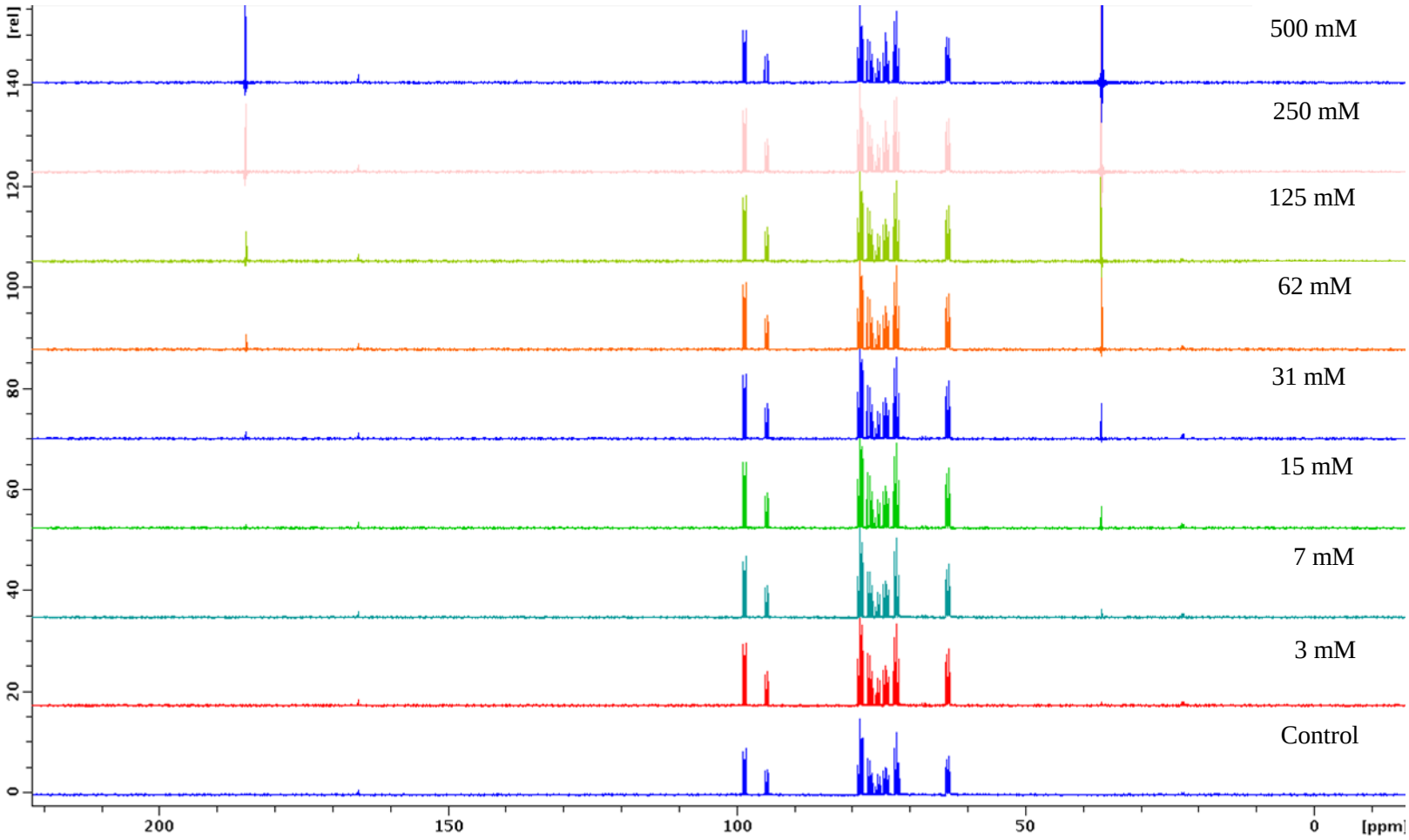

Figure 4.9: ^{13}C spectra of sperm samples incubated with different concentrations of succinate. Succinate chemical shift are 184.94 ppm and 36.83 ppm (HMDB, 2010).

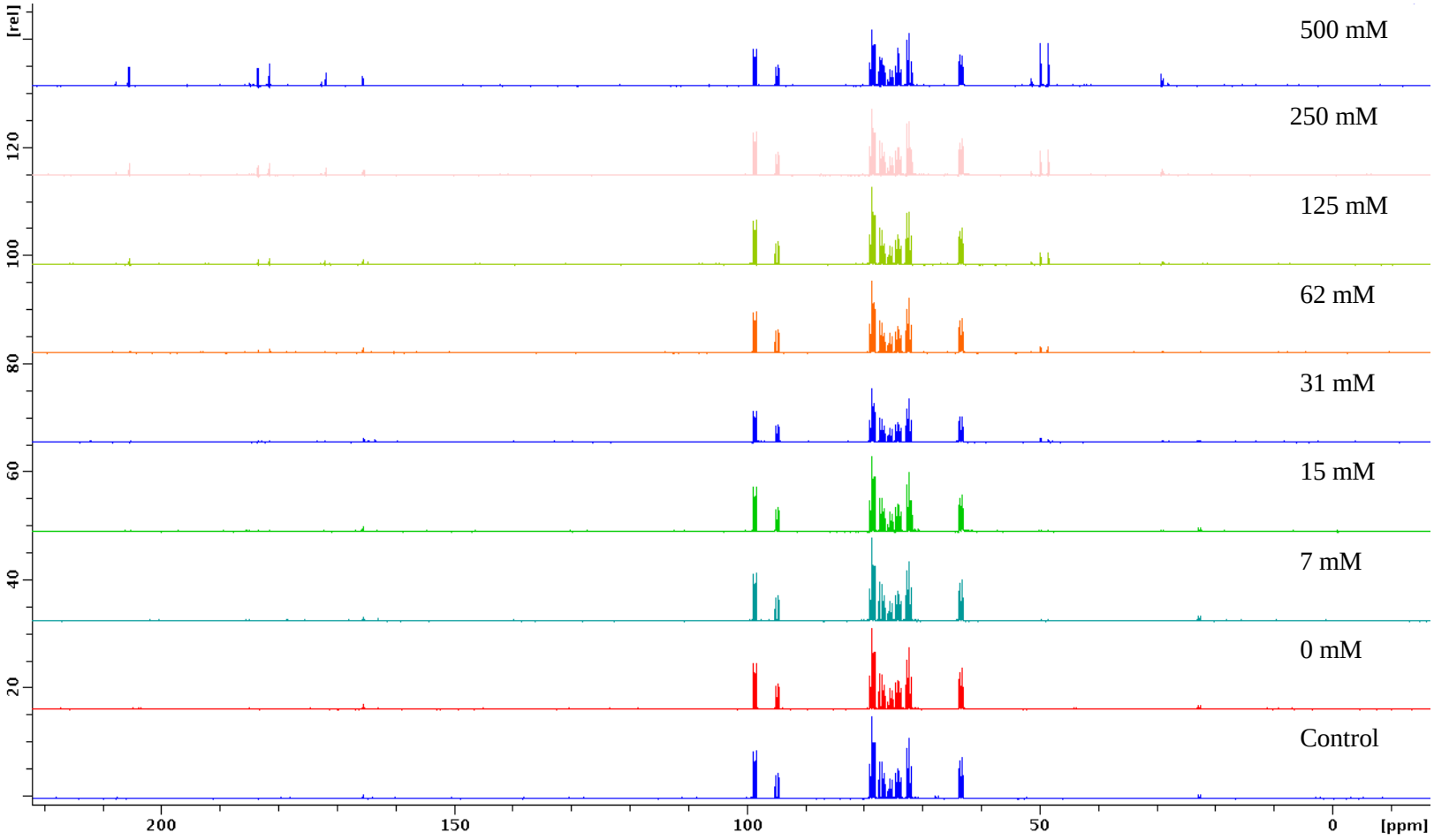

Figure 4.10: ^{13}C spectra of sperm samples incubated with different concentrations of oxaloacetate.

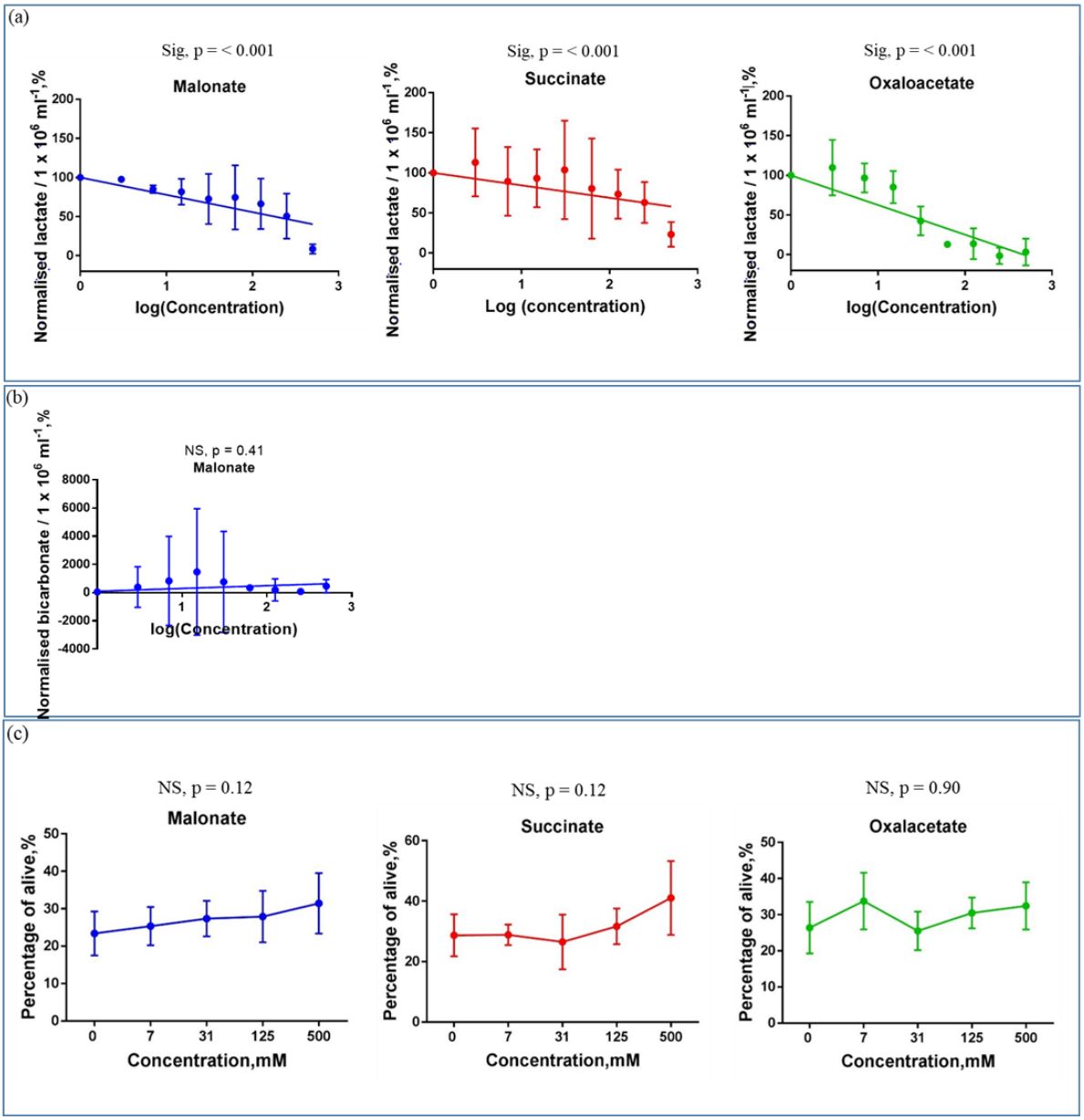

Figure 4.11: Effect of increasing concentration of the inhibitors: malonate, succinate, and oxaloacetate, on detected metabolite and sperm vitality. (a) lactate integral (b) bicarbonate integral and (c) sperm vitality were normalised relative to their respective control metabolite integral or vitality for each sample. First data point, for (c), is the percentage of alive sperm for control sample after 18 h incubation time. Sig = significant, NS = Not significant.

Table 4.1: Statistical comparison of lactate, bicarbonate and vitality for malonate, succinate and oxaloacetate using Ordinary Two-way ANOVA with Dunnett's mutiple comparison test. Reported concentration value in the statistical analysis column represents the concentration of inhibitor that produced a significantly different change compared to the respective control. Sig = significant, NS = Not significant, and NA = Not available.

Inhibitor	Lactate		Bicarbonate		Vitality
	Detection, N	Statistical analysis	Detection, N	Statistical analysis	Statistical analysis
Malonate	5	Sig, > 250 mM	2	NS	NS
Succinate	5	Sig, 500 mM ($p < 0.001$)	0	NA	Sig, 500 mM ($p = 0.008$)
Oxaloacetate	5	Sig, > 31 mM	0	NA	NS

Apart from the lactate concentration decrease being caused by an inhibition reaction, it could also be due to sperm death. The results from vitality experiments showed that there was no significant difference between sperm death due to the natural dying process and sperm death due to the inhibitor. The decision to carry out the vitality assessment was taken after analysis of the result from the MRS experiments. This is because sperm could die over incubation period, hence reduce the glucose intake as well its metabolite products such as lactate. Therefore, to investigate whether a lactate decrease, measured in the MRS experiment was due to an inhibition process or sperm death, the percentage of sperm death was calculated in the vitality experiment. Though sperm from different ejaculates (as well as sperm from the same ejaculate) might behave differently with inhibitors, to ensure the validity of the analytical approach, only samples with the similar sperm quality (motile) variance and not significantly different were used for the vitality experiments (coefficient of variance: MRS = 3.76% , Vitality = 4.73%; unpaired t-test = 0.702). Therefore, the result from the vitality experiment could represent the sperm from the MRS experiment.

Indeed, after incubation with inhibitors, particularly succinate, the sperm vitality improved. These findings fit with a previous study where succinate has been reported to be able to stimulate respiration in the boar sperm without improving sperm motility (Mann and Lutwak-Mann, 2012). Respiration is a process to generate energy, which involves either mitochondrial OXPHOS or a cytosol related pathway such as lactate fermentation and glycolysis (Piomboni *et al.*, 2012). Thus, this may suggest that, succinate, which is the substrate of Complex II of the respiratory chain (Ford and Harrison, 1981), has resulted in improvement of boar sperm energy metabolism (Stovell *et al.*, 2018). Therefore, this may indicate that lactate concentration changes were not caused by inhibitor toxicity on sperm but by the inhibition reactions.

The fact that lactate in the sperm sample (which may represent lactate fermentation) decreased after incubation with Krebs cycle inhibitors, suggests that the inhibitor may have interfered with the availability of cofactors which could have been responsible for the observed change in lactate. Thus, as hypothesised, it may indicate there might be an accumulation of Krebs cycle intermediates too. This assumption fits with the findings reported by (Peterson and Freund, 1974), where lactate decreased while citrate increased when they incubated human sperm with succinate and analysed the metabolic changes using fluorimetry. The difference between our current findings and those of Peterson may be due to a difference in the detection sensitivity. Fluorimetry enabled detection of a single photon thus making it a highly sensitive methodology (Malicka *et al.*, 2004). Therefore, fluorimetry, as well as other methodologies such as mass spectroscopy and enzyme assays, could be used in future studies to confirm the present findings.

Unsuccessful detection of intermediates by ^{13}C MRS could be due to the concentration of the intermediate being below the level of MRS detection even after a sample was subjected to inhibitors. To be detected by non-hyperpolarised MR, the lowest suggested concentration of metabolite is 0.1 µmol/g (Mishkovsky, Comment and Gruetter, 2012).

The concentration of Krebs cycle intermediates in boar sperm is unclear. However glutamate, which is the most concentrated amino acid generated from the Krebs cycle, was hardly detected by ^{13}C MRS (Henry *et al.*, 2006). Most of the glutamate detections were from cardiac (Lewandowski *et al.*, 1996) and brain (Sonnewald *et al.*, 1993; Gruetter *et al.*, 1998; Shen *et al.*, 1999) studies but none in sperm of any species (to the best of our knowledge). The fact that brain cells, for instance, consume much more substrate (120 g daily) and require a continuous supply of substrate might have an influence on this finding (Berg, Tymoczko and Stryer, 2002b). It is likely that, a higher metabolic rate could enable detection of Krebs cycle intermediates.

Although bicarbonate is the end product of the Krebs cycle, analysis of the impact of inhibitors on bicarbonate production was difficult as peak detection was not possible due to its low concentration. The reason why some samples produced detectable bicarbonate and some did not remains unanswered.

Finally, therefore, it can be concluded that inhibition reactions did take place in sperm incubated with inhibitors which resulted in a decrease of lactate concentration. However, accumulation of Krebs cycle intermediates was below the level of ^{13}C MRS detection.

Chapter 5: Effects of temperature, labelled substrate and inhibitors on boar sperm metabolism

5.1 Introduction

In the previous chapter, the experimental results suggested that the inhibitors; malonate, succinate and oxaloacetate, influenced the lactate production which likely affected Krebs cycle intermediates production as well. However, Krebs cycle intermediate concentrations changes were unable to be observed by MRS. Besides that, even though the lactate peak was always visualized in the spectra, it was tricky to analyse due to its relatively small intensity. Therefore, it was hypothesised that if the metabolism rate could be increased, it would result in more frequent metabolite peak detection and potentially allow detection of Krebs cycle intermediates, if an inhibitor was used.

The boar is an endotherm which can regulate its metabolism reactions to maintain a relatively constant body temperature (Lopez Rodriguez *et al.*, 2017) of 39°C ± 0.5 (Mark L. Lorschy, 2005). Below body temperature, at 15°C to 20°C, boar sperm become immotile. If the temperature is too low, it could result in sperm death (Lasley and Bogart, 1944). However, immotile sperm can regain their motility by re-warming them to body temperature (Aalbers, Mann and Polge, 1961).

Metabolism is a sum of a complex set of biochemical reactions and the temperature can affect the rate of these reactions. The relationship between temperature and the metabolic rate can be described using a Boltzmann or Arrhenius factor in Equation 5.1.

$$Q = e^{-E/kT} \qquad \text{Equation 5.1}$$

Where;

Q = metabolic rate,

E = activation energy for the biochemical reactions of metabolism, kJ/mol

k = Boltzmann's constant, 1.381×10^{-23} J/K

T = absolute temperature, K

Equation 5.1 describes that the metabolic rate increases exponentially with temperature. The effect of temperature on the metabolic rate was modelled by considering the minimum energy that must be available for the chemical reaction to occurred. Chemical reactions only occur if the substrate has enough energy to overcome the activation energy to form products. Temperature could contribute some energy, in form of heat energy, to the substrate to overcome the activation energy for the chemical reaction to be occurred (DeLong *et al.*, 2017).

Previous studies using boar sperm have used temperatures between 35 - 40°C (Lasley and Bogart, 1944; Monin, Lambooy and Klont, 1995; He, Bailey and Buhr, 2001). They have found that metabolism was significantly increased when the incubation temperature increased between 20°C to 37°C (Osinowo, 1981). Another study reported that boar sperm metabolism rate at 40°C was higher than that at 35°C (Monin, Lambooy and Klont, 1995). Eng at al., (1986) also emphasized the importance of conducting the experiment at the normal body temperature of the species under investigation. It would be interesting to find out the metabolism rate of boar sperm at its normal body temperature, 39°C, compared to 37°C, which was used in studies in the previous chapter.

It is known that mammalian spermatozoa meet their energy needs by switching between different metabolic pathways depending on the substrate availability (Hereng *et al.*, 2011). Glucose, pyruvate and lactate are the preferred substrates for metabolic studies in mammalian sperm (Hoshi, Tsukikawa and Sato, 1991; Mukai and Okuno, 2004) however this preference of substrate varies between species (Storey, 2008). One of the factors that determines the choice of labelled substrate is the metabolic pathway to be studied. By considering specific carbon labelling of the substrate, interesting metabolic pathways can be monitored. Even though the end product is the same for both U-^{13}C glucose and 2-^{13}C pyruvate, the labelled carbon from 2-^{13}C pyruvate will label specifically carbon position two pyruvate and its subsequent product along its the metabolism pathway (Rodrigues and Cerdán, 2005) (Figure 5.1).

In the previous chapter (Chapter 4), it was found that, there was a possibility that there was an accumulation of the Krebs cycle intermediates by incubating the sperm with inhibitors. Therefore, this chapter further investigates the effect of one of the inhibitors, succinate, on sperm 2-^{13}C pyruvate metabolism.

MRS has the ability to acquire metabolite resonance signals from a sample using the same acquisition parameters at multiple time points. This allows measurement of the rate of the labelled substrate metabolism throughout the incubation period.

In order for successful fertilization of eggs in vivo, sperm must leave the environment of the seminal plasma within minutes following ejaculation and penetrate the cervical mucus. Consequently, sperm are subjected to multiple physiological environments that influence their metabolism particularly to sustain the energy needed for motility. This includes changes in temperature and substrate availability. For example, the temperature for fallopian tube isthmus, which is the sperm storage site, is 1-2° C cooler than the fallopian tube ampula (fertilisation site) (Bahat, 2005). These changes are important in order

to prolong sperm quality for some time before fertilisation occur. Therefore, the biological purpose for this chapter is to evaluate the influence of these factors upon sperm metabolism.

This chapter aims to: (i) identify and compare the metabolism of U-^{13}C glucose and 2-^{13}C pyruvate, as the ^{13}C labelled substrates for sperm metabolism, at different incubation temperatures; (ii) measure the kinetic rate of U-^{13}C glucose and 2-^{13}C pyruvate metabolism; and (iii) examine the effect of succinate on the metabolites derived from 2-^{13}C pyruvate metabolism in boar sperm samples.

5.2 Methods

After the sperm sample (see Section 2.1) was prepared using Percoll/PBS DGC (see Section 2.2.3), the re-suspended sperm were incubated with (aim i) 60 µl of 100 mM U-^{13}C glucose or 2-^{13}C pyruvate respectively for 18 hours at 37°C or 39°C (Process (a) in Figure 5.2) before freeze-thawing and scanning by MR (see Section 2.6) (Process (b) in Figure 5.2).

For aim ii and iii, (Process (c and d) in Figure 5.2)) the re-suspended sperm had 60 µl of 100 mM U-^{13}C glucose, 60 µl of 100 mM 2-^{13}C pyruvate or 60 µl of 100 mM 2-^{13}C pyruvate with 500 mM of succinate added respectively (selected concentration was based on the experiments from Chapter 4), and was scanned continuously in the scanner (see Section 2.6) at 39°C over 18 hours where each scan took 3 hours.

For each sample, an aliquot from the re-suspended sperm was pipetted for sperm quality assessment (see Section 2.5). The summary of the sample number was illustrated in Figure 5.3.

5.3 Data analysis

5.3.1 U-^{13}C glucose and 2-^{13}C pyruvate metabolism in the sperm sample at 37°C and 39°C (aim i)

The 2-^{13}C lactate peak from U-^{13}C glucose metabolism was obscured by the intense neighbouring peaks of the ^{13}C glucose at 71.2 ppm so only half of the quartet peak from 2-^{13}C lactate was integrated. To obtain its full concentration, the integrated value was multiplied by two. This is based on the assumption that the full concentration was divided into quartet peaks. 3-^{13}C lactate from U-^{13}C glucose was integrated as well. Comparison was then made between 2-^{13}C, and 3-^{13}C lactate from U-^{13}C glucose and 2-^{13}C lactate from 2-^{13}C pyruvate using one-way ANOVA with Tukey's test. Same statistical test was used for ^{13}C bicarbonate from U-^{13}C glucose and 2-^{13}C pyruvate. In all of these, metabolites integral were normalised to the relative sperm concentration.

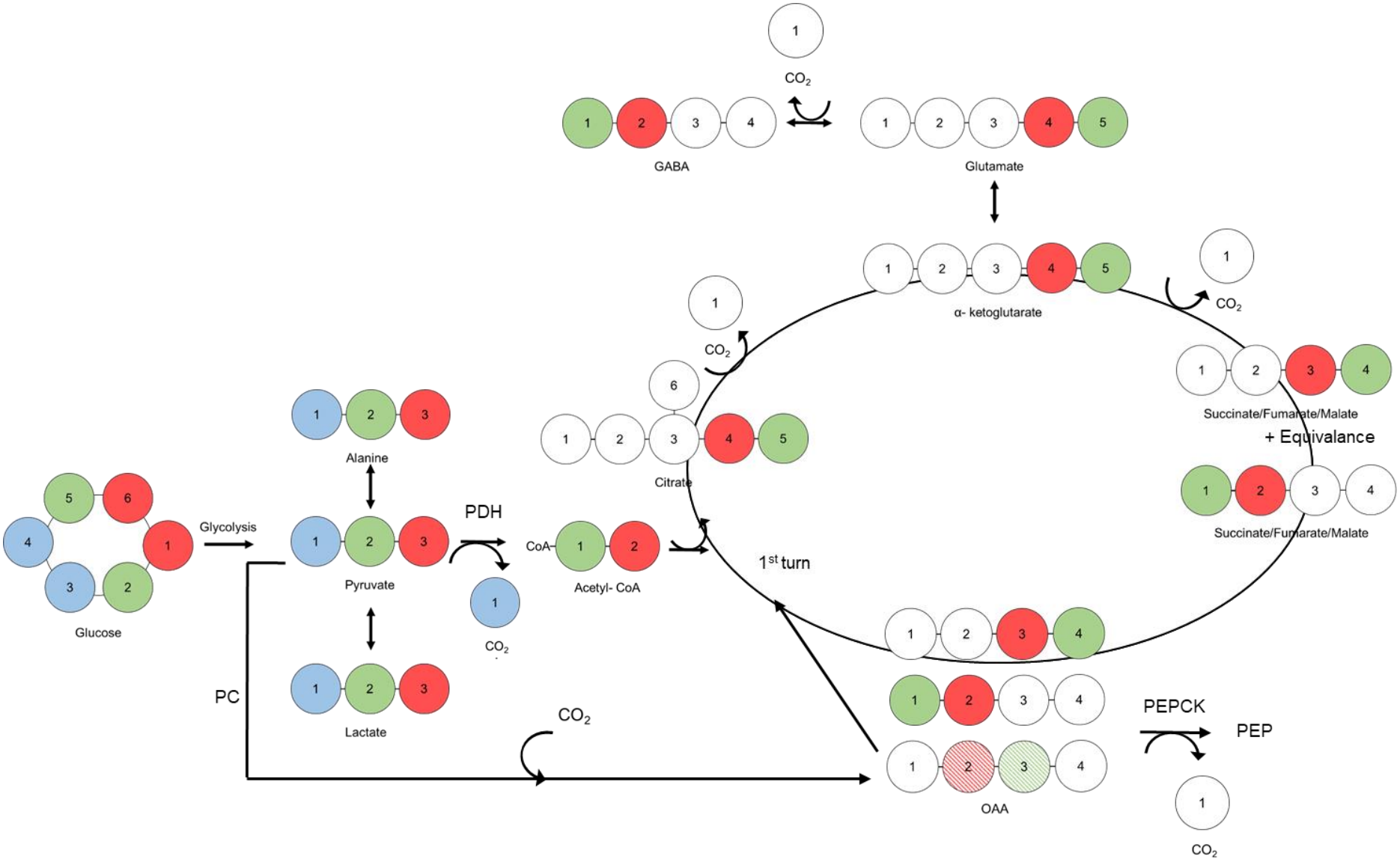
GABA
Glutamate
α- ketoglutarate
Succinate/Fumarate/Malate
+ Equivalance
Succinate/Fumarate/Malate
Citrate
Alanine
Glucose
Glycolysis
Pyruvate
PDH
Acetyl- CoA
CoA
1st turn
PC
Lactate
OAA
PEPCK
PEP

Figure 5.1: Through glycolysis, U-^{13}Cglucose generates 1, 2 and 3-^{13}C pyruvate. Pyruvate can then be metabolised either through LDH, PDH, PC or transamination. Through transamination, it is converted to 1, 2, and 3-^{13}C alanine. Through LDH, 1, 2 and 3-^{13}C pyruvate yields 1, 2 and 3-^{13}C lactate (Rodrigues *et al.*, 2013). Through PDH, 1-^{13}C atom of pyruvate was released as ^{13}C bicarbonate while 2, 3-^{13}C pyruvate is transported into the mitochondria for oxidative metabolism as 1, 2-^{13}C Acetyl CoA for the Krebs cycle. 1, 2-^{13}C acetyl-CoA, then combine with an unlabelled molecule of oxaloacetate to generate citrate labelled at the C4 and C5 position (Henry *et al.*, 2006). Subsequently, α-ketoglutarate becomes labelled at the C4 and C5 position (Rodrigues and Cerdán, 2005). The glutamate then becomes labelled at the C4 and C5 position through transamination of 4, 5-^{13}C α-ketoglutarate (Rodrigues and Cerdán, 2005). ^{13}C-label then continues on to label 4, 5-^{13}C glutamine and 1, 2-^{13}C GABA with the release of unlabelled bicarbonate. At the same time, ^{13}C label continues to flow into the TCA cycle, labelling succinate, fumarate and malate at C4 and C5 or C1 and C2 (since succinate is a symmetric molecule, the C1 and C2 positions of succinate cannot be distinguished and become labelled with equal probability). The first turn of the TCA cycle is completed when oxaloacetate becomes labelled at the C3 and C4 or C1 and C2 positions. Labelled oxaloacetate can combine again with the labelled acetyl-CoA and labels all the carbon positions of citrate, or 1,2,3 and 4 citrate if combined with unlabelled acetyl-CoA, and subsequent labelled decarboxylation at level isocitrate dehydrogenase and α-ketoglutarate dehydrogenase (Chance *et al.*, 1983). If the 2-^{13}C pyruvate enters the mitochondria through PC, 2, 3-^{13}C oxaloacetate will be labelled, then continuing the labelling on 1, 2-^{13}C α-ketoglutarate (or incorporated into PEP while releasing CO_2). Subsequently, 1-^{13}C and 4-^{13}C succinate, fumarate, malate and oxaloacetate are produced (Rodrigues and Cerdán, 2005).

5.3.2 Rates of the U-^{13}C glucose, and 2-^{13}C pyruvate metabolism (aim ii)

A single experiment from each ejaculate included six spectra which were sequentially acquired every 3 hours over 18 hours. Each peak from each spectrum was integrated and collated into a set of peak integral time courses. Integral versus time for each detected peak was plotted and fitted using non-linear exponential regression. Only experiments that had $R^2 > 0.5$ were retained in order to avoid misinterpretation. The mean ± standard error (SE) was determined for each peak from U-^{13}C glucose and 2-^{13}C pyruvate. Differences between metabolic rates were analysed using one-way ANOVA with Tukey's test.

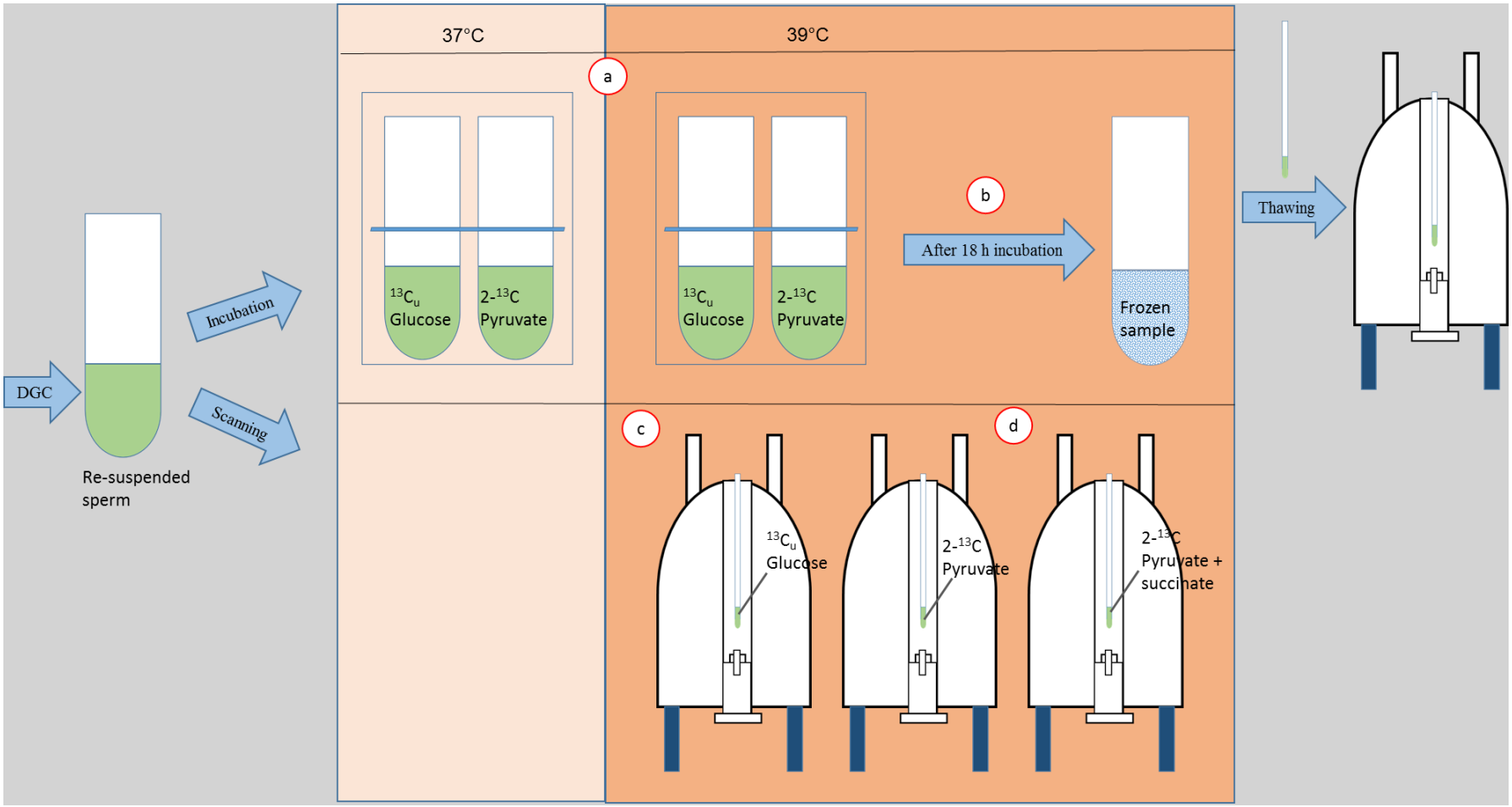

Figure 5.2: Overview of the MRS sample preparation.

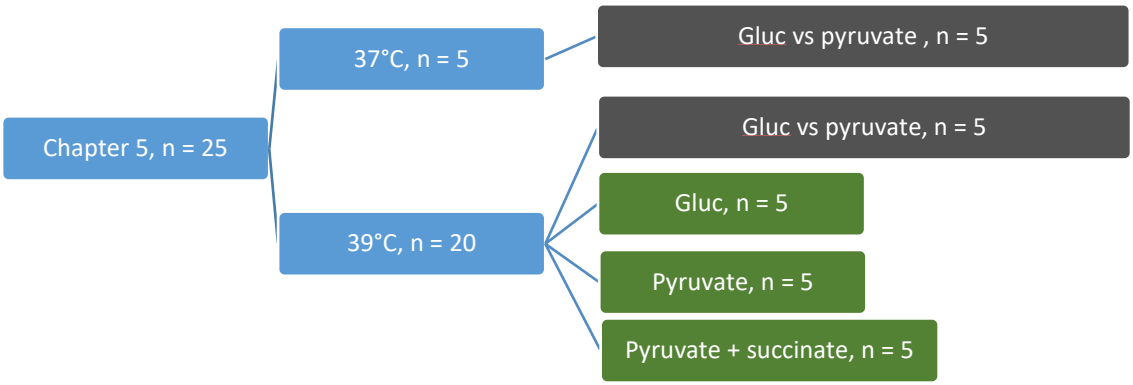

Figure 5.3: Summary of the sample usage. Gluc = U-^{13}C glucose, Pyruvate = 2-^{13}C pyruvate.

5.3.3 Effect of succinate on the metabolite products detected from 2-^{13}C pyruvate metabolism (aim iii)

For this aim, the spectrum acquired at 18 hours was selected. Each metabolite product peak that was detected from the 2-^{13}C pyruvate metabolism was integrated. The same integration range was then used as for the spectra of 2-^{13}C pyruvate with succinate. All metabolite integrals were normalised to the respective sperm concentration. The comparison was performed using an unpaired t-test with Welch's correction. For comparison between two groups, which have the same sample size and standard deviation, a T-test is performed by Prism. But in this chapter, the standard deviations between groups were different. Therefore, the Welch test was chosen. It yields a different t ratio compared to an ordinary T-test because it adjusts the P value to control for Type 1 errors (Lee, 2018).

5.4 Results

5.4.1 U-^{13}C glucose and 2-^{13}C pyruvate metabolism in the sperm samples at 37°C and 39°C

At both the 37°C and 39°C incubation temperatures, lactate and bicarbonate were detected in the spectra. At 37°C, only 3-^{13}C lactate (C3) was detected following incubation with U-^{13}C glucose but at 39°C, all lactate carbons, (C1, C2, and C3), were detected. For 2-^{13}C pyruvate, lactate was detected in all samples regardless of the temperature (Table 5.1) and the 2-^{13}C lactate integral was significantly increased when the incubation temperature was 39°C compared to 37°C. The 2-^{13}C lactate integral from 2-^{13}C pyruvate metabolism was statistically higher than 2-^{13}C lactate from U-^{13}C glucose at both 37°C and 39°C (Figure 5.4 (a)). The same result was found when a comparison was made between 2-^{13}C lactate from pyruvate and 3-^{13}C lactate from the U-^{13}C glucose (Figure 5.4 (b)). Bicarbonate was always detected in the spectra when the sperm samples were incubated with 2-^{13}C pyruvate at 37°C and 39°C, and U-^{13}C glucose at 39°C only. The bicarbonate integral from 2-^{13}C pyruvate was statistically higher at 39°C than 37°C (Figure 5.4 (c)).

5.4.2 Rates of the U-^{13}C glucose and 2-^{13}C pyruvate metabolism

Sequentially acquired spectra showed a rise and decline in metabolite products and substrates respectively. For U-^{13}C glucose, detected metabolite products were lactate and bicarbonate. The 3-^{13}C lactate peak was first detected in the spectrum acquired at the 9 h time point, where the magnitude of the 3-^{13}C lactate peak was > 2 fold greater than 1-^{13}C lactate. 2-^{13}C lactate was visualised, however it was quite difficult to quantify as the peak for the ^{13}-C glucose obscured the 2-^{13}C lactate (Figure 5.5). The lactate peak then rapidly built up but then slowed down after reaching 15 h scanning time. The bicarbonate peak was first visualised in the spectrum acquired at 15 h and slowly increased up to 18 h.

For 2-^{13}C pyruvate, both lactate and bicarbonate were first seen in the first scan at 3 h (first spectrum) where the magnitude of the lactate peak was about the same size as the 3-^{13}C lactate from U-^{13}C glucose at 15 h scanning. Both lactate and bicarbonate peaks slowly increased and reached maximum concentration at 15 h and 18 h respectively. Apart from 2-^{13}C lactate and bicarbonate, there was visualisation of natural abundance 1-^{13}C lactate in the 2-^{13}C pyruvate metabolism spectra (Figure 5.6).

For 2-^{13}C pyruvate with 500 mM of succinate, no metabolite products were detected in any of the spectra (Figure 5.7).

The rates of lactate and the bicarbonate formation are listed in Table 5.2. From a statistical comparison between 1-^{13}C lactate, 2-^{13}C lactate and 3-^{13}C lactate from U-^{13}C glucose metabolism, there was no statistical difference between those rates, therefore only 3-^{13}C lactate was chosen for subsequent rate comparisons. There were no significant difference between 3-^{13}C and 2-^{13}C lactate rate ($p = 0.801$) for U-^{13}C glucose and 2-^{13}C pyruvate. The same result was observed for bicarbonate rate ($p = 0.548$). However the rate of lactate and bicarbonate conversion from 2-^{13}C pyruvate (lactate = 0.19 ± 0.01 s^{-1}, bicarbonate = 0.39 ± 0.10 s^{-1}) was faster than U-^{13}C glucose (lactate = 0.05 ± 0.03; s^{-1}, bicarbonate = 0.21 ± 0.12 s^{-1}).

5.4.3 The effect of succinate on the metabolite products detected from 2-^{13}C pyruvate metabolism

Lactate and bicarbonate were detected from 2-^{13}C pyruvate metabolite rate measurement spectra but not after succinate was added to 2-^{13}C pyruvate. The presence of succinate significantly affected conversion of pyruvate into lactate ($p < 0.001$) and bicarbonate ($p = 0.004$) (Figure 5.8). The detected peaks in the spectra were 1, 2 and 3-^{13}C succinate and 2-^{13}C pyruvate.

5.5 Discussion

In this chapter, U-^{13}C glucose and 2-^{13}C pyruvate metabolism by boar sperm incubated at 37°C and 39°C were compared. Their conversion rate at 39°C as well as the effect of succinate on the 2-^{13}C pyruvate metabolism was also studied. The result showed that 2-^{13}C pyruvate generated higher lactate and bicarbonate concentrations which were consistently detected especially when the sperm was incubated at 39°C. Moreover, both lactate and bicarbonate were not visualised in the 2-^{13}C pyruvate metabolism spectra after succinate had been added.

Table 5.1: Number of visually detected metabolites peaks in the spectra when the sperm was incubated at 37°C and 39°C with U-^{13}C glucose and 2-^{13}C pyruvate.

Temperature	Substrate	Lactate, N	Bicarbonate, N
37°C	U-^{13}C glucose	3 (C3)	1
	2-^{13}C pyruvate	5 (C2)	5
39°C	U-^{13}C glucose	3 (C1), 3(C2), 5(C3)	5
	2-^{13}C pyruvate	5 (C2)	5

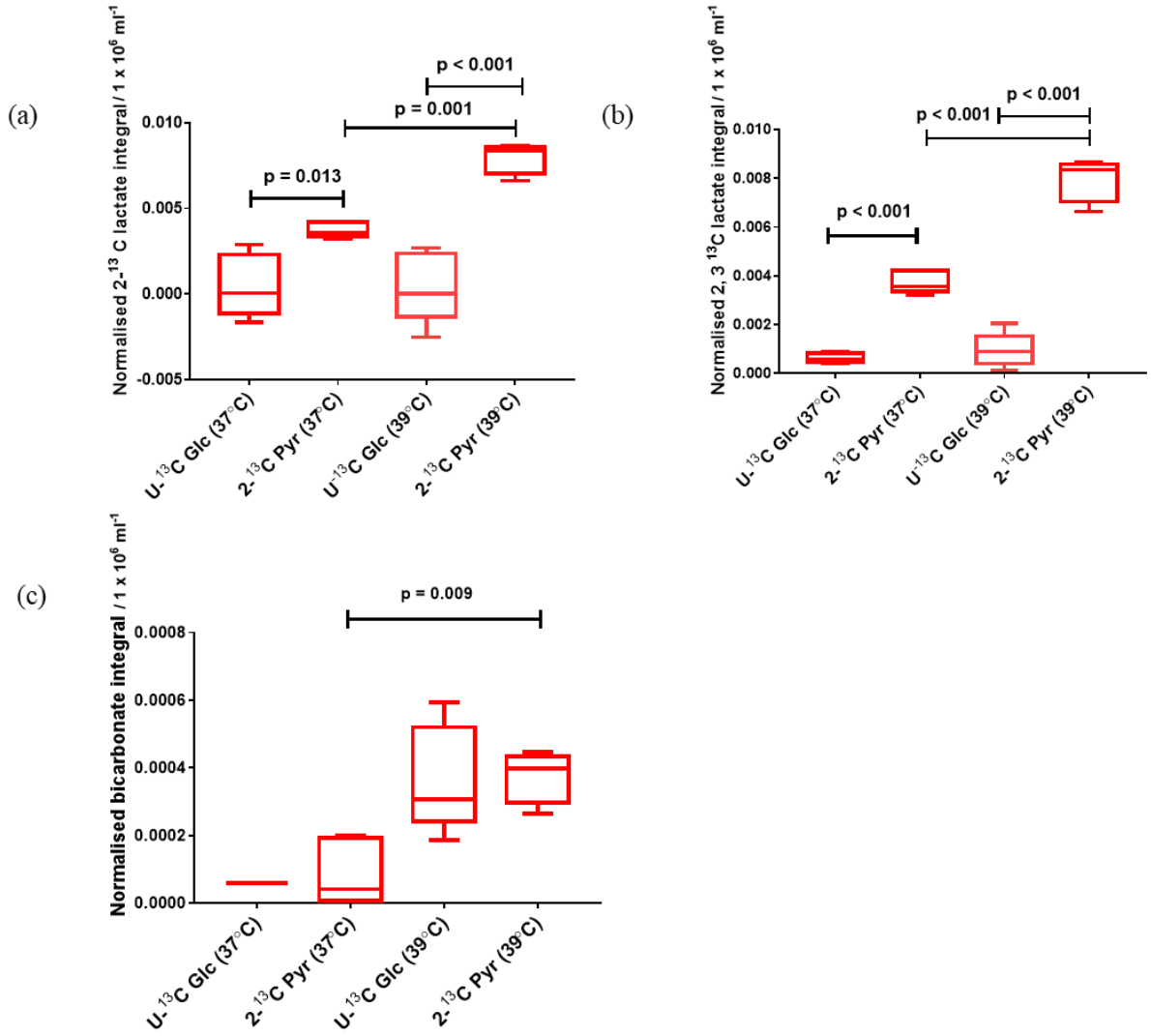

Figure 5.4: Graphs of normalised (by sperm concentration) integrals for (a) 2-^{13}C lactate, (b) 2-^{13}C lactate (from pyruvate) and 3-^{13}C lactate (from glucose) and (c) bicarbonate, from U-^{13}C glucose (Glc) and 2-^{13}C pyruvate (Pyr) respectively. p = p value.

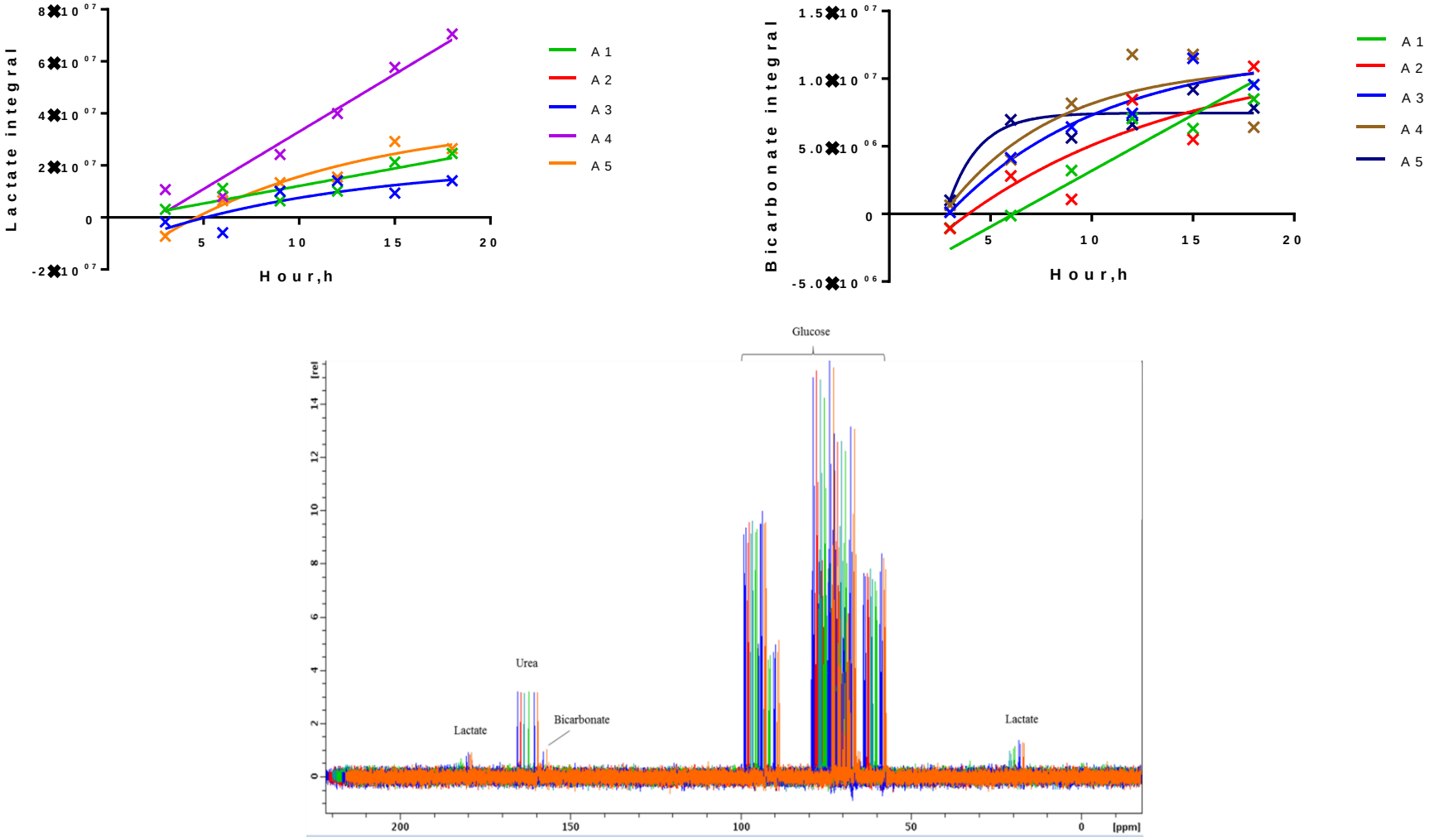

Figure 5.5: (Bottom) Six U-^{13}C glucose rate spectra which were sequentially acquired every 3 hours over 18 hours. Each spectrum is shift in the chemical shift axis to aide visualisation; with the left most spectrum (dark blue) the 1st acquired spectrum, followed by red, dark green, light green, light blue and orange. ^{13}C-urea was added as a chemical shift reference peak. Integrated detected peak: 2-^{13}C lactate (Left, upper); and bicarbonate (Right, upper) were plotted versus time and fitted using non-linear exponential regression ($R^2 > 0.5$). A1-A5 is the number of the boar sperm sample.

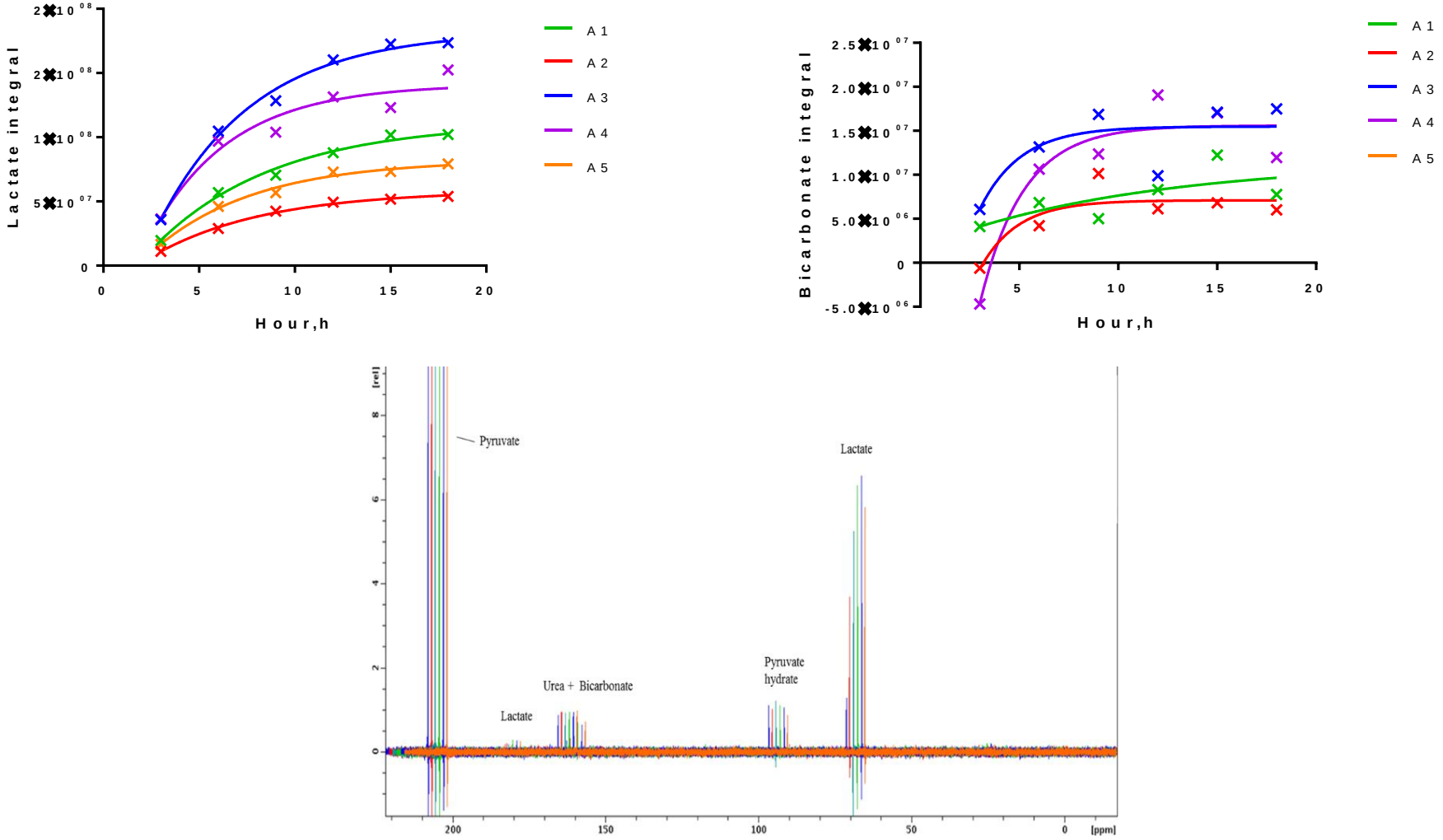

Figure 5.6: (Bottom) Six 2-^{13}C pyruvate rate spectra which were sequentially acquired every 3 hours over 18 hours. Each spectrum is shift in the chemical shift access and zoom in (top of pyruvate peak was purposely cut off) to aide visualisation. Dark blue is the 1st acquired spectrum, followed by red, dark green, light green, light blue and orange. Urea was added to provide a chemical shift reference peak. Integrated detected peak: lactate (Left, upper); and bicarbonate (Right, upper) were plotted versus time and fitted using non-linear exponential regression ($R^2 > 0.5$). A1-A5 is the number of the boar sperm sample.

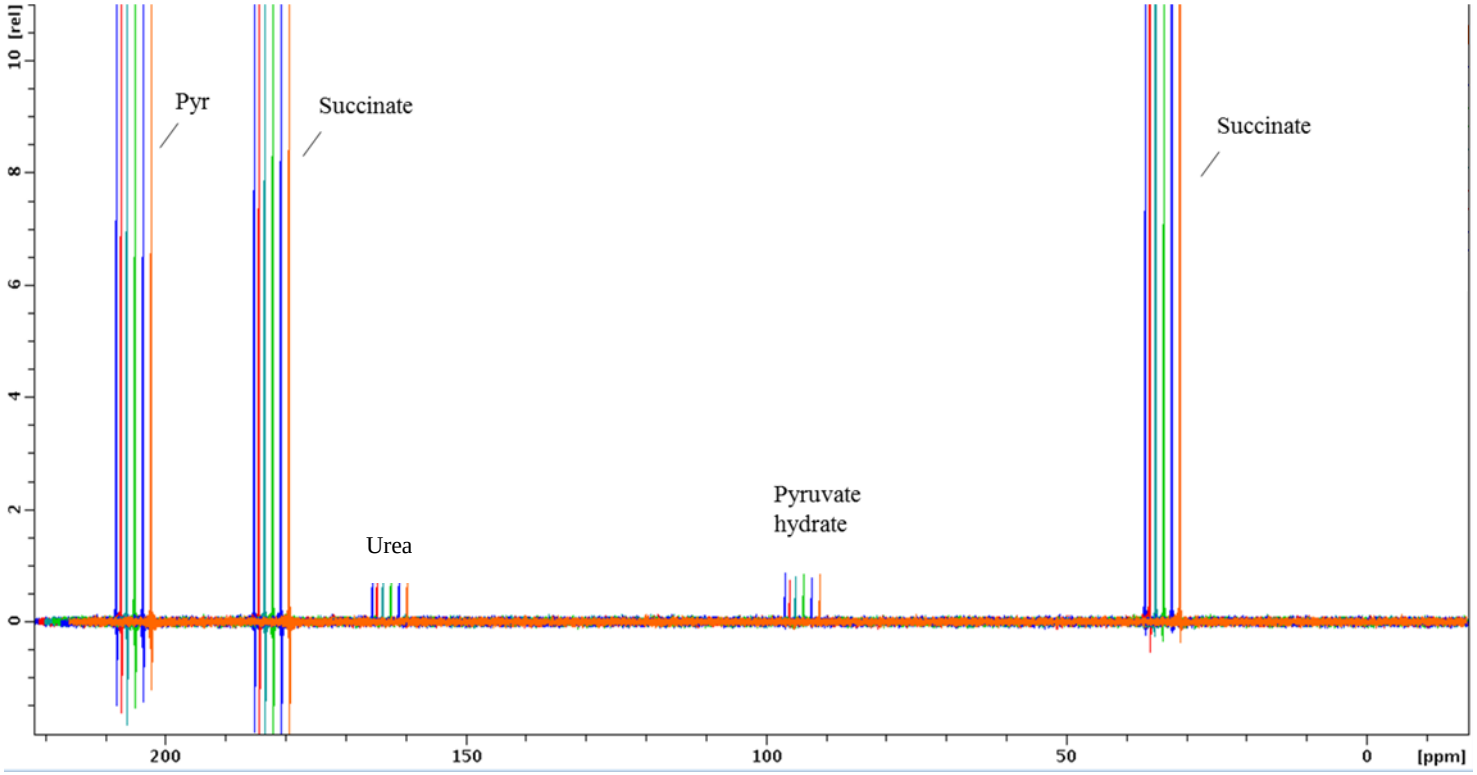

Figure 5.7: Six 2-^{13}C pyruvate with succinate rate spectra which were sequentially acquired every 3 hours over 18 hours. Each spectrum is shift in the chemical shift access and zoom in (top of pyruvate and succinate peaks were purposely cut off) to aide visualisation Dark blue is the 1st acquired spectrum, followed by red, dark green, light green, light blue and orange. Urea was added to provide a chemical shift reference peak.

Table 5.2: Mean rate of metabolite production from U-^{13}C glucose and 2-^{13}C pyruvate metabolism (N = 10).

Metabolite substrate	Metabolite product	Mean rate ± SEM, s^{-1}	No of spectra in where R^2 > 0.5.
U-^{13}C glucose	1-^{13}C lactate	0.03±0.05	3
	2-^{13}C lactate	0.02±0.01	2
	3-^{13}C lactate	0.05±0.03	4
	^{13}C bicarbonate	0.21±0.12	5
2-^{13}C pyruvate	2-^{13}C lactate	0.19±0.01	5
	^{13}C bicarbonate	0.39±0.10	4

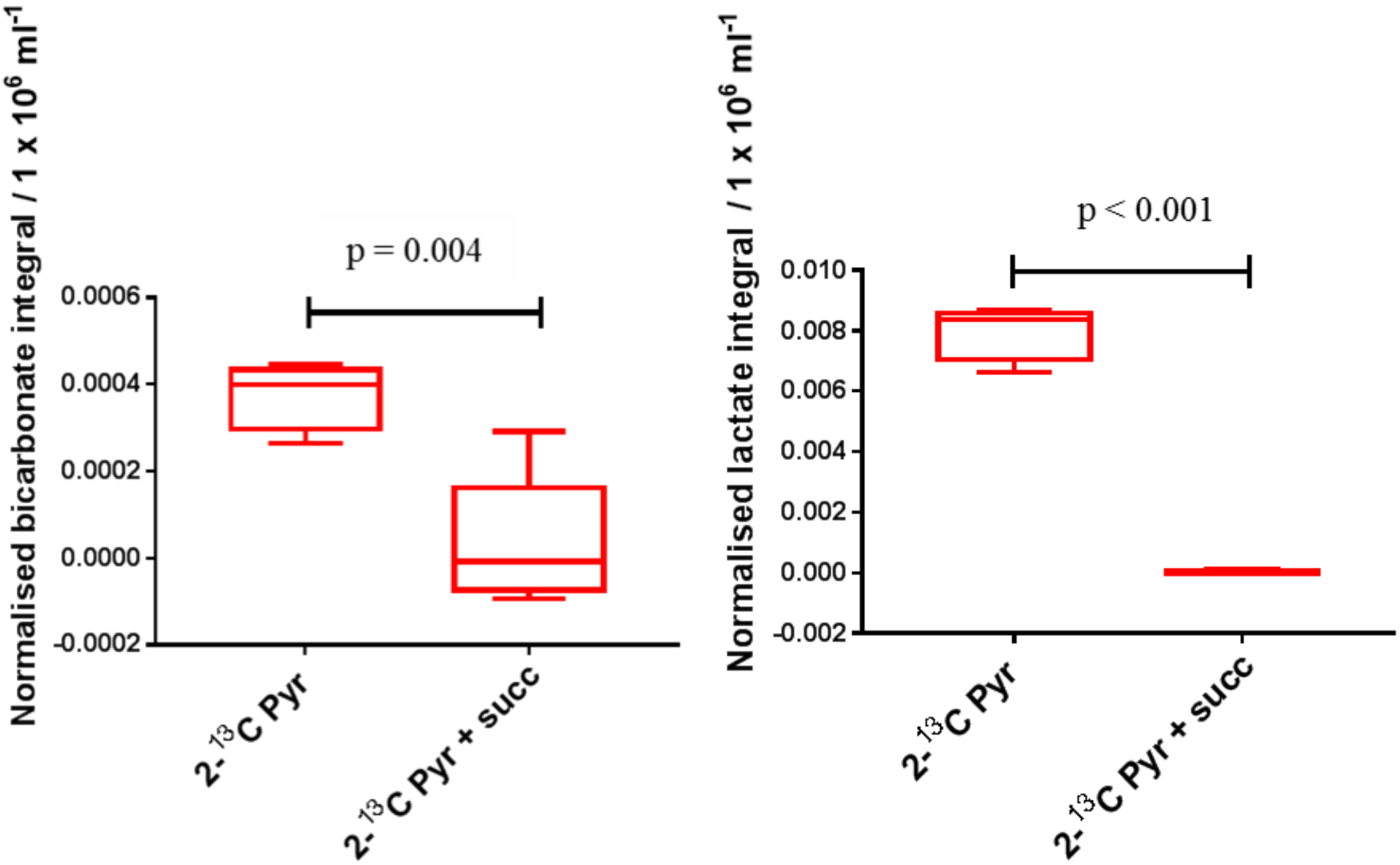

Figure 5.8: (Left) Bicarbonate integral for 2-^{13}C pyruvate and 2-^{13}C pyruvate with succinate (succ). (Right) lactate integral for 2-^{13}C pyruvate and 2-^{13}C pyruvate with succinate (succ). p = p value. Bicarbonate and lactate integral were normalised to sperm concentration.

A previous study by Eng *et al* (1986) found that at 39°C, the rate of pig polar body formation during oocytes development was better than at 37°C. Even though they focused on oocyte development, it is known that oocyte development requires higher energy compared to the immature oocyte stage (Babayev and Seli, 2015). Their finding is interesting for the experiments outlined in this chapter which found that at 39°C, sperm metabolism was increased markedly. More lactate and particularly bicarbonate were derived from both U-^{13}C glucose and 2-^{13}C pyruvate. As expected, higher temperature results in a higher metabolic rate. This happens when the energy, which is produced from the collision of molecules, is converted into chemical potential energy of the molecules. That chemical potential energy was provided to the substrate and may cause it to change its chemical state. Consequently more chemical reaction will occur (Cooper, 2000). Furthermore, high temperature increases the probability of collision and binding between enzyme and substrate, thus greater substrate will be converted into product (Wharton, 2007). Although Shelby and Foley (1971) reported that lactate concentration accumulated more at 38°C rather than 39°C, the difference between current findings and Shelby and Foley (1971) may be due to a difference in the incubation period (6 hours incubation for Shelby and Foley study and 18 hours incubation for this study). This suggests that the combination of incubation time and temperature may influence lactate production.

2-^{13}C pyruvate was chosen rather than U-^{13}C glucose in the subsequent experiment with succinate for two reasons. Firstly, it was found that lactate and bicarbonate were consistently detected in the spectra and their concentrations were significantly higher than those from U-^{13}C glucose regardless of the incubation temperature. This was also supported by the results from the rate experiments (aim ii) where the conversion of 2-^{13}C pyruvate into 2-^{13}C lactate and ^{13}C bicarbonate was faster than with U-^{13}C glucose. This is to be expected as the production of lactate from glycolysis involves 11 reactions compared to a single reaction for pyruvate. Secondly, despite achieving increased U-^{13}C glucose and 2-^{13}C pyruvate metabolism rates by sperm, Krebs cycle intermediates were still not detected by MRS. However, consistent detection of bicarbonate from 2-^{13}C pyruvate might be from the Krebs cycle. For U-^{13}C glucose, bicarbonate may emerge from several different metabolism pathways, such as PDH, PC, or a forward turn of the Krebs cycle after PC (Comment and Merritt, 2014). However, for 2-^{13}C pyruvate, C2 pyruvate is transported into the Krebs cycle by incorporation into Acetyl CoA. Thus, any detected metabolite from 2-^{13}C pyruvate is most likely from Krebs cycle processes. Clark *et al* (1994) reported the detection of lactate, alanine, glutamate and acetate when they used 2-^{13}C pyruvate in glial cells. Citrate is one of the intermediates of the Krebs cycle while glutamate is a flux through exchange reactions with α-ketoglutarate, which is an intermediate of the Krebs cycle (Henry *et al.*, 2006). Therefore, 2-^{13}C pyruvate is a more useful substrate in determining the origin of bicarbonate under the influence of succinate than U-^{13}C glucose.

The experiments conducted in aim iii shown that both bicarbonate and lactate, which were always detected from the 2-^{13}C pyruvate metabolism in the sperm samples without addition of succinate, were not visualised in the spectra during the 18 h incubation time with succinate. This may suggest that detected bicarbonate in the control sample (without succinate) may have emerged from a subsequent turn of the Krebs cycle from 4-^{13}C isocitrate, 1-^{13}C α-ketoglutarate, or 1- ^{13}C glutamate (Chance *et al.*, 1983). As shown in Figure 5.1, in the first turn of 2-^{13}C pyruvate metabolism, bicarbonate is not labelled, however, due to rapid exchange with a symmetric molecule of succinate, fumarate and malate respectively, a labelled bicarbonate molecule will be produced in a further turn of the Krebs cycle. Most probably, production of the bicarbonate did not occur due to the fact that succinate blocked the reaction between α-ketoglutarate to succinate, resulting in obstruction of bicarbonate production in the further turn.

In the normal equilibrium state, the carbon 2 atom from pyruvate incorporates into acetyl-CoA which then enters the Krebs cycle. However, an excessive concentration of acetyl-CoA may incorporate in other pathways. As the pyruvate concentration was much higher than physiological levels, the excess acetyl-CoA produced may have changed the equilibrium state and led to incorporation into other pathways (Cruz *et al.*, 2001; Park *et al.*, 2013). Possible metabolic pathways include: (i) conversion into ketone bodies, (ii) lipogenesis, and (iii) synthesis of cholesterol and other steroids (Hu *et al.*, 2012). Typically, most of the detected metabolites, for instance 1,3-^{13}C acetoacetate which represent ketone bodies, and 1-^{13}C acetylcarnitine which represent lipogenesis (Schroeder *et al.*, 2009; Hu *et al.*, 2012), were detected when MRS was used in conjunction with the highly sensitive methodology, which is DNP, along with an excessive amount of hyperpolarised 2-^{13}C pyruvate or inhibitor. Therefore, the next chapter will utilise DNP in order to confirm this finding.

Though the exact relationship between α-ketoglutarate inhibition and lactate production by pyruvate is unclear, the result showed that, apart from resulting in the decrease of the bicarbonate concentration, α-ketoglutarate also decreased the lactate concentration. This might suggest that the effect of the α-ketoglutarate inhibition influenced the conversion of pyruvate to lactate. For example, Corbet at al., (2018) reported that inhibiting the transport of pyruvate into the mitochondria can block lactate metabolism in cancer cells and also reduces oxygen consumption rate.

In summary, the incubation of boar sperm samples at 39°C with 2-^{13}C pyruvate was shown to be superior to the U-^{13}C glucose in increasing the conversion rate into lactate and bicarbonate as well as increasing their concentrations. Succinate utilisation with 2-^{13}C pyruvate was unable to increase the Krebs cycle intermediates to a level detectable by MRS. However, disappearance of the lactate and bicarbonate signal from 2-^{13}C pyruvate metabolism after addition of succinate suggests that bicarbonate was indeed produced in the Krebs cycle and there is a link between the Krebs cycle and lactate production.

Chapter 6: Sperm metabolism measured using hyperpolarised 2-^{13}C pyruvate

6.1 Introduction

In the previous chapter, bicarbonate detection from 2-^{13}C pyruvate was assumed to be the result of reactions from the Krebs cycle. This assumption was confirmed when the bicarbonate peak disappeared completely after introducing succinate into the boar sperm sample. As the lactate peak also disappeared, it may indicate, there is a relationship between the Krebs cycle and lactate production. Therefore, this chapter is intended to further confirm this observation by using a higher MR detection sensitivity methodology, known as Dynamic Nuclear Polarisation (DNP).

As explained in Chapter 1, in the presence of an external magnetic field, two energy populations will be created among nuclei. The energy difference between these two populations (known as polarisation) determines the MR signal intensity (Schroeder *et al.*, 2012). At body temperatures and routine external magnetic field strength found in research and clinical practice, the difference in these populations is very low (Hurd *et al.*, 2012). A potential strategy to overcome this drawback is by using a hyperpolarisation technique. This technique increases MR signal intensity by increasing spin polarisation. It temporarily aligns more of the nuclei in the lower energy state, which results in a bigger difference in populations, and stronger MR signal (Rodrigues *et al.*, 2013).

DNP operates on the principle of the Nuclear Overhauser Effect which was proposed by Overhauser (Overhauser, 1953). He suggested the transfer of spin polarisation from electron spins to nuclear spins by microwave irradiation of the electron spins. The idea was extended by Beljers (1954) and Griesinger *et al*. (2012) in which the polarisation was transferred from free radicals to solvent molecules. The potential use of DNP in metabolomics studies became clear after Ardenkjaer-Larsen *et al*. (2003) demonstrated that a hyperpolarised sample in the solid state can be rapidly dissolved into a liquid solution while preserving its nuclear polarisation. It has been shown that, dissolution-DNP method could enhance ^{13}C nuclear polarisation to almost 50% (Hurd *et al.*, 2012) with a SNR > 10, 000 times compared to conventional MRS in the solution state (Marjańska *et al.*, 2010).

Dissolution-DNP transfers hyperpolarised electron polarisation to nuclear spins of a ^{13}C- labelled molecule by microwave irradiation (Comment and Merritt, 2014). This is achieved by adding unpaired electrons (typically from an organic radical agent) into the proximity of the ^{13}C molecules. The choice of radical agent depends on several factors: (i) it should be chemically stable and dissolve quickly in the ^{13}C molecule solution, and (ii) the electron paramagnetic resonance (EPR) spectrum of the radical should possess a width that allows DNP to be effective for the nucleus of interest (Hurd *et al.*, 2012). Based on those factors, typical radical agents utilized in DNP are nitroxide and trityl (Marco-Rius,

2014). For ^{13}C, trityl is superior to nitroxides in term of line width. The line width for trityl radicals is 0.80% of the resonance frequency. It is a suitable match with ^{13}C, which has 0.37% of the resonance frequency (Hurd *et al.*, 2012). As a consequence, this increases the probability of polarisation transfer to ^{13}C spins hence producing a larger maximal ^{13}C polarisation (Weissleder, 2010).

The radical agent molecule has a tendency to crystallize as a saturated aqueous solution. This prevents the radical agent from forming a homogeneous distribution around the ^{13}C molecules and results in poor polarisation efficiency. To ensure that ^{13}C molecules stay amorphous when frozen, a solvent such as dimethylsulfoxide (DMSO) is added into the mixture of ^{13}C molecules and radical agent (Marco-Rius, 2014).

The polarisation process begins by freezing the mixture at very low temperature in a high magnetic field. The final temperature, which is ~ 1 K, is achieved using liquid helium and vacuum pumping the mixture to very low pressure (~ 1 mbar) (Schroeder *et al.*, 2012). At 1 K and high magnetic field, for instance 5 T, electron spin polarisation can reach almost 100% (in which all electrons align in the antiparallel direction to the external magnetic field) compared to 77 K (liquid nitrogen temperature) where the polarisation is ~ 4% (Comment and Merritt, 2014). The electron spin polarisation can be increased more by lowering the temperature and increasing the magnetic field, however, the time to build up the electron polarisation could become very long. To transfer polarisation from the electrons to the ^{13}C molecule molecules, microwave irradiation at a frequency determined by the properties of the ^{13}C molecule, the radical and the magnetic field strength, is then applied (Maly *et al.*, 2008). This procedure commonly takes between 30 minutes to a few hours for ^{13}C molecules which result in a ^{13}C polarisation of up to 50% (Schroeder *et al.*, 2012). By increasing the power for microwave irradiation, polarisation build up time (for the certain radical agent (Smith *et al.*, 2012)) could be reduced, but this would generate excessive heating to the mixture and might actually result in a decrease in polarisation efficiency (Comment and Merritt, 2014).

To make the polarised solid ^{13}C molecule useful for in vivo experiments, it needs to be dissolved in a suitable buffer which will increase its temperature from 1 K to a physiological temperature. This is achieved by rapidly dissolving the solid sample with a superheated and pressurised bolus of aqueous solvent. Depending on the ^{13}C molecule, the solution may need to be neutralised in order to maintain pH within the physiologic range of 6.8 to 8.1 (Comment and Merritt, 2014). The polarisation is preserved almost completely in the dissolution step. The polarisation produced then steadily decays back to the normal thermal equilibrium level at a rate dependent on the relaxation properties of the molecule under study (typically 1 – 2 min) (Chen *et al.*, 2009). Thus, to preserve the nuclear polarisation, the polarised agent to be transferred rapidly into the sample under study, followed by efficient and rapid ^{13}C spectroscopic imaging sequences.

The polarisation, irradiation and dissolution process requires hardware known as a hyperpolariser. Thus, the location of the hyperpolariser with respect to the MR system is of importance. It should be located close to the MR scanner. Its main components are: (i) a superconducting magnet, to provide the external magnetic field, (ii) a helium cryostat which is connected to vacuum pumps in order to cool the mixture sample to ~ 1 K, and (iii) a microwave source to allow the polarisation transfer from electron spins to the nuclear spins and a dissolution system (Comment and Merritt, 2014).

Commonly, dissolution DNP for ^{13}C MR studies has used ^{13}C pyruvate as the labelled substrate because it polarises efficiently, has a relatively long decay (time constants of signal decay are approximately 45 s) and speed of uptake (Comment and Merritt, 2014). ^{13}C studies have been conducted on the cardiac system, brain, prostate, breast and cancer cells, following infusion of hyperpolarised 1-^{13}C pyruvate. These have shown that pyruvate catabolism and its products can be measured effectively. In sperm, only one study has been reported which was conducted by Reynolds *et al*. (2017) to investigate the relationship between sperm energy metabolism and motility. However, pyruvate labelled at the C1 position does not allow investigation of the Krebs cycle involvement for detected bicarbonate as discussed in the previous chapter. This is due to the labelled C1 nucleus being transferred to bicarbonate/CO_2 following the PDH reaction, and hence does not incorporate into Krebs cycle intermediates.

By using 2-^{13}C pyruvate, incorporation of the enriched pyruvate C2 into the Krebs cycle can be monitored. It has been shown that hyperpolarised 2-^{13}C pyruvate can be used to assess Krebs cycle metabolism (Schroeder *et al.*, 2009; Marjańska *et al.*, 2010; Josan *et al.*, 2014). Some of the related metabolites which were detected from 2-^{13}C pyruvate metabolism include 1-^{13}C citrate in the first turn of the Krebs cycle, 5-^{13}C glutamate, which is in exchange with the Krebs cycle intermediate α-ketoglutarate, 1-^{13}C acetylcarnitine generated from acetyl-CoA via carnitine acetyltransferase and 1,3-^{13}C acetoacetate, which is a ketone body produced from two molecules of acetyl-CoA (Josan *et al.*, 2014). As this chapter is intended to confirm the assumption from the previous chapter, which involved reactions in the Krebs cycle, 2-^{13}C pyruvate seemed a more suitable candidate compared to other substrates, particularly 1-^{13}C pyruvate.

Therefore, the biological purpose of this chapter is to determine the source of the detected bicarbonate, focusing on rapid changes of pyruvate metabolism through the Krebs cycle. Thus, not only can the relationship with sperm motility be investigated but information concerning the kinetics of 2-^{13}C pyruvate could be studied. The aim in this chapter was to acquire hyperpolarised 2-^{13}C pyruvate metabolism in boar sperm using dissolution-DNP.

6.2 Methods

6.2.1 Sperm preparation

The sperm sample (see Section 2.1) was prepared using Percoll/PBS DGC (see Section 2.2.3), after which the supernatant was aspirated and the sperm pellet was re-suspended in ~ 400 - 600 ml of PBS. An aliquot from the re-suspended sperm sample was then prepared for concentration and motility assays (see Section 2.5.1 and 2.5.2) in which concentration of the re-suspended sperm was adjusted using PBS and a haemocytometer so that the final sperm concentration was < 100 x 10^6/ml. Once the desired sperm concentration was achieved, 400 µl of the re-suspended sperm was added to a NMR tube with 10 µl D_2O for immediate MR scanning (if needed, the sperm sample was kept at the specified temperature (37°C or 39°C) before being scanned in the MRS system) (Figure 6.1 (a)).

6.2.2 Hyperpolarisation

For hyperpolarisation experiments, a mixture consisting of ~ 2.5 – 5 mg of 2-^{13}C labelled pyruvate acid, 15 mM OXO63 (Oxford Instruments, Abingdon, UK) and ~ 1.5 mM of Dotarem (Guerbet, Roissy. France) was polarised using a HyperSense dissolution DNP polariser (Oxford Instruments). The mixture was polarised until it achieved > 90% of its maximum polarisation which took approximately 40 minutes (Figure 6.1 (b)).

The hyperpolarised 2-^{13}C pyruvate acid was dissolved with a superheated 40 mM HEPES buffer solution and transferred to 20 µl of 2.0 M NaOH solution via an open vessel for the neutralisation process. The final dissolved 2-^{13}C pyruvate had a concentration of 19 mM and a pH of ~ 7.2 - 7.5. 20 µl of dissolved 2-^{13}C pyruvate solution was immediately pipetted into the sperm sample and well mixed. The final pyruvate concentration after it was added to the sample was ~ 0.9 mM. The time from sample dissolution to initiation of the spectrum acquisition was 20 – 30 seconds.

Immediately after infusion of hyperpolarised 2-^{13}C pyruvate, MR acquisition was initiated.

6.2.3 MRS experiment

All experiments were performed on a 9.4 T Bruker Avance III NMR spectrometer, with a 5 mm broadband observe probe at 37°C or 39°C (Figure 6.1 (c)). The acquisitions were acquired using a ^{13}C {^{1}H} inverse-gated pulse sequence for every 1 second over the course of 3 minutes (Time Domain Points = 38458, Flip Angle = 16°, Sweep Width = 239 ppm, Number of Averages = 1, Repetition Time = 1 s, Number of Repeats = 180).

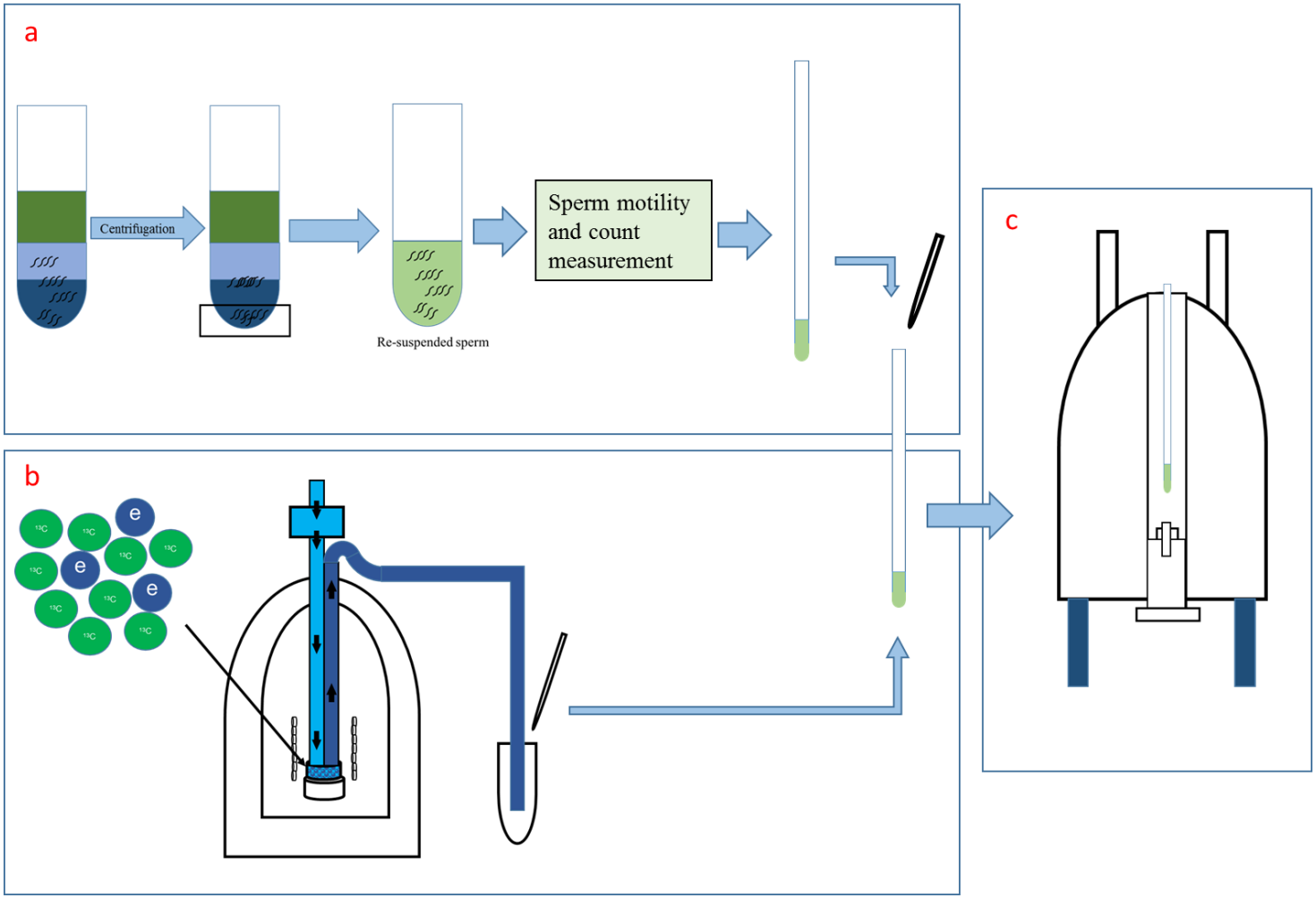

Figure 6.1: Summary of the experiment. (a) Sperm sample was prepared using DGC technique and then the sperm pellet was re-suspended with PBS. Sperm sample concentration was adjusted to the desired concentration before it was aliquoted into an NMR tube. (b) The sample had dissolved hyperpolarised 2-^{13}C pyruvate added, which was polarised to > 90% of its maximum value in the DNP polariser beforehand (c) The sample was immediately scanned in the MR scanner for 3 minutes.

6.3 Data analysis

Raw time domain data was Fourier transformed (FT) into a stack of 1D spectra. The first 40 spectra were summed together to create a single 1D spectrum for detection of low SNR metabolite peaks. Both 1D and 2D spectra were inspected visually for the evidence of 2-^{13}C pyruvate metabolism and the appearance of metabolic products. They were also compared to the 1D spectra of a 2-^{13}C pyruvate phantom which was carried out according to the same protocol as the hyperpolarisation experiment except without the addition of the sperm sample. Assignment of the detected peaks was based on previous reported literature.

6.4 Results

Figure 6.2 shows the spectrum acquired from boar sperm (N = 2), where 5 mg of pyruvate acid was polarised and the sample was scanned at 37°C. The signal from 2-^{13}C pyruvate peak had the highest intensity at 207.8 ppm. The maximal intensity for 2-^{13}C pyruvate was at time zero which decreased over 180 s. Another detected peak was pyruvate hydrate at 94.5 ppm, which is in chemical equilibrium with pyruvate. Naturally abundant 1-^{13}C pyruvate at 170.7 ppm appeared after the 40 first spectra were summed. None of the metabolite products from 2-^{13}C pyruvate were observed.

With an assumption that the intense 2-^{13}C pyruvate peak hindered visualisation of the small peak, which might be derived from pyruvate metabolism, the experiment setting was slightly modified. Two further samples were added with the dissolved solution from the polarised 2.5 mg pyruvate acid. The hyperpolarised spectra (Figure 6.3) showed the same peaks with a slightly lowered intensity of pyruvate and pyruvate hydrate. To ascertain whether sperm may require a longer time to metabolise pyruvate, after the sperm sample hyperpolarisation experiment was performed, the same sample was subsequently incubated in a water bath for 18 h at 37°C (without transferring into another tube or adding any other chemical compound) and re-scanned after a freeze and thaw process (see Section 2.6). From the incubation spectrum analysis (see Section 2.7), there was visualization of the 2-^{13}C lactate peak (N = 2) (Figure 6.3).

To investigate further, another sperm sample was added with the dissolved solution from polarised 2.5 mg (N = 2) and 5 mg (N = 2) of 2-^{13}C pyruvate acid, respectively, and was scanned at 39°C (each sample was subsequently incubated and re-scanned as described in the paragraph above). From the hyperpolarised spectra (Figure 6.4), the same peaks were detected for the sample which were prepared from 2.5 mg of 2-^{13}C pyruvate acid (N = 2). However, there were new peaks detected in the sperm sample which was prepared from 5 mg of 2-^{13}C pyruvate acid (N = 2) (Figure 6.5). Their chemical shifts were at 181.7 ppm (peak 1) and 85.8 ppm (peak 2).

Lactate was detected in the incubation spectra for all samples (N = 4). From a comparison with the 2-^{13}C pyruvate phantom (Figure 6.6 and Figure 6.7), those new peaks were confirmed as impurities that were present in the supplied 2-^{13}C pyruvate.

6.5 Discussion

The aim for this chapter was to confirm the origin of bicarbonate observed in Chapter 5 by acquiring hyperpolarised 2-^{13}C pyruvate metabolism in sperm using dissolution DNP. The result has shown that, despite several experimental modifications, no pyruvate metabolic products were observed in the spectra.

This study followed a similar experimental protocol as implemented in the Reynolds *et al*. (2017) study except they used 1-^{13}C pyruvate, as the hyperpolarised substrate and human sperm as the sample. A few changes were applied in this study to better suit boar sperm; for instance, the sperm preparation and temperature setting during MR acquisition. Reynolds *et al* (2017) found evidence of 1-^{13}C pyruvate metabolism in human sperm by detecting 1-^{13}C lactate and ^{13}C bicarbonate. However, this study did not detect any of those products (2-^{13}C lactate instead of 1-^{13}C lactate for this study). This study attempted to compare 1-^{13}C and 2-^{13}C pyruvate metabolism in boar sperm however this was difficult due to impurities detected in 1-^{13}C pyruvate spectrum.

However, isotopically, 1-^{13}C pyruvate and 2-^{13}C pyruvate label the pyruvate at different carbon positions within a molecule. Isotopic labelling replaces those carbon atoms by their nuclear isotope, but this process does not change their chemical properties. For example, both 1-^{13}C and 2-^{13}C pyruvate are converted to lactate by the same enzyme which is LDH. However, the nuclear spin lattice relaxation time, $T_{1,}$ might be different between them, given that lactate carbon position 1 is in a carbonyl group whist lactate carbon position 2 is a methane group (Gebelin 1987). This is because, T_1 is influenced by other nuclei in the same molecule and other molecules (Landheer *et al.*, 2016). Due to carbonyl lactate not having any protons directly bound to it (the neighbouring proton is three bonds away from 1-^{13}C), it relaxes slowly, compared to a methane lactate, which has a directly attached proton (Marjańska *et al.*, 2010). T_1 for the 1-^{13}C lactate is thus expected to be longer than that for 2-^{13}C lactate. This will result in different peak intensities between them if the same acquisition time is used; the former will be higher than the latter (Golman, in ’t Zandt and Thaning, 2006; Shchepin, Pham and Chekmenev, 2014). This is in accordance with the findings of Marjańska *et al*. (2010). They reported that, infusion of 1-^{13}C pyruvate and 2-^{13}C pyruvate into rat brain, produced a 2-^{13}C lactate SNR which was lower than 1-^{13}C lactate (Marjańska *et al.*, 2010).

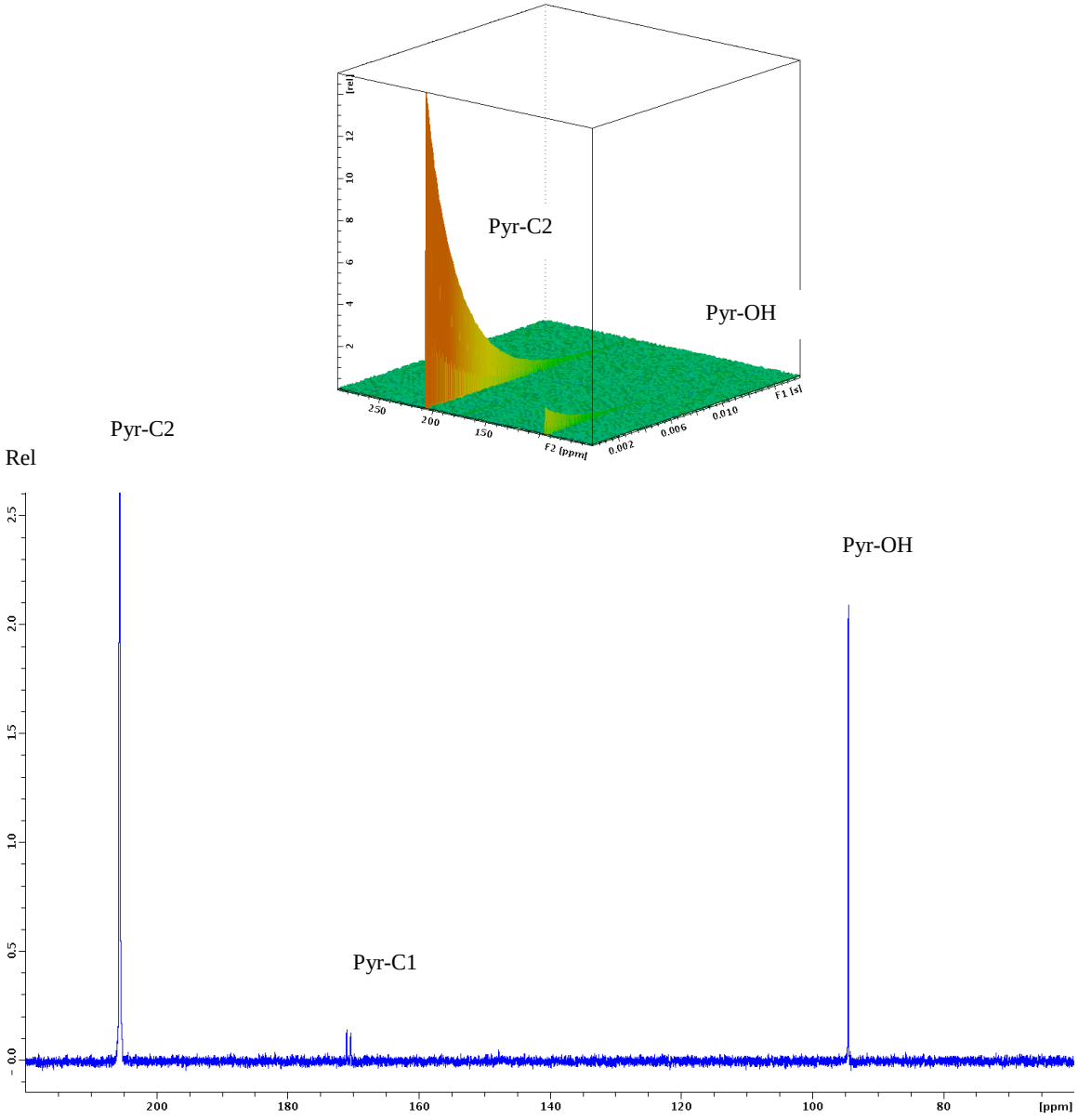

Figure 6.2: Spectra obtained from boar sperm which had polarised 5 mg 2-^{13}C pyruvate and acquired at 37°C. (Top) Dynamic spectra acquired every 1 s showed that the Pyr-C2 and Pyr-OH signal decreased over 180 s. (Bottom) The spectrum is the sum of first 40 rows and the observed peaks were: (i) 2-^{13}C pyruvate (Pyr-C2), (ii) 1-^{13}C pyruvate derived from natural abundance (Pyr-C1) and (iii) C2-pyruvate-hydrate (Pyr-OH).

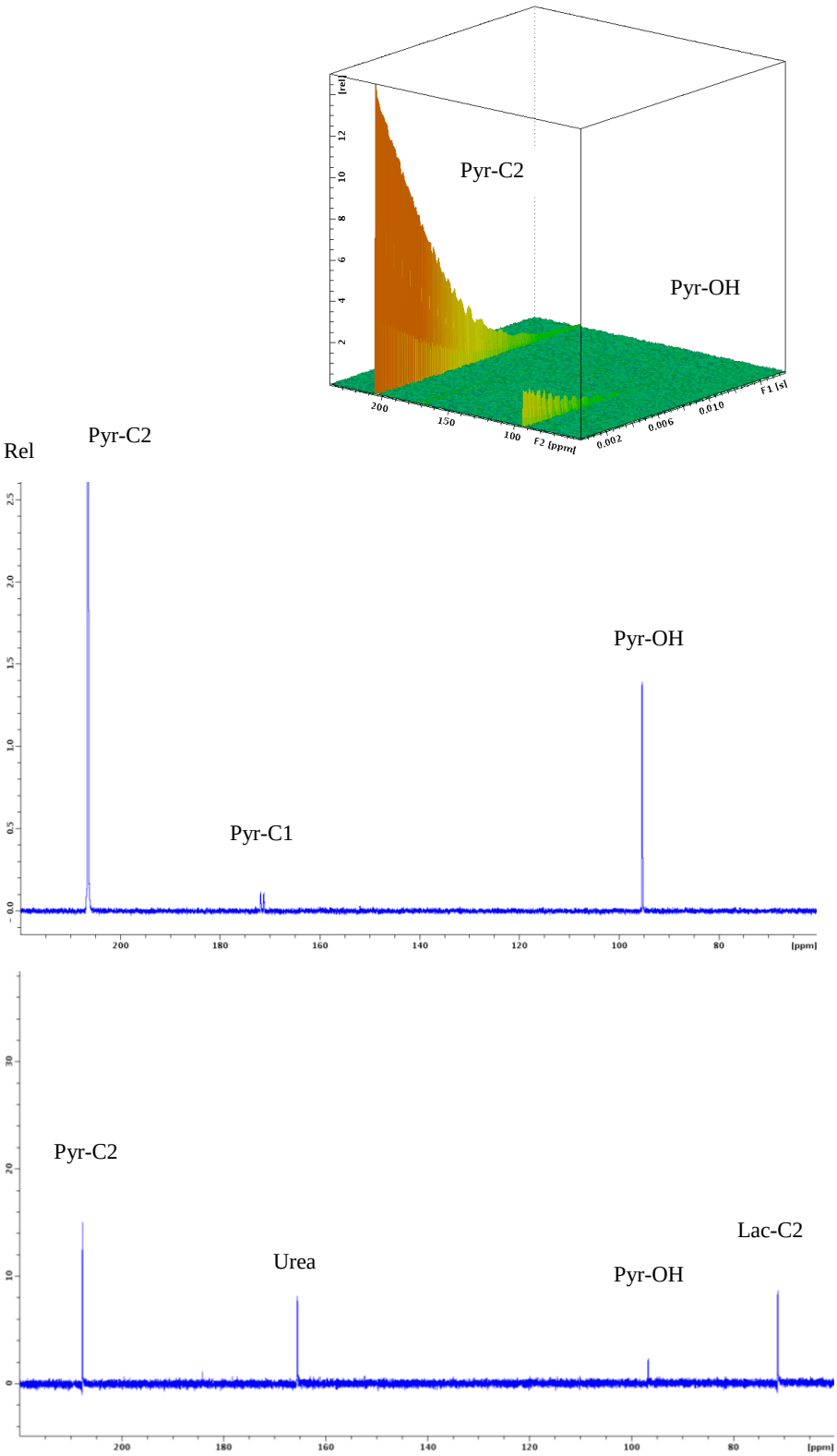

Figure 6.3: Spectra obtained from the boar sperm which had polarised 2.5 mg 2-^{13}C pyruvate and acquired at 37°C. (Top) Dynamic spectra acquired every 1s showed Pyr-C2 and Pyr-OH that the signal decreased over 180 s. (Middle) The spectrum is the sum of first 40 rows and the observed peaks were: (i) 2-^{13}C pyruvate (Pyr-C2), (ii) 1-^{13}C pyruvate (Pyr-C1) and (iii) pyruvate-hydrate (Pyr-OH). (Bottom) Same peaks were detected in the 18 h incubation spectra except 2-^{13}C lactate (Lac-C2).

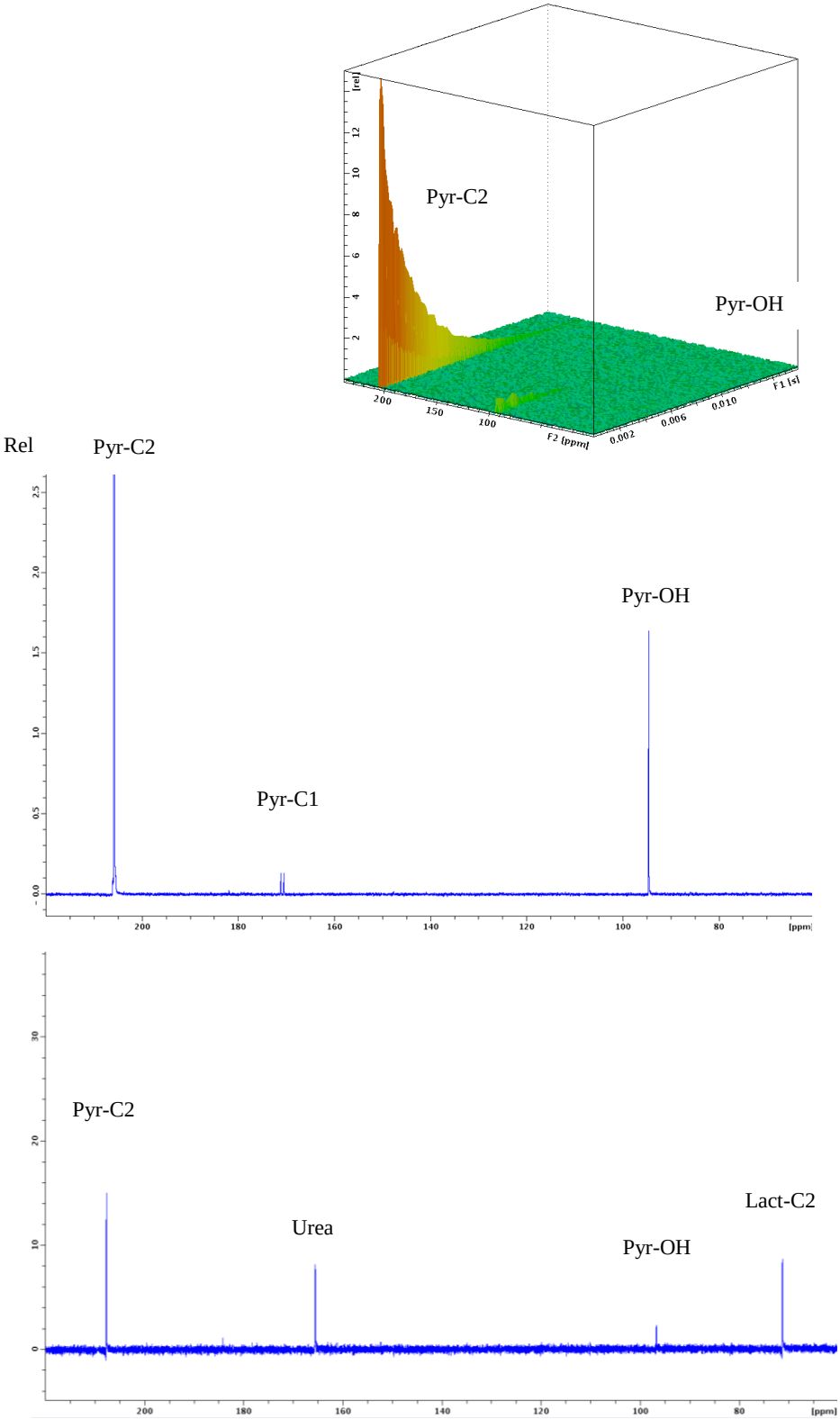

Figure 6.4: Spectra obtained from the boar sperm which had polarised 2.5 mg 2-^{13}C pyruvate and acquired at 39°C. (Top) Dynamic spectra acquired every 1 s showed that the Pyr-C2 and Pyr-OH signal decreased over 180 s. (Middle) The spectrum is the sum of first 40 rows and the observed peaks were: (i) 2-^{13}C pyruvate (Pyr-C2), (ii) 1-^{13}C pyruvate (Pyr-C1) and (iii) pyruvate-hydrate (Pyr-OH). (Bottom) Same peaks were detected in the 18 h incubation spectra except for 2-^{13}C lactate (Lac-C2).

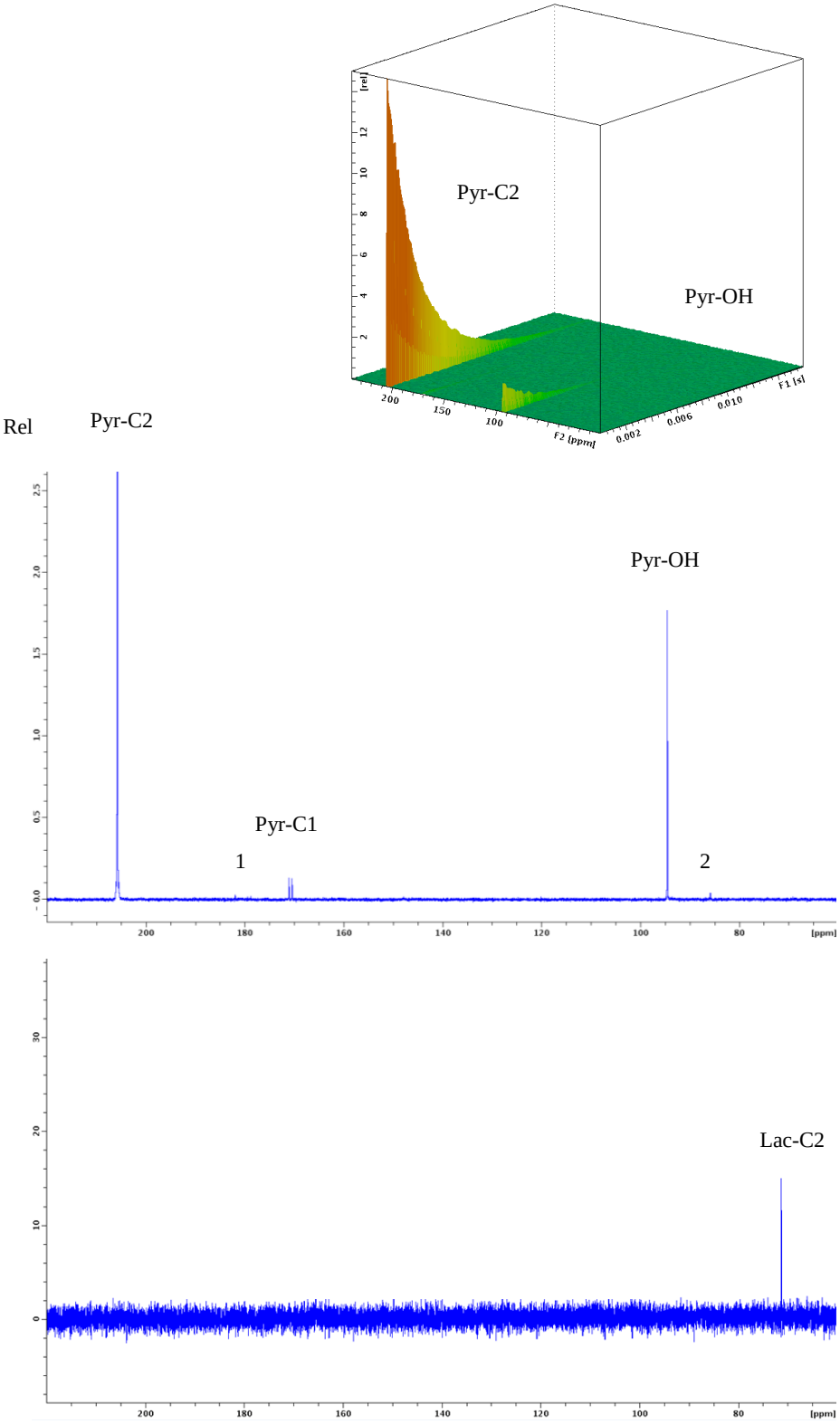

Figure 6.5: Spectra obtained from boar sperm which had polarised 5 mg 2-^{13}C pyruvate and acquired at 39°C. (Top) Dynamic spectra acquired every 1 s showed that the Pyr-C2 and Pyr-OH signal decreased over 180 s. (Middle) The spectrum is the sum of the first 40 rows and the observed peaks were: (i) 2-^{13}C pyruvate (Pyr-C2), (ii) 1-^{13}C pyruvate (Pyr-C1) and (iii) pyruvate-hydrate (Pyr-OH). Other identifiable peaks were Peak 1 and 2. (Bottom) Only 2-^{13}C lactate (Lac-C2) peak was detected in the 18 h incubation spectra. Absence of the 2-^{13}C pyruvate and pyruvate hydrate peak might be due to they being completely converted into 2-^{13}C lactate.

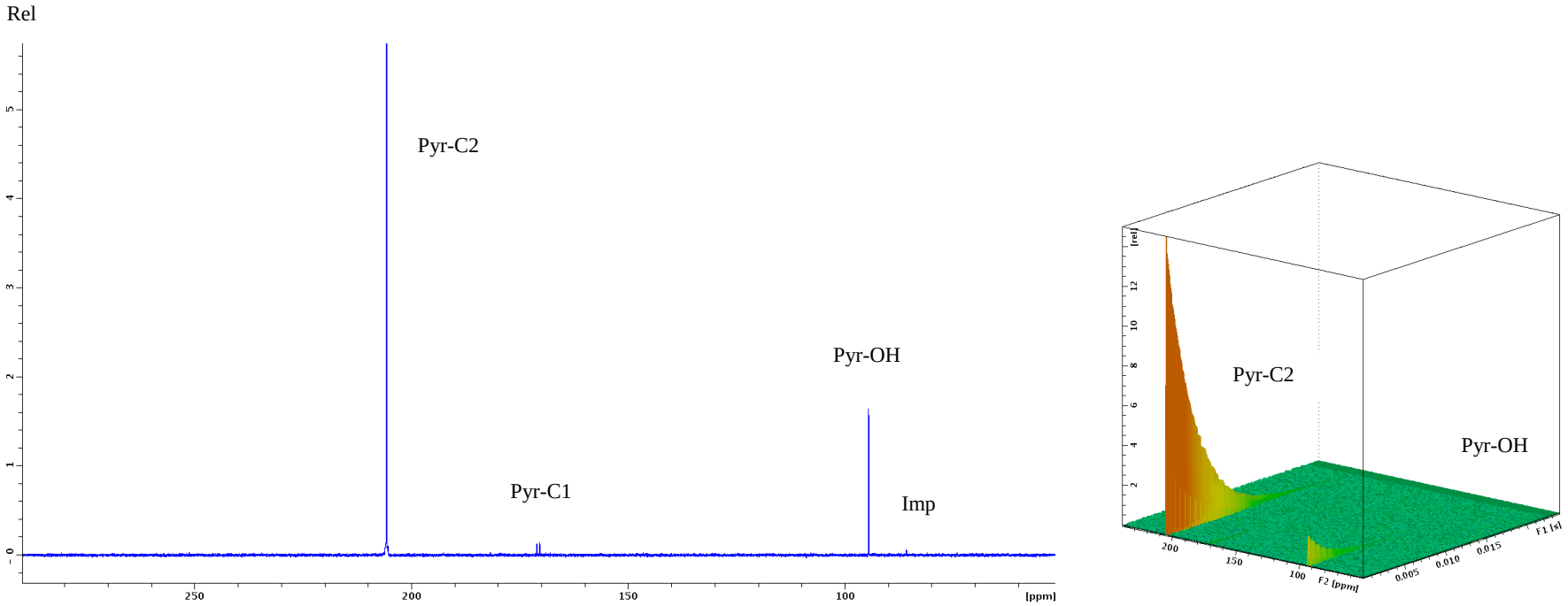

Figure 6.6: Spectra obtained from polarised 5 mg 2-^{13}C pyruvate (phantom spectra) and acquired at 39°C. (Left) The spectrum is the sum of first 40 rows and the observed peaks were: (i) 2-^{13}C pyruvate (Pyr-C2), (ii) 1-^{13}C pyruvate (Pyr-C1), (iii) pyruvate-hydrate (Pyr-OH) and (iv) impurity (Imp). (Right) Dynamic spectra acquired every 1s showed that the Pyr-C2 and Pyr-C1 signal decreased over 180 s.

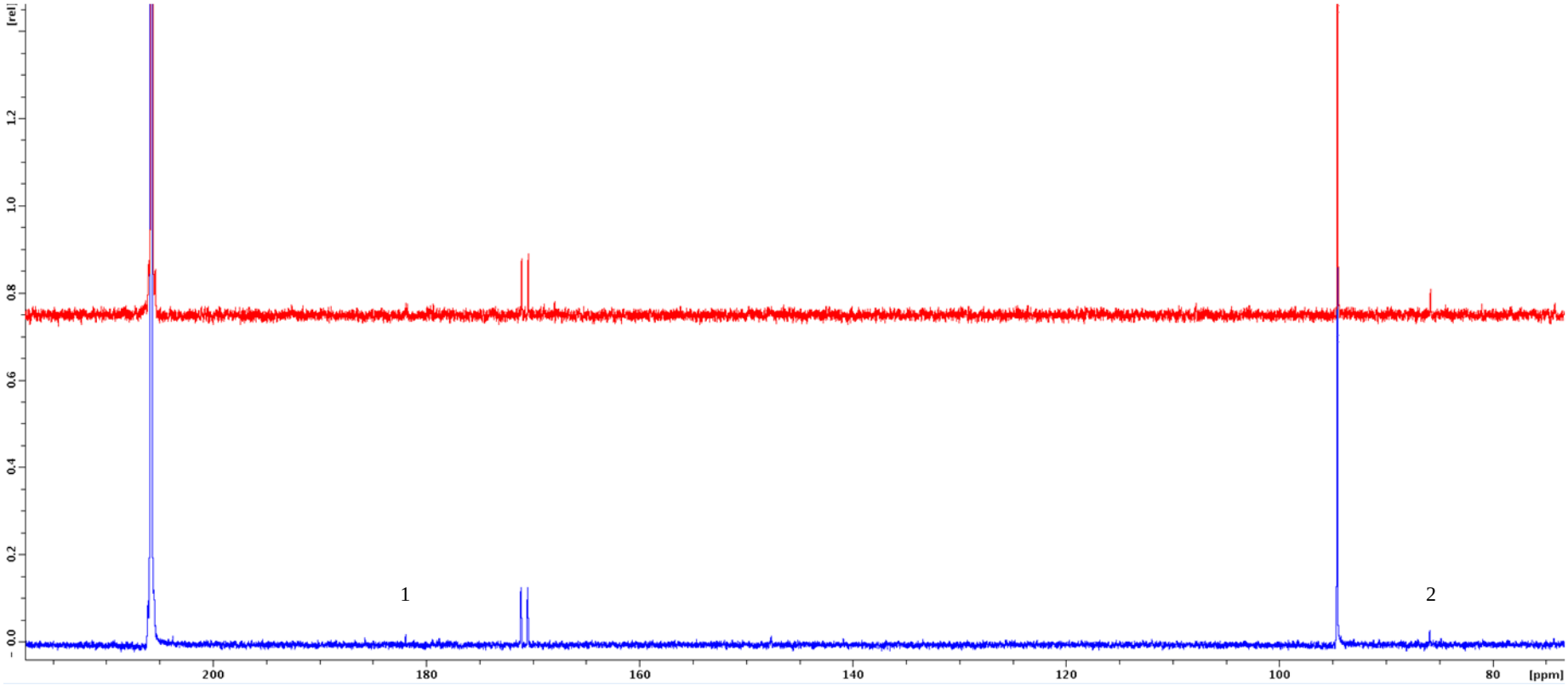

Figure 6.7: Comparison between spectra of the 2-^{13}C pyruvate phantom (red line) and the boar sperm sample which had polarised 5 mg 2-^{13}C pyruvate and acquired at 39°C (blue line). Peaks 1 and 2 match the peaks (impurities) visualised in the 2-^{13}C pyruvate phantom spectrum.

This suggests that, if the human and boar sperm metabolise the hyperpolarised substrate at a similar rate, metabolite peaks derived from the 2-^{13}C pyruvate in boar sperm should be detected too. Typically, in other hyperpolarised studies, undetectable or relatively small peaks during dynamic acquisition became visible when multiple rows were added together (Schroeder *et al.*, 2009). In this study, even after 40 rows were summed, no metabolite product peaks were detected. Therefore, this may indicate, the difference in relaxations time between pyruvate carbon positions was not the reason for the absence of a lactate peak in this study but species variation.

Interestingly, by allowing a longer incubation time (18 h) for the same sperm samples, which had undergone the hyperpolarisation experiment, lactate and bicarbonate peaks were then visible in the spectra. This suggests that pyruvate metabolism has taken place in the sperm sample over the incubation period. This accumulation of lactate and bicarbonate after 18 h, was enough to be detected by MRS (as found in experiments in Chapters 4 and 5). It also suggests that, 3 minutes, which was the time frame for this hyperpolarisation study, was not enough for boar sperm to metabolise pyruvate sufficiently so that the metabolism product's concentration was detectable by MRS.

This phenomenon may suggest that the flux of pyruvate through LDH or OXPHOS in boar sperm is lower than for human sperm. Especially for the pyruvate metabolism taking place in the mitochondria, the process requires a pyruvate transporter, known as a Mitochondrial Pyruvate Carrier (MPC or MCT) (Mccommis and Finck, 2016). MPC acts as a regulatory point and as a pyruvate transporter across the inner mitochondrial membrane for further metabolism reactions to take place (Bucci *et al.*, 2011; Piomboni *et al.*, 2012; Mccommis and Finck, 2016). It is likely that, existence, location and distribution of these MPC in boar sperm is not the same (or lower) as for human sperm. Moreover, the fact that freshly ejaculated human sperm has very high glycolytic activity (it can generate 95% more ATP than boar sperm (Marin *et al.*, 2003)) might contribute to this observed result.

Pyruvate has a long signal half-life, ~ 30 s, compared to other labelled hyperpolarised substrates for Krebs cycle assessment such as glucose and citrate. Perhaps by adding (or increasing the concentration) other enriched atoms, such as deuterium could prolong pyruvate's half-life as was observed for hyperpolarised U-^{13}C glucose (Allouche-Arnon *et al.*, 2013) thus enabling the observation of pyruvate metabolism. Furthermore, the impurity signal became prominent when the boar sperm was scanned at higher temperature and higher concentration of hyperpolarised 2-^{13}C pyruvate. Due to the fact that 2-^{13}C pyruvic acid is a reactive compound, the generation of impurities are difficult to prevent. As the 2-^{13}C pyruvic acid is polarised, the ^{13}C labelled carbon of these impurities will be hyperpolarised too (Harris *et al.*, 2018). Using higher hyperpolarised 2-^{13}C pyruvate concentration, these impurities become more noticeable.

It is well known that mitochondrial metabolism requires an aerobic environment whereas glycolysis requires an anaerobic environment in order to work efficiently. However, all previous experiments were done under ambient oxygen concentration. By considering this requirement, it is likely that results might be influenced by oxygen concentration.

In conclusion, even though dissolution-DNP could overcome the sensitivity issue faced by MRS, presently it has limitations in detecting metabolites of interest in boar sperm due to the short half-life of the hyperpolarisation substrate. As a consequence, the origin of the bicarbonate measured in the previous chapter cannot yet be confirmed.

Chapter 7: The effect of oxygen concentration on sperm metabolism

7.1 Introduction

In the previous chapters, all experiments were performed at ambient oxygen concentration. Therefore, there was a possibility that the oxygen concentration, during sperm incubation, affected all the previous findings, especially on the DNP experiments (Chapter 6). So, in this chapter, the oxygen concentration in the sperm incubation atmosphere was manipulated and the changes were observed using MR spectroscopy.

Mammalian sperm, including boar sperm, are specialised cells. They can undergo both anaerobic and aerobic metabolism (Rodríguez-Gil and Bonet, 2016). An aerobic atmosphere contains oxygen molecules while an anaerobic atmosphere does not. ATP generation through glycolysis take place in anaerobic conditions while OXPHOS occurs in an aerobic atmosphere (Berg, Tymoczko and Stryer, 2002a). The former occurs in the cytosol at the principal piece of the flagellum and the latter occurs in the mitochondrial mid-piece (Piomboni *et al.*, 2012). This has been suggested due to the principle piece being devoid of mitochondria and the presence of enzymes which are responsible for glycolysis, such as hexokinase, phosphoglucokinase isomerase, phosphofructokinase, glyceraldehyde 3-phosphate dehydrogenase, and aldolase (Krisfalusi *et al.*, 2006).

Glycolysis occurs in the absence of oxygen. However, at the end of glycolysis, at the step where pyruvate is produced, the subsequent fate of pyruvate metabolism depends on oxygen. Oxygen may be used for OXPHOS in the mitochondria or reduction may take place in the cytosol without using oxygen (Berg, Tymoczko and Stryer, 2002b). The former will convert the pyruvate to Acetyl CoA while the latter will produce lactate. This choice is influenced by several factors including the role played by an electron carrier, namely, the NADH molecule.

In glucose metabolism, NADH is formed in step six of glycolysis, which is the conversion of glyceraldehyde-3-phosphate into 1, 3-Biphosphoglycerate (**Error! Reference source not found.**). Regardless of whether aerobic or anaerobic metabolism is taking place, the NADH molecule must be re-oxidised to NAD^+.

The ratio of $NADH/NAD^+$ is constant. As the NADH was being produced through glycolysis, the ratio of $NADH/NAD^+$ will be changed as the concentration of NADH is higher than NAD^+. This will result in an accumulation of NADH, especially in anaerobic conditions, when the re-oxidation of NADH in the mitochondria is not possible due to an absence of the electron acceptor, O_2. To maintain NAD^+ levels, as well as to allow further glycolysis to occur in the absence of oxygen, pyruvate is forced to

undergo an oxidation-reduction reaction with NADH. This leads to oxidation of NADH to NAD^+ and the formation of lactate via the enzyme LDH (Cruz *et al.*, 2001). In aerobic conditions, the NADH molecule will continue the reduction in OXPHOS (Storey, 2008).

Sperm are able to switch between different energy pathways based on the available substrate, process and oxygen concentration of the environment in which they operate (Ferramosca and Zara, 2014). The preferred metabolic pathway seems to be highly species specific (Piomboni *et al.*, 2012). Oxygen tension from spermatogenesis up to the final fertilization site, which is the oviduct, varies (Free, Schluntz and Jaffe, 1976; Yedwab *et al.*, 1976; Aitken and Roman, 2008). For most mammalian species, in the oviduct, oxygen tension is between 2-8%, (Yedwab *et al.*, 1976) which is lower than in ambient air (García-Martínez *et al.*, 2018). The level of oxygen tension depends on several factors. One of which is supply of oxygen to the cell (Aitken and Roman, 2008). Poor vascularization of the testes indicates that oxygen tension in the testes is low.

In a normal ambient atmosphere, or normoxia, the concentration of oxygen is 20 – 21% in air (McKeown, 2014). A condition where the concentration of oxygen is lower than in air is called hypoxia and when it is higher it is called hyperoxia. There is a possibility that the sperm will shift their energy producing pathway in different oxygen concentrations. It was hypothesized that sperm will favour use of anaerobic glycolysis rather than OXPHOS during hypoxia as the latter is impaired by lack of oxygen to oxide NADH. In hyperoxia, as electron receptor is in abundance, OXPHOS (and Krebs cycle) will dominate rather than anaerobic glycolysis.

The detrimental effects of high oxygen concentration on spermatozoa in humans has been known for many years (Macleod, 1943). When human sperm were exposed to high oxygen concentrations, 95%, sperm rapidly lost motility. Of the total uptake of oxygen for the respiration process by sperm, 0.2 – 2% is thought to be converted to reactive oxygen species (ROS) (Harper *et al.*, 2004; Murphy, 2009). ROS are a group of free radicals which can interact with other molecules. They include superoxide anions, hydrogen peroxide, hydroxyl radicals, lipid hydroperoxides, peroxyl radicals and peroxynitrite (Guerriero *et al.*, 2014). In sperm, mitochondrial Complex I and Complex III are the major sites for ROS production (Koppers *et al*., 2008). Complex I produces the superoxide in the mitochondrial matrix while Complex III releases superoxide into both sides of the inner membrane of mitochondria (Piomboni *et al.*, 2012).

When the ROS concentration in the sperm mitochondrial membrane becomes too high, sperm might enter oxidative stress, potentially leading to alteration of mtDNA (Hagedorn *et al.*, 2012). Consequently, mtDNA alteration is likely to have an effect on sperm motility (Aitken and West, 1990; Kumar *et al.*, 2009).

On the contrary, it has been found that small amounts of ROS are beneficial for spermatozoa as they can stimulate sperm capacitation, hyperactivation, acrosome reaction and oocyte fusion (Griveau *et al*., 1994; Aitken, 1995; Kodama *et al*., 1996). ROS can therefore have beneficial or detrimental effects on sperm quality in dependence on concentration.

Sperm also have an ability to respond to and counteract the adverse effects of oxidative stress. For instance, sperm have an enzyme, a catalase (CAT), that is able to efficiently reduced superoxide (Macleod, 1943; Kovalski, de Lamirande and Gagnon, 1992). CAT has a signal sequence at its N terminus. This helps in directing and binding CAT to the receptor protein, protease, which is located in the mitochondrial membrane (Alberts *et al*, 2002). Once in the mitochondrial matrix, this signal sequence is rapidly removed and binds with the superoxide (hydrogen peroxide). CAT is able to remove the hydrogen peroxide by converting it into water and oxygen (Heck *et al.*, 2010). However, boar sperm has very low CAT concentration, hence, superoxide has been suggested to be a major ROS responsible for oxidative damage (Awda, Mackenzie-Bell and Buhr, 2009). Possibly, adding exogenous CAT to the boar sperm could reduce the ROS effect when sperm are incubated in a high oxygen atmosphere.

Previous studies, Nevo (1969) and Aalbers (1961) using fructolysis have shown that lactate production from fructose metabolism in boar sperm was higher in anaerobic compared to aerobic conditions. However, for hyperoxia, to the best of our knowledge, the effect of oxygen concentration on sperm metabolism has not been investigated, particularly in the boar. Most of the previous studies have focused on the effect on the acrosome reaction and motility in other sperm species such as human (Macleod, 1943; Whittington and Ford, 1998) and salmon (Bencic *et al.*, 2000).

Therefore, the biological purpose was to find out how the hyperoxia and hypoxia conditions affect boar energy metabolism. It is hypothesised that the OXPHOS rate will increase together with an increase in the Krebs cycle intermediates and bicarbonate formation in hyperoxia while lactate production will increase in hypoxia. This will answer the question of which pathway dominates energy production in boar sperm. Ultimately, the role of the Krebs cycle in supporting sperm motility, both aerobically and anaerobically, associated with in vivo fertilization could be investigated. This study aimed to: (i) intentionally induce hypoxic and (ii) hyperoxic atmospheres in which the sperm are incubated with U-^{13}C glucose and measure the metabolism changes using MRS, and (iii) to compare sperm energy metabolism with and without the present of CAT in a hyperoxic atmosphere.

7.2 Methods

7.2.1 Oxygenation chamber for hyperoxia experiment

An air and water tight clear plastic container, 12 cm x 12 cm x 8 cm, was used to construct an oxygenation chamber for producing a hyperoxic atmosphere. Two small holes were made at the centre of the lid's container to fit 4 mm outer diameter (OD) push fittings (IMI Norgren Ltd, UK). Those fittings were connected with polyurethane tubing (Norgren Ltd, UK), which had 4 mm OD and 2.5 mm in inner diameter (ID), as an inlet Port A, and an outlet Port B (Figure 7.1).

Tubing for Port A allowed flow of the gas mixture from the gas cylinders (Medical grade, Compressed Oxygen and Nitrogen (oxygen free), BOC, UK). In order to mix the gases, a Y connector (4 mm OD) (IMI Norgren Ltd, UK) was used. Each inlet for the Y connector connected with the tubing for oxygen and nitrogen gas while the outlet connected to the push fitting on the lid. Another tube was inserted into the push fitting located inside the container. This tubing was connected during the media equilibration process only and removed afterwards. Its end was inserted almost to the bottom of the tube which contained the media to eliminate the medium surface barrier and provide a humidified condition in the chamber. This provided effective diffusion of the gas into the media and speed up the media equilibrium process.

Port B allowed flow of gas from the container to the oxygen monitor (Crowcon, UK) in the fume hood. Another four holes were made in the base of the container to fit a 10 mm OD cable gland (HellermannTyton, UK) and were sealed with a nut and washer. Gas leakage was tested using a soapy water solution to monitor the presence of bubbles forming in the water when the gas flowed into the container. Any leakage was sealed using nuts and washers and araldite glue.

On the day of experiment, the conical tubes (which contained media) were inserted into the glands which were subsequently tightened and the gas tubing was inserted into each sample tube. The container was then closed with the lid and placed on a rack. A 3.5 liter per minute (LPM) flow of oxygen and 0.2 LPM of the nitrogen gas were mixed in order to provide a 95% oxygen concentration atmosphere in the container (the flowrates were determined based on the calibration curve, see section 7.2.2 for detailed information). The gas flow was controlled by a flowmeter with a valve (Cole-Parmer, UK). Once the desired flow rate was achieved, flow was maintained constant during the media equilibration process and the hyperoxia experiments.

After the media was treated, the container lid was opened to allow for the sperm sample to be added into the media. This process was done quickly to minimise the time that the media was exposed to ambient oxygen concentration. The container was then closed, and the sample was checked to ensure that the entire sample was in the water bath. The timer for the total incubation time was initiated after ~ 5 minutes to allow restoration of the hyperoxic oxygen atmosphere in the chamber.

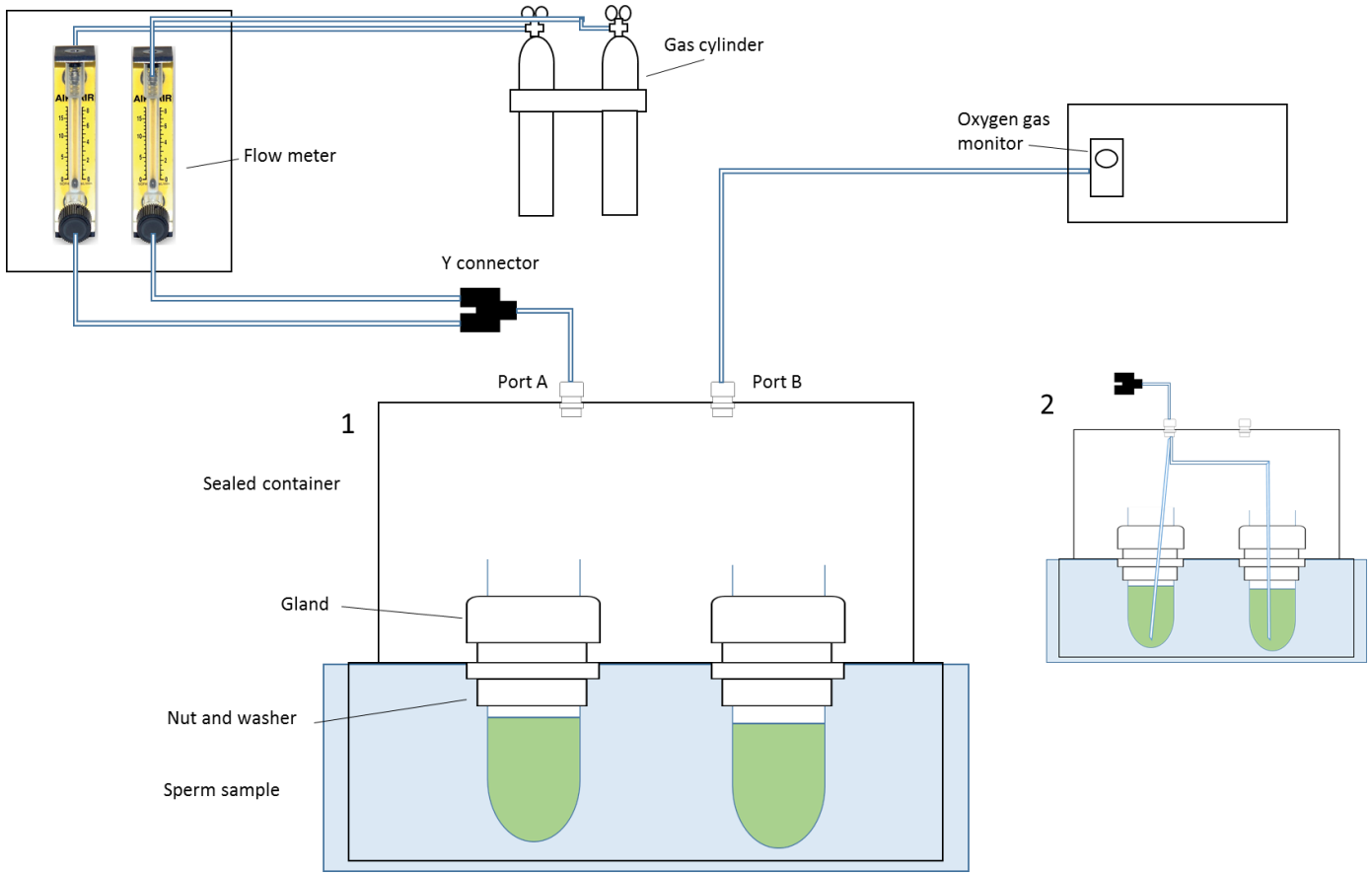

Figure 7.1: Diagram of the oxygenation chamber for the hyperoxia experiment. (1) is the diagram after sample was added into the equilibrated media. The flow rate of the oxygen and nitrogen gases were controlled using the flowmeters. To obtain mixed gases, they flowed through the Y connector before entering the sealed oxygenation chamber through Port A. Port B was the gas outlet connected to the oxygen gas monitor in the fume hood. The chamber was supported by a rack to make sure that the whole sperm sample was in the water bath (blue boxes). Panel (2) represents the setup during the media equilibration process. Tubing was inserted almost to the bottom of the media tubes and removed afterwards.

7.2.2 Oxygen calibration curve

To obtain the gas calibration curve, various Oxygen gas flows, X_{LPM}, (X_{LPM} = 0.0, 0.2, 0.4, 0.6, 0.8, 1.0, 1.2 LPM), and 3.5 LPM nitrogen gas, $Y_{LPM,}$ flowed into the oxygenation chamber and the Oxygen gas concentration, Z, in %, obtained from the Oxygen monitor was tabulated. This step was repeated three times for each X_{LPM}. X_{LPM} was then converted into Oxygen concentration percentage, Equation 7.1.

$$X_{cal} = \frac{X_{LPM}}{X_{LPM}+Y_{LPM}} \times 100 \qquad \text{Equation 7.1}$$

A linear regression graph of X_{cal} versus Z was plotted (Figure 7.2) to get the calibration equation, Equation 7.2. Using the calibration equation to obtain Z = 95%, yielded X_{cal} of 95.95%. To convert into flow rate, (using Equation 7.1) to achieve X_{cal} = 95.95%, the required flow rate was 3.5 LPM for Oxygen and 0.2 LPM for Nitrogen. This yielded 95% Oxygen concentration with 1% percentage error between X_{cal} and Z.

$$Z = 1.01 \times X_{cal} \qquad \text{Equation 7.2}$$

7.2.3 Sample preparation for oxygenation experiments.

Boar sperm (see Section 2.1), was prepared by washing using Percoll/PBS DGC (see Section 2.2.3). 100 µl of re-suspended sperm was added to the media (see Section 2.4) of the respective groups without taking the media out from the oxygenation chamber, Figure 7.1. For the hypoxia group (aim i), the media was equilibrated for > 19 h prior to the day of the experiment, in a hypoxic chamber (Baker Ruskinn, Maine, USA) which contained 0.8% oxygen, 5% carbon dioxide and 94.2% nitrogen . For the normoxia group, the media was left untreated at atmospheric oxygen concentration (21% oxygen, 78% nitrogen, 0.04% carbon dioxide and other gases). For the hyperoxia group (aim ii), the media was equilibrated for 2 h prior the experiment, in a hyperoxia chamber (95% oxygen, 5% nitrogen). To investigate aim iii, a sample which was from the same re-suspended sperm as for the hyperoxia sample, had 10 µl of CAT (Sigma Aldrich, Missouri, USA) added per 1 $x10^6$ sperm (the concentration of the catalase varied depending on the sperm concentration). It was calculated based on the catalase concentration used by Hagedorn *et al*. (2012). All groups were incubated for 4 hours at 37°C in their respective oxygen condition before freezing. For each sample, an aliquot from the re-suspended sperm was pipetted for sperm quality assessment in the normoxia atmosphere (see Section 2.5). MR scanning was done as described in Section 2.6). Detected spectra was then analysed (see Section 2.7). The summary of the sample number and methods was summarised in the Figure 7.3 and 7.4).

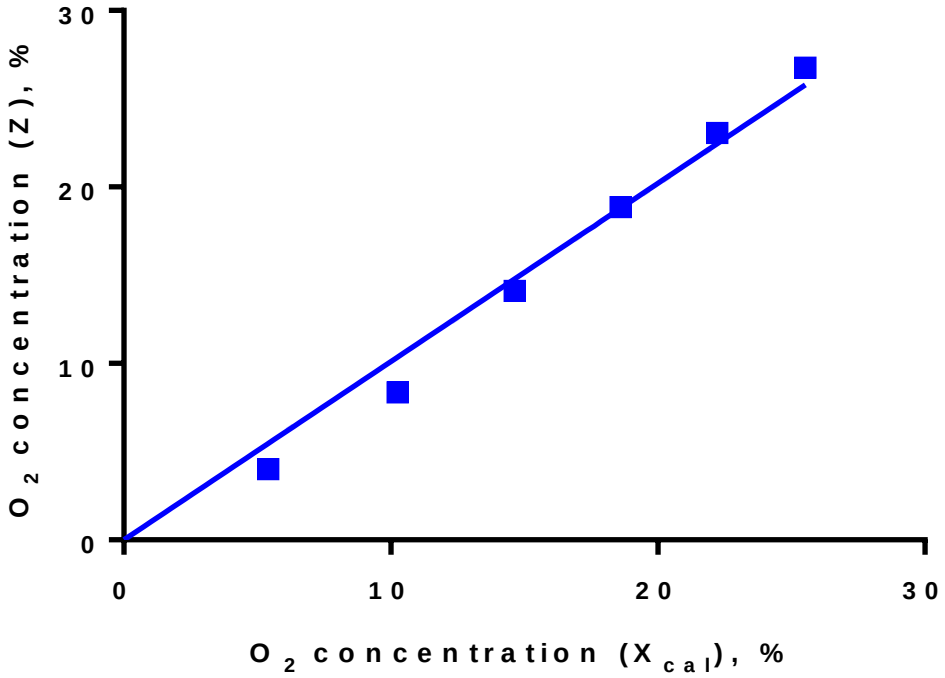

Figure 7.2: Linear regression graph of oxygen concentration, X_{cal} versus oxygen concentration, Z was plotted in order to obtain the calibration equation.

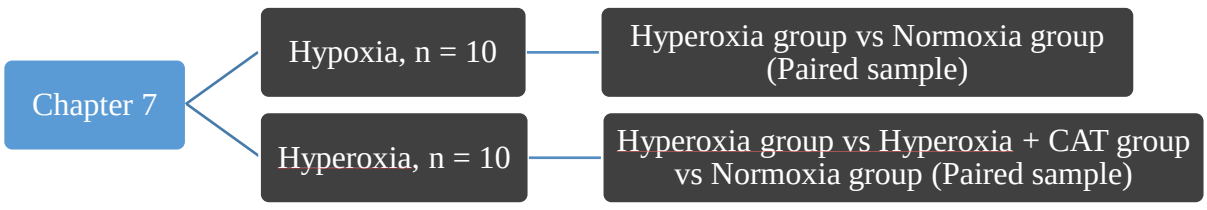

Figure 7.3: Summary of the sample numbers used for Chapter 7.

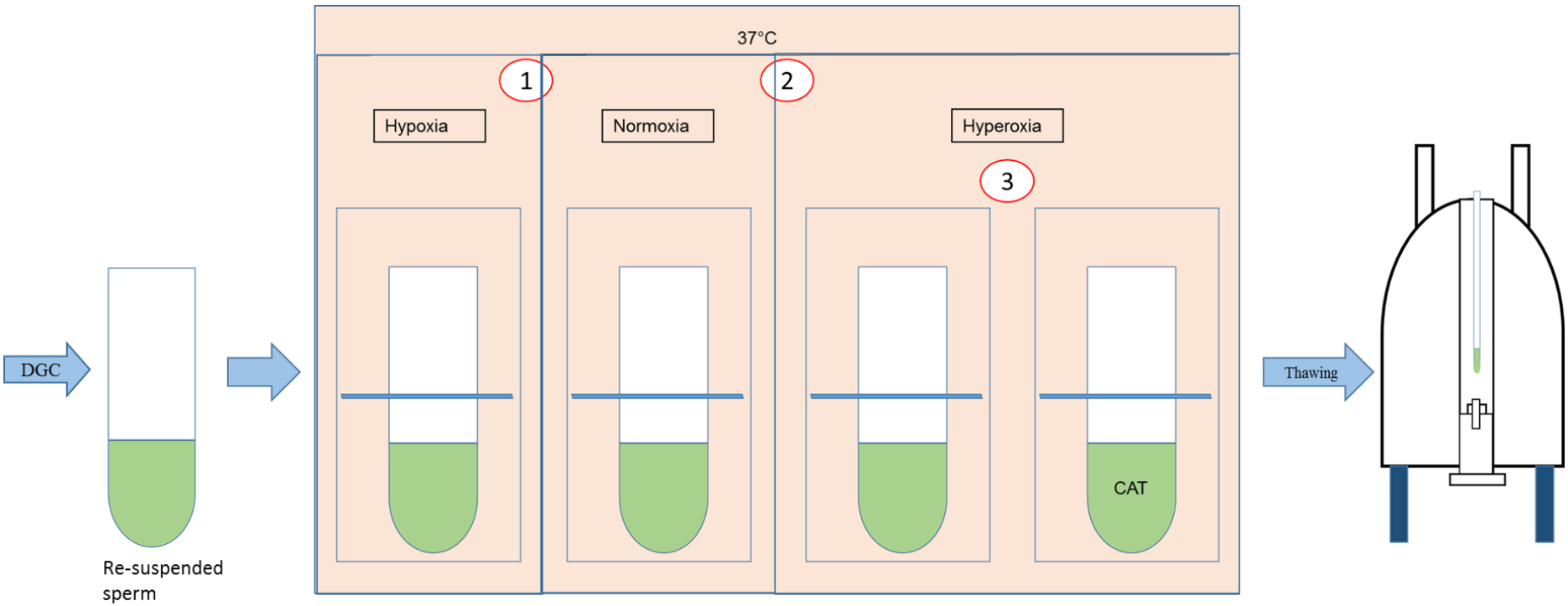

Figure 7.4: Summary of the sperm sample preparation method for the oxygenation experiments. After the sperm sample was prepared using the DGC technique, the re-suspended sample was added into the respective media and incubated in (1) hyperoxic, (2) normoxic, and (3) hyperoxic environment at 37°C for 4 h. After that, they were subsequently frozen before thawing and scanning in the MR scanner. CAT represents catalase.

7.3 Data analysis

A paired Student's t-test was used for comparison between metabolite product integrals, for the normoxia and hypoxia groups whereas a one-way ANOVA with Sidek's test was used for comparison between metabolite product integrals, for the normoxia, hyperoxia and hyperoxia + CAT groups. In all of these, metabolite integrals were normalised to the relative sperm concentration.

7.4 Results

Sperm concentrations used for all oxygenation experiments were 107 – 402 x 10^6/ml with progressive motility between 3% and 16% and motility between 30% to 95%. The calculations were made on the sample without undergone any oxygenation treatment (ambient oxygenation condition).

No Krebs cycle intermediates were observed but lactate and bicarbonate were detected in the spectra (Figure 7.5 and Figure 7.6). Lactate was always observed in each sample for all groups but bicarbonate was intermittently detected.

For aim (i), lactate integrals in the hypoxia group were significantly higher ($4.97 \pm 1.28 \times 10^{-4}$, n = 10) than in the normoxia group ($0.75 \pm 0.85 \times 10^{-4}$, n = 10) ($p < 0.001$) (Figure 7.7). No bicarbonate peak was detected in the hypoxia group but the sperm incubated under normoxia group (n = 3), produced a detectable bicarbonate peak ($0.13 \pm 0.45 \times 10^{-4}$). Therefore statistical analysis was not carried out.

For aims (ii) and (iii), lactate was always detected in the spectra but its integral was not significantly different between all groups (normoxia = $0.80 \pm 0.88 \times 10^{-4}$; hyperoxia = $1.87 \pm 1.55 \times 10^{-4}$; hyperoxia + CAT = $2.47 \pm 2.15 \times 10^{-4}$) (Figure 7.8). Bicarbonate was detected in only one sample from hyperoxia + CAT group, therefore statistical analysis was not carried out.

7.5 Discussion

The aims of this chapter were to investigate the effect of low and high oxygen atmospheres (with or without adding CAT) on boar sperm metabolism. It was found that the change of oxygen concentration during sperm incubation, from a normal to hypoxic condition, resulted in a significant increase in the lactate integral. Moreover, hyperoxia produced a higher (but not significant) lactate integral than normoxia.

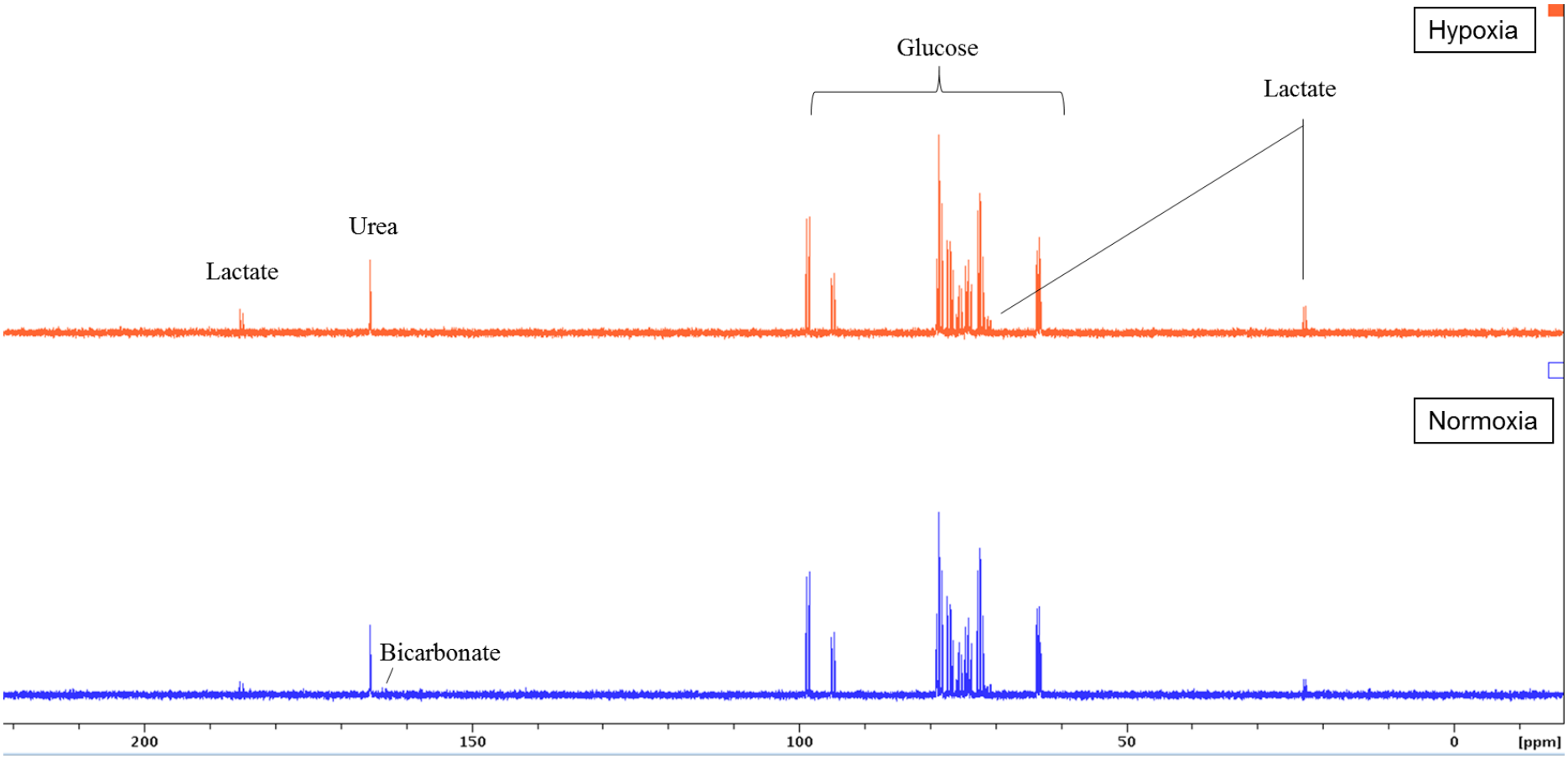

Figure 7.5: Incubation ^{13}C spectra of sperm metabolism for normoxia (blue) and hypoxia (orange) groups.

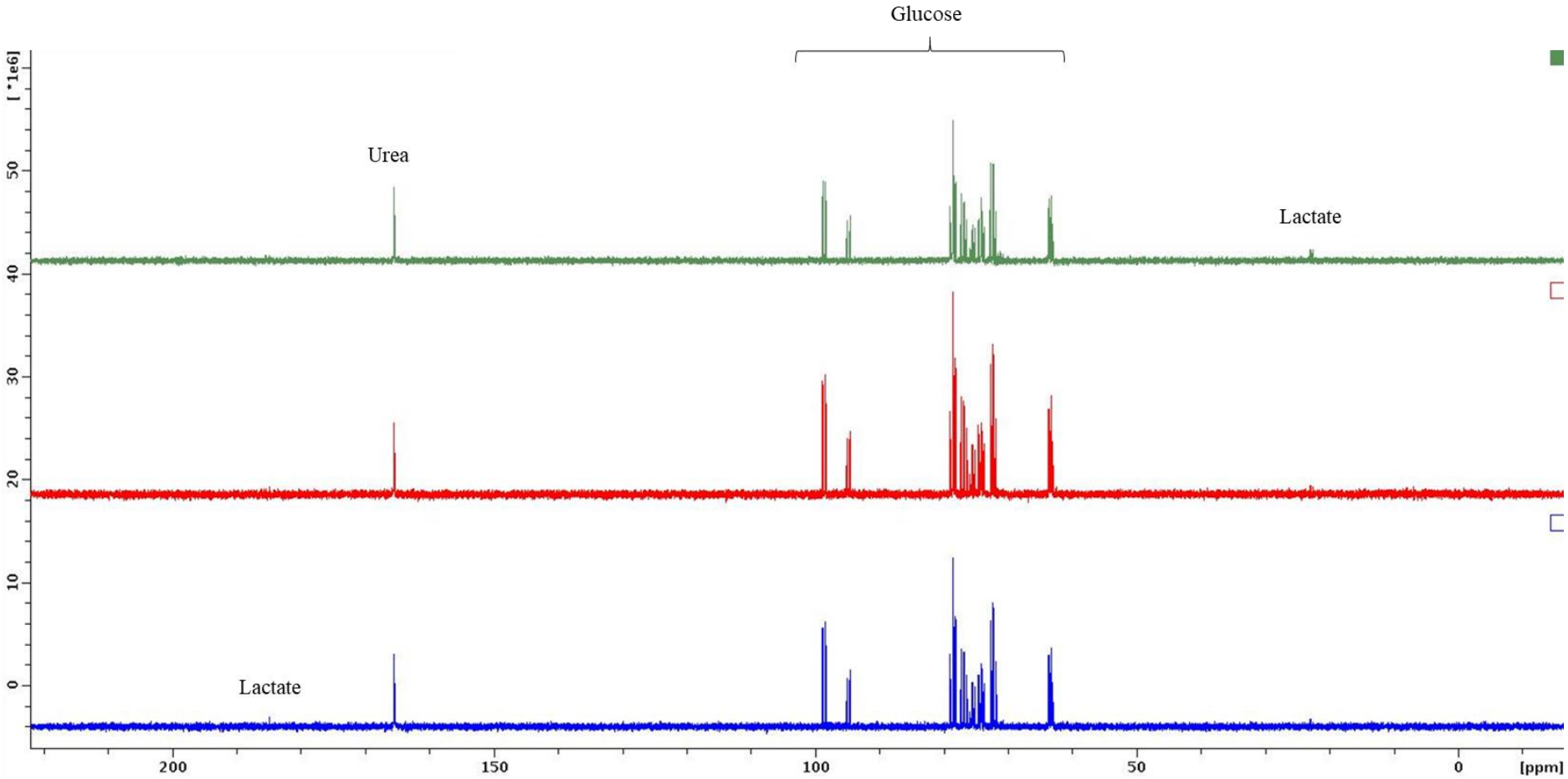

Figure 7.6: ^{13}C spectra of sperm metabolism for incubation in normoxia (blue), hyperoxia (red) and hyperoxia with CAT (green) groups.

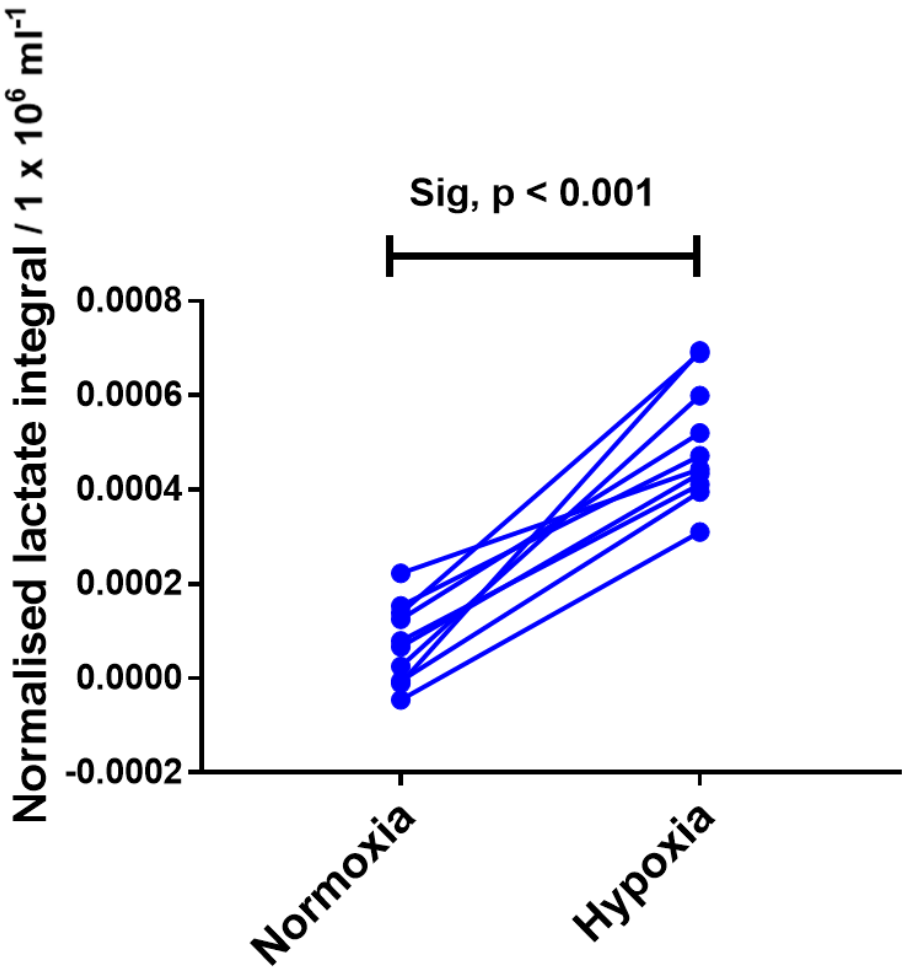

Figure 7.7: Normalised (to sperm concentration) lactate integral with statistical p value for sperm incubated under normoxia and hypoxia conditions. Sample number, n = 10; lactate, n = 10. Sig represents significance.

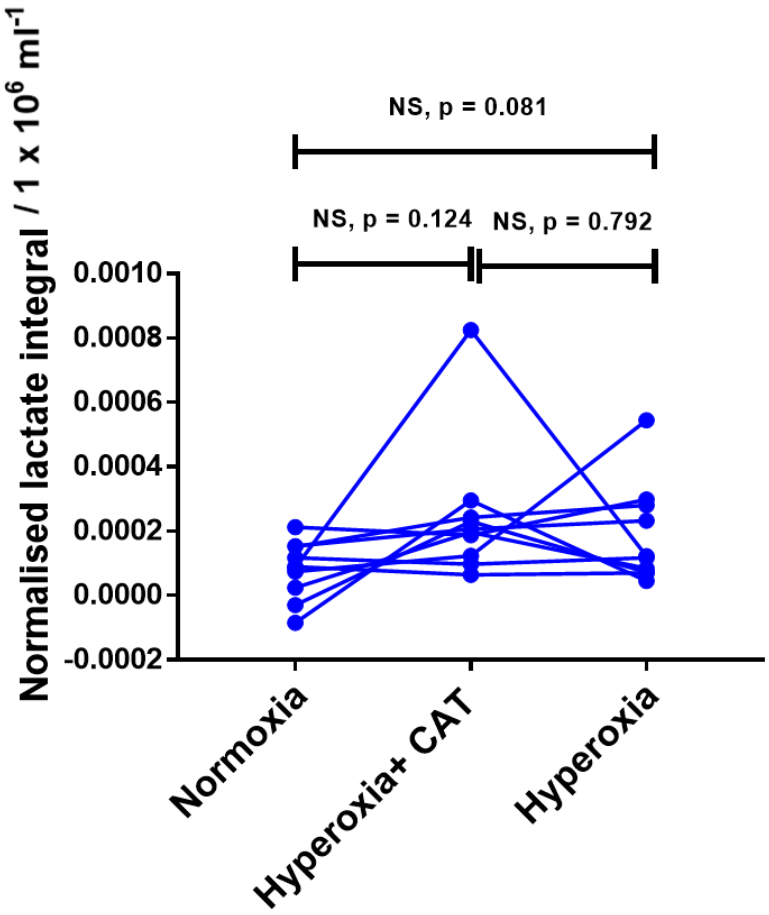

Figure 7.8: Normalised (to sperm concentration) lactate integral with the statistical p value for the sperm sample in normoxia, hyperoxia and hyperoxia + CAT groups. Sample number, n = 10 and lactate, n = 10. NS represents not significant.

The concentrations of oxygen used in this work were 0.8% and 95%, to avoid nitrogen and oxygen toxicity on sperm based on the reported literature (Macleod, 1943; Whittington and Ford, 1998). Macleod (1943) reported that sperm loss motility in 95% oxygen atmosphere but have maximal motility in 95% nitrogen. Contrary, Whittington (1998) did not found any significant different of motility between samples incubated under 95% oxygen and 95% nitrogen. Although their finding are different, toxicity is expected to occur more abundantly as more oxygen or nitrogen are available (Catt, 2000). Whilst these values are not physiologically realistic for the female reproductive system (see Section 1.4 for details), they allow investigation of which pathway is dominant and the ability of the boar sperm to change their metabolism according to oxygen availability.

The increase in concentration of lactate may indicate that pyruvate was converted more rapidly into lactate by LDH. As mentioned briefly in Chapter 1, this reaction could happen in the cytosol or in the mitochondrial matrix by LDH-X, a specific LDH isoform for the sperm LDH (Piomboni *et al.*, 2012). As the re-oxidation of NADH in the mitochondria is limited due to very little O_2 in the hypoxia atmosphere, the significant increase in concentration of lactate may indicate that the needed energy was predominantly provided by LDH-X in the cytosol. This finding fits with a previous study which showed a higher lactate concentration for boar sperm which had been incubated in an anaerobic (achieved by constant overflow of the nitrogen gas) than in the aerobic condition (achieved by constant stirring with air) (Nevo *et al*., 1970).

The higher lactate which was detected under hyperoxia compared to normoxia may indicate that some proportion of the detected lactate in the hyperoxia experiment was generated from the mitochondria LDH-X. Medrano *et al* (2006) could support this assumption whereas they found LDH-X in boar sperm. They also added that this enzyme is located mainly at the principal piece of the tail. Compared to normoxia, hyperoxia possibly gives rise to a higher number of NADH molecules being produced by the Krebs cycle. It is likely that this NADH is used to facilitate mitochondrial pyruvate to lactate conversion and consequently an increasing in the lactate concentration.

Moreover, the presence of mitochondrial LDH-X might be considered to be one of the possible reasons for the scarce OXPHOS reactions found in this study. This may suggest that low OXPHOS was not due to the low rate of the Krebs cycle but due to the NADH, the product of the Krebs cycle, competing with LDH-X to facilitate mitochondrial pyruvate to lactate conversion (as discussed in the previous paragraph). This hypothesis is supported by a report from Peterson & Freund (1974) where they found that the respiration rate of human sperm increased after addition of succinate. In fact, a similar result was observed in Chapter 4, where sperm vitality was found to increase after addition of succinate. Succinate is a substrate of Complex II, which is one of the protein complexes in OXPHOS. By adding

exogenous succinate into the cell, extra electrons will be generated, beside the ones from NADH, for the subsequent OXPHOS process.

It was thought that bicarbonate detection would be detected more frequently with a higher possibility to detect Krebs cycle intermediates when the boar sperm was incubated in an aerobic atmosphere especially hyperoxia. However, the fact that boar sperm produced lactate more than bicarbonate in these conditions might be explained by several reasons, one of which is the ATP shuttle system (Kamp *et al.*, 2003). For sperm motility, it is necessary for the produced ATP to be diffused (or be transported) to the dynein ATPases (Kamp *et al.*, 2003). Consequently, ATP which is generated in the mid-piece (from the Krebs cycle or OXPHOS in the mitochondria), must be transported to the principal piece (which contains dynein ATPases). This process requires an ATP protein transporter, for instance phosphorylcreatine - creatine kinase (Piomboni *et al.*, 2012). However, boar spermatozoa do not have this transporter (Kaldis *et al.*, 1997). Consequently, ATP production in the principal piece (from the anaerobic glycolysis) is crucial and dominant, compared to that from the mid-piece, for boar spermatozoa to function properly.

No significant difference of lactate concentrations measured for sperm samples that were incubated in exogenous CAT and those that were not (both incubated in the same oxygen condition) indicates that addition of CAT did not influence metabolism. This could be due to the fact that there was no ROS produced under hyperoxic conditions. Therefore, CAT could not further reduce the level of ROS. This is supported by the findings of Whittington & Ford (1998) where incubation of normal sperm under 95% O_2 and 5% CO_2 did not produce detectable levels of ROS. The adverse effect of ROS was only observed in samples that had a history of ROS production (Whittington and Ford, 1998). However, it would be helpful if the ROS level for the sperm sample to be used in future studies is assessed beforehand.

Considering only one sperm sample (from hyperoxia + CAT group) produced detectable bicarbonate and undetectable Krebs cycle intermediates may suggest that increasing the oxygen concentration alone was not adequate to increase their concentrations to the detection level of MRS. Another possibility is that the protein complexes in the OXPHOS chain are not of sufficient concentration to accommodate any higher OXPHOS activity. Typically, cells which have a very high OXPHOS activity have a prominent intra-mitochondrial inner membrane crest, which is localised by protein complexes (Berg, Tymoczko and Stryer, 2002b). However, boar sperm have almost flat inner membrane crests (Rodriguez-gil, 2006). Therefore, it is not surprising that bicarbonate concentration was unable to be detected by the MRS.

A separate study to investigate the effect of CO_2 on sperm metabolism during oxygenated incubation would be interesting. Most commercial oxygenation chambers have CO_2 control. CO_2 is used for maintaining a proper pH level. Typically 5% CO_2 is used in oxygenation chambers to maintain an acceptable pH level for several days of incubation (Wenger *et al.*, 2015). The pH for diluent used in this study was PBS, was ~ 7.4 (Nallella *et al.*, 2005). The pH matches those of boar sperm which is between 7.2 to 7.5 in freshly ejaculated semen (Johnson *et al.*, 2000). Therefore, while further investigation would be useful, these issues are not thought to drastically affect the results presented here.

Other methodology could be used to confirm the present findings, for instance, by NADH/NAD^+ cytochemical staining. It could demonstrate NAD^+ distribution in the cytosol and mitochondria (VanLinden *et al.*, 2015). Thus, differences in NAD^+ production between mitochondria and cytosol metabolism under hypoxia or hyperoxia can be investigated. However, NADH might be retained in the cytoplasm during spermatogenesis (Zini *et al.*, 1998; Riammer *et al.*, 2016). Therefore, precautions should be taken when measuring NADH/NAD^+ concentration between mature and immature sperm.

As a conclusion, the energy producing pathway for boar sperm is dominated by anaerobic glycolysis rather than OXPHOS regardless of the oxygen concentration in the environment that they operate. Consequently, Krebs cycle intermediates were not observed even in an oxygen rich atmosphere.

Chapter 8: General discussion, conclusions and future work

For sperm analysis, numerous analytical techniques have been utilised, but the advantages offered by MRS metabolomics potentially make it as a useful methodology for in vivo sperm studies.

MRS analyses can be categorised into two groups: targeted or untargeted analyses. Untargeted analysis focuses on the detection of naturally abundant metabolites in the sperm. The advantage of using this technique is the high number of metabolites that can be detected simultaneously in a few minutes. For instance, ^{1}H MRS spectrum can quantify around 42 metabolites in a sample of human sperm (Paiva *et al.*, 2015). This contributes a huge amount of information on human metabolism at a given point in time. Whilst this is an excellent capability of ^{1}H MRS, there is an issue in terms of determining the source of the metabolite because of the complicated background signals (Dona *et al.*, 2016).

The targeted metabolomics technique focuses on the detection of selected metabolites, for instance, metabolite production in a specific metabolic pathway as the product of drug administration or of substance intake by sperm. In targeted analysis, the metabolites under investigation are usually predictable. This technique employs isotopically labelled nuclei such as ^{13}C. One important advantage of ^{13}C over ^{1}H studies is the chemical shifts cover a larger range of values which is over 20 times that of ^{1}H MRS (Dona *et al.*, 2016). Thus, it can be used to monitor the ability of sperm to metabolise a range of labelled substrates and the conversion process through various metabolic pathways. In addition, it could detect small metabolic changes occuring during capacitation and hyperactivation and directly monitor the substrate metabolism process and kinetic rates in live sperm (Clendinen *et al.*, 2014). The non-destructive and high reproducibility of MRS mean that several analyses can be carried out on the same sperm sample, which makes MRS suitable for this study.

In this study, the main aim was to attempt to detect Krebs cycle intermediates by ^{13}C MRS in boar sperm. Several variables were investigated including Krebs cycle inhibitors, incubation temperature, U-^{13}C glucose and 2-^{13}C pyruvate labelled substrates, hyperpolarised 2-^{13}C pyruvate and manipulation of oxygen availability.

8.1 Summary of the results

Present findings shows that boar sperm efficiently utilises U-^{13}C glucose and 2-^{13}C pyruvate as sole energy sources in the absence of other energy substrates, as reflected by the detection of lactate and bicarbonate peaks in the ^{13}C MRS spectrum, induced by both substrates. This utilisation may take place through anaerobic glycolysis and the Krebs cycle. U-^{13}C glucose conversion into lactate was always observed, especially in the control samples, whereas bicarbonate was rarely detected in spectra. In

contrast, both lactate and bicarbonate were consistently detected in the spectrum when 2-^{13}C pyruvate was used as the sole substrate for boar sperm.

The lactate integral significantly decreased after addition of the inhibitors to sperm samples suggesting that there might be an accumulation of Krebs cycle intermediates. However, unsuccessful detection of intermediates by ^{13}C MRS could be due to the concentration of those accumulated intermediates being below the MRS detection level. This assertion is reinforced by the fact that the lactate decrease was not the result of sperm death. Furthermore, the results also indicate that addition of succinate boasted sperm vitality.

By incubating the sample with 2-^{13}C pyruvate, lactate and bicarbonate concentrations were significantly higher and were consistently detected compared to when using U-^{13}C glucose. Indeed, these changes became obvious when the sperm samples were incubated at 39°C. Despite achieving increased lactate and bicarbonate concentration, the Krebs cycle intermediates were still not detected by MRS. However, it was expected that detected bicarbonate had emerged from the Krebs cycle. This assumption was confirmed by the finding that inhibition of the Krebs cycle by succinate where it prevents the formation of bicarbonate (and lactate) from 2-^{13}C pyruvate, thus indicating that bicarbonate is indeed metabolised through the Krebs cycle. Furthermore, disappearance of the lactate peak suggests that there is a link between the Krebs cycle and lactate production. Possibly, by inhibiting the Krebs cycle, it also inhibits formation of the cofactor that it is needed for lactate production.

Unfortunately, an attempt to confirm the association of bicarbonate and the Krebs cycle using DNP was unsuccessful as no evidence of 2-^{13}C pyruvate metabolism was detected throughout the acquisition period. The result may indicate that 3 minutes, which was the time frame for this hyperpolarisation study, was not enough for boar sperm to metabolise pyruvate sufficiently so that the metabolism product's concentration was detectable by ^{13}C MRS. This assumption was proven when lactate and bicarbonate peaks were detected in the spectra by allowing a longer time for the same samples to metabolise.

The energy production pathway for boar sperm takes place mainly through anaerobic glycolysis rather than the Krebs cycle as the rate of lactate and bicarbonate production showed in the hypoxic and hyperoxic experiments. The change of oxygen concentration during sperm incubation, from a normal to hypoxic condition, resulted in a significant increase in the lactate integral. Sperm which were incubated in the normoxia atmosphere produced a lower lactate integral than hyperoxia. This may suggest that in a hypoxic atmosphere, lactate generation was switched from mitochondrial to cytosol metabolism. Thus, under conditions of hypoxia, lactate was predominantly generated by LDH-X in the

cytosol while part of the detected lactate in the hyperoxia experiment was generated from mitochondrial LDH-X.

8.2 Contribution to the wider knowledge and other methodology.

The use of other techniques in future studies, such as liquid chromatography (LC)-Mass Spectroscopy (MS), as well gas chromatography-Mass Spectroscopy (GC/MS) could confirm the present findings. MS could separates different isotopes of an element based on their mass to charge ratio (Choi and Antoniewicz, 2011). ^{13}C is heavier than ^{12}C, thus allowing ^{13}C labelled compounds to be differentiated from unlabelled compounds containing ^{12}C (Choi and Antoniewicz, 2011). However, a well-known drawback of MS is only isotopologues can be distinguished unless tandem MS analysis is used (Henry *et al*., 2011). The coupling technique could be by using gas or liquid chromatography. By coupling the chromatography to MS, it can potentially increase the amount of labelled data (Choi and Antoniewicz, 2011).

Marin *et al* (2003) have reported similar findings to the present study where they used GC/MS to investigate the involvement of the Krebs cycle in boar sperm metabolism. They investigated the distribution of 1,2-$^{13}C_2$ glucose on glycolysis and the pentose phosphate pathway and ^{14}C glucose on $^{14}CO_2$. They also investigated the contribution of PDH and PC to the Krebs cycle using an inhibitor for PC. Though MS is more sensitive than ^{13}C MRS, apparently MS was unable to detect Krebs cycle intermediates too. They assessed the involvement of the Krebs cycle by monitoring glutamate production and reported that glutamate was produced equally from PC and PDH before adding an inhibitor. However, in the presence of the inhibitor, more glutamate was produced from PDH compared to those from the PC pathway hence suggesting that the Krebs cycle is active in boar sperm metabolism with a very low flux rate.

Contrary to this, this study proved the involvement of the Krebs cycle in boar sperm metabolism by monitoring bicarbonate production. As described in Chapter 1, bicarbonate can be generated via several metabolic pathways. These pathways, for example PDH, PC, and Krebs cycle, may influence sperm motility differently.

The Krebs cycle not only contributes mostly to the production of ATP but it also provides an intermediate for other biosynthetic reactions intersecting the Krebs cycle. For instance, α-ketoglutarate is an importance intermediate for the biogenesis of glutamine, glutamate, arginine, and proline, while oxaloacetate is used to generate aspartate and asparagine (Owen *et al*., 2002). Oxaloacetate and citrate also contribute to gluconeogenesis and lipogenesis, respectively. The key role of the Krebs cycle is providing an electron, from NADH and FADH, to OXPHOS so that more ATP can be generated.

Therefore, any aberration in Krebs cycle regulation could result in various cellular processes being affected, with the motility process being particularly vulnerable because of its dominant reliance on ATP production.

Given the Krebs cycle's role in mitochondrial metabolism, therapeutics modulating Krebs cycle metabolism may be a fruitful area for future study in the treatment of infertility. For example, investigating the ratio or relationship of bicarbonate production from the PDH, PC, and Krebs cycle between infertile and healthy sperm samples might provide insight on how to control the pathway producing bicarbonate and ultimately the ability of sperm to fertilise.

It was reported that by incubating boar sperm with bicarbonate, which is a stimulator of adenylyl cyclase, increased sperm motility (Holt and Harrison, 2002). Bicarbonate activates the motility by stimulating adenylyl cyclase to produce an increased level of cyclic adenosine monophosphate (cAMP) hence initiating the protein phosphorylation pathway (Holt and Harrison, 2002). Protein phosphorylation influences ATP production where it is involved in esterifying the phosphate from ATP to amino acids by protein kinases. Holt e*t al* (2002) reported that after incubating boar sperm with bicarbonate, a subpopulation of them had a faster, more linear type of progressive motility while the other population was not affected by bicarbonate. The response was maintained for up to 2 hours before declining. The response was significantly increased for sperm which contained few progressive motile sperm before the incubation process. They claimed that the difference in response to bicarbonate stimulation was not due to sperm death but due to genetic variability of the protein in individual sperm hence, difference respond to bicarbonate treatment could be expected.

Therefore, it suggests that, by stimulating specific bicarbonate producing pathways, potentially it may be possible to increase motility for all populations. Reynolds *et al* (2017), who studied human sperm metabolism using hyperpolarised 1-^{13}C pyruvate, reported that there was a relationship between the bicarbonate, which was generated by PDH and human sperm fast progressive motility. To investigate the ability of sperm to metabolise pyruvate over the time, bicarbonate production was analysed at two different time points. The first time point was when the pyruvate was added immediately after sperm wash. The second time point was addition of pyruvate to the same sample after one hour from the first addition. They reported that only the second pyruvate addition was significantly correlated with sperm fast progressive motility. Since they also found a correlation between lactate from the first pyruvate addition and sperm fast progressive motility, they suggested that there was a change from anaerobic glycolysis to OXPHOS over time.

Although there were several variations in the experimental parameters used, there are some differences, which have been noticed between human and boar sperm metabolism. Firstly, no bicarbonate peak was

detected using ^{13}C MRS when human sperm was incubated with the labelled pyruvate (Calvert *et al.*, 2018) but rather, bicarbonate was always observed in boar pyruvate metabolism for this study. Secondly, by using hyperpolarised pyruvate, both bicarbonate and lactate peaks were observed in human sperm (Reynolds *et al*. 2017) but not in boar sperm.

These differences might be due to different phenotypes characteristic between human and boar sperm. Boar sperm was reported to have a lower average motility than human sperm (Rodríguez-Gil and Bonet, 2016). This low motility problem is more apparent in the AI provided sperm. Therefore, by using a freshly ejaculated boar sperm, this issue might be overcome.

8.3 Limitations and strength

Whilst the link between Krebs cycle metabolism (which might be observed by the bicarbonate production) and sperm motility could be investigated in this study, some aspects should be further improved so that the result is more reliable. One of which is to assess the boar sperm motility using a computer-assisted analyser with increased sample size. This would reduce the well-known errors which are associated with visual motility assessment such as bias and inaccuracy (Amann and Waberski, 2014). In addition, to perform MRS and other related experiment, such as vitality assessment, on the sample from the same ejaculate. Although each sperm might has different sperm quality but it will avoid potential limitation and could show that, the sperm from the other experiment are truly representative of the sperm from the MRS experiment.

However, the present findings showed the strength of this work when the metabolism of 2-^{13}C pyruvate was consistently detected with a relatively high SNR. In addition, the metabolism process can be frozen at a desired time point to track live metabolic conversion to several pathways over an 18 hours period. Therefore, the present technique is potentially able to track different stages of sperm life, such as during capacitation and hyperactivation.

8.4 Recommendations and future studies

There are several recommendations, which can be suggested for future work. Firstly, for the oxygenation experiments, use of a gas analyser or a pre-mixed gas cylinder is recommended. This would provide more accurate gas concentration in the oxygenation chamber particularly if using a mixture of gasses. Besides that, exploration of other oxygen concentrations would be useful. Extremely low and high oxygen levels were chosen in this study because the oxygen level for the hypoxic chamber could not be changed and the latter was based on previous literature which had succeeded in detecting Krebs cycle intermediates (Schroeder *et al.*, 2009). In addition, the present oxygenation study investigated the

influence of the oxygen at 37°C only. It might be useful if the work could be repeated at 39°C in the different incubation atmospheres. This might need a new variable temperature oxygenation chamber because the present hypoxic chamber temperature setting is fixed for communal usage.

Lastly, increase sample size, especially for the hyperpolarisation experiment would be useful. As DNP is a very sensitive methodology, the result shown here is believed to be reliable even though the sample size was relatively small (n = 8). Although the hyperpolarisation method offers a new approach to understanding sperm metabolism, presently it has limitations in detecting metabolite of interests in boar sperm metabolism due to the fast decay rate of the hyperpolarised substrate. There are other factors which could improve metabolite product detection. These could include decreasing the time between substrate dissolution and transfer to the sample, using a highly motile sperm sample and adding or increasing other enriched atoms to prolong the hyperpolarised substrate's decay rate.

8.5 Conclusion

None of the investigated variables, in this study, enabled the detection of Krebs cycle intermediates using ^{13}C MRS. However, from the present findings, it can be concluded that bicarbonate indeed emerged from the Krebs cycle suggesting that Krebs cycle metabolism is involved in boar sperm energy production. In addition, anaerobic glycolysis is a dominate pathway compared to OXPHOS in producing energy for boar sperm.

References

Aalbers, J. G., Mann, T., & Polge, C. (1961). Metabolism of boar semen in relation to sperm motility and survival. *Journal of Reproduction and Fertility*, *2*(1), 42–53.

Aaronson, D. S., Iman, R., Walsh, T. J., Kurhanewicz, J., & Turek, P. J. (2010). A novel application of 1H magnetic resonance spectroscopy: Non-invasive identification of spermatogenesis in men with non-obstructive azoospermia. *Human Reproduction*, *25*(4), 847–852.

Aitken, R. J., & Roman, S. D. (2008). Antioxidant systems and oxidative stress in the testes. *Oxidative Medicine and Cellular Longevity*, *1*(1), 15–24.

Aitken, R. J., & West, K. M. (1990). Analysis of the relationship between reactive oxygen species production and leucocyte infiltration in fractions of human semen separated on Percoll gradients. *International Journal of Andrology*, *13*(6), 433–51.

Alberts, B., Johnson, A., Lewis, J., Raff, M., Roberts, K., & Walter, P. (2009). *Molecular Biology of the cell*. Garland Science.

Allouche-Arnon, H., Wade, T., Waldner, L. F., Miller, V. N., Gomori, J. M., Katz-Brull, R., & McKenzie, C. A. (2013). In vivo magnetic resonance imaging of glucose - initial experience. *Contrast Media & Molecular Imaging*, *8*(1), 72–82.

Amann, R. P., & Waberski, D. (2014). Computer-assisted sperm analysis (CASA): Capabilities and potential developments. *Theriogenology*, *81*(1), 5–17.

Ardenkjaer-Larsen, J. H., Fridlund, B., Gram, A., Hansson, G., Hansson, L., Lerche, M. H., … Golman, K. (2003). Increase in signal-to-noise ratio > 10,000 times in liquid-state NMR. *Proceedings of the National Academy of Sciences of the United States of America*, *100*(18), 10158–63.

Awda, B. J., Mackenzie-Bell, M., & Buhr, M. M. (2009). Reactive oxygen species and boar sperm function. *Biology of Reproduction*, *81*(3), 553–561.

Babayev, E., & Seli, E. (2015). Oocyte mitochondrial function and reproduction. *Current Opinion in Obstetrics & Gynecology*, *27*(3), 175–81.

Balci, M. (2005). *Basic 1H- and 13C-NMR Spectroscopy*. Elsevier.

Barratt, C. L. R., De Jonge, C. J., & Sharpe, R. M. (2018). 'Man Up': the importance and strategy for placing male reproductive health centre stage in the political and research agenda. *Human Reproduction*, *33*(4), 541–545.

Barratt, C. L. R., Kay, V., & Oxenham, S. K. (2009). The human spermatozoon - a stripped down but refined machine. *Journal of Biology*, *8*(7), 63.

Barskiy, D. A., Coffey, A. M., Nikolaou, P., Mikhaylov, D. M., Goodson, B. M., Branca, R. T., … Chekmenev, E. Y. (2017). NMR Hyperpolarization Techniques of Gases. *Chemistry - A European Journal*. Wiley-VCH Verlag.

Beckmann, N. (1995). *Carbon-13 NMR spectroscopy of biological systems*. Academic Press.

Belkic, D., & Belkic, K. (2010). *Signal Processing in Magnetic Resonance Spectroscopy with*

Biomedical Applications. CRC Press.

Bencic, D. C., Krisfalusi, M., Cloud, J. G., & Ingermann, R. L. (2000). Short-term storage of salmonid sperm in air versus oxygen. *North American Journal of Aquaculture*, *62*(1), 19–25.

Berg, J. M., Tymoczko, J. L., & Stryer, L. (2002). *Biochemistry. 5th Edition*. W.H. Freeman.

Berg, J. M., Tymoczko, J. L., & Stryer, L. (2002). Entry to the Citric Acid Cycle and Metabolism Through It Are Controlled. In *Biochemistry* (5th ed.). W H Freeman.

Berg, R. (2008). Lecture 12 Enzymes : Inhibition, 225–236.

Berger, T., & Horton, M. B. (1988). Evaluation of assay conditions for the zona-free hamster ova bioassay of boar sperm fertility. *Gamete Research*, *19*(1), 101–111.

Berruti, G., & Paiardi, C. (2011). Acrosome biogenesis: Revisiting old questions to yield new insights. *Spermatogenesis*, *1*(2), 95–98.

Bhabha, G., Johnson, G. T., Schroeder, C. M., & Vale, R. D. (2016). How Dynein Moves Along Microtubules. *Trends in Biochemical Sciences*, *41*(1), 94–105.

Bhagavan, N. V., & Ha, C. E. (2011). *Essentials of Medical Biochemistry*. *Essentials of Medical Biochemistry*. Elsevier.

Bohnensack, R., & Halangk, W. (1986). Control of respiration and of motility in ejaculated bull spermatozoa. *Biochimica et Biophysica Acta*, *850*(1), 72–9.

Bone, W., Jones, N. G., Kamp, G., Yeung, C. H., & Cooper, T. G. (2000). Effect of ornidazole on fertility of male rats: inhibition of a glycolysis-related motility pattern and zona binding required for fertilization in vitro. *Reproduction*, *118*(1), 127–135.

Bonechi, C., Collodel, G., Donati, A., Martini, S., Moretti, E., & Rossi, C. (2015). Discrimination of human semen specimens by NMR data, sperm parameters, and statistical analysis. *Systems Biology in Reproductive Medicine*, *61*(6), 353–359.

Boron, W. F., & Boulpaep, E. L. (2009). *Medical physiology : a cellular and molecular approach*. Saunders/Elsevier.

Brown, M. A., & Semelka, R. C. (2003). *MRI Basic Priciple and Applications*. *John Wiley & Sons,Inc*. Wiley-Liss.

Brown, T. R., Kincaid, B. M., & Ugurbil, K. (1982). NMR chemical shift imaging in three dimensions. *Proceedings of the National Academy of Sciences of the United States of America*, *79*(11), 3523–6.

Bucci, D., Rodriguez-Gil, J. E., Vallorani, C., Spinaci, M., Galeati, G., & Tamanini, C. (2011). Gluts and mammalian sperm metabolism. *Journal of Andrology*, *32*(4), 348–355.

Buescher, J. M., Antoniewicz, M. R., Boros, L. G., Burgess, S. C., Brunengraber, H., Clish, C. B., … Fendt, S.-M. (2015). A roadmap for interpreting (13)C metabolite labeling patterns from cells. *Current Opinion in Biotechnology*, *34*, 189–201.

Burgess, S. A., Walker, M. L., Sakakibara, H., Knight, P. J., & Oiwa, K. (2003). Dynein structure and power stroke. *Nature*, *421*(6924), 715–718.

Bussalleu, E., Pinart, E., Rivera, M., Briz, M., Sancho, S., Yeste, M., … Bonet, S. (2009). Effects of matrix filtration of low-quality boar semen doses on sperm quality. *Reproduction in Domestic Animals*, *44*(3), 499–503.

C.G Gebelin. (1987). *Advances in Biomedical Polymers*. Springer US.

Calvert, S. J., Reynolds, S., Paley, M. N., Walters, S. J., & Pacey, A. A. (2018). Probing human sperm metabolism using 13C-magnetic resonance spectroscopy. *MHR: Basic Science of Reproductive Medicine*, *25*(1), 30-41.

Cates, W., Farley, T. M. M. M., & Rowe, P. J. (1985). Worldwide patterns of infertility: Is Africa different? *The Lancet*, *326*(8455), 596–598.

Chance, E. M., Seeholzer, S. H., Kobayashi, K., & Williamson, J. R. (1983). Mathematical analysis of isotope labeling in the Citric Acid Cycle with applications to 13C NMR studies in perfused rat hearts. *Journal of Biological Chemistry*, *258*(22), 13785–13794.

Chen, A. P., Tropp, J., Hurd, R. E., Van Criekinge, M., Carvajal, L. G., Xu, D., … Vigneron, D. B. (2009). In vivo hyperpolarized 13C MR spectroscopic imaging with 1H decoupling. *Journal of Magnetic Resonance (San Diego, Calif. : 1997)*, *197*(1), 100–6.

Cho, C., & Vale, R. D. (2012, January). The mechanism of dynein motility: Insight from crystal structures of the motor domain. *Biochimica et Biophysica Acta - Molecular Cell Research*. NIH Public Access.

Choi, J., & Antoniewicz, M. R. (2011). Tandem mass spectrometry: A novel approach for metabolic flux analysis. *Metabolic Engineering*, *13*(2), 225–233.

Chung, J., Chen, C., & Paw, B. H. (2012). Heme metabolism and erythropoiesis. *Current Opinion in Hematology*, *19*(3), 156–162.

Claridge, T. D. W. (2016). *High-Resolution NMR Techniques in Organic Chemistry: Third Edition*. *High-Resolution NMR Techniques in Organic Chemistry: Third Edition*. Elsevier.

Clendinen, C. S., Lee-McMullen, B., Williams, C. M., Stupp, G. S., Vandenborne, K., Hahn, D. A., … Edison, A. S. (2014). ^{13}C NMR metabolomics: applications at natural abundance. *Analytical Chemistry*, *86*(18), 9242–50.

Comment, A., & Merritt, M. E. (2014). Hyperpolarized magnetic resonance as a sensitive detector of metabolic function. *Biochemistry*, *53*(47), 7333–7357.

Cooper, G. M. (2000). *The Cell: A Molecular Approach. The Cell: A Molecular Approach*. Sunderland (MA): Sinauer Associates.

Cox, M., & Nelson, D. L. (2008). *Lehninger Principles of Biochemistry*. *Lehninger Principles of Biochemistry* (4th ed.). Palgrave Macmillan.

Cruz, F., Villalba, M., García-Espinosa, M. a., Ballesteros, P., Bogónez, E., Satrústegui, J., & Cerdán, S. (2001). Intracellular compartmentation of pyruvate in primary cultures of cortical neurons as detected by 13C NMR spectroscopy with multiple 13C labels. *Journal of Neuroscience Research*, *66*(5), 771–781.

Dahlbom, M., Andersson, M., Vierula, M., & Alanko, M. (1997). Morphometry of normal and teratozoospermic canine sperm heads using an image analyzer work in progress. *Theriogenology*, *48*(4), 687–698.

DeLong, J. P., Gibert, J. P., Luhring, T. M., Bachman, G., Reed, B., Neyer, A., & Montooth, K. L. (2017). The combined effects of reactant kinetics and enzyme stability explain the temperature dependence of metabolic rates. *Ecology and Evolution*, *7*(11), 3940–3950.

Demain, L. A. M., Conway, G. S., & Newman, W. G. (2017). Genetics of mitochondrial dysfunction and infertility. *Clinical Genetics*, *91*(2), 199–207.

Devlin, T. M. (2006). *Textbook of biochemistry: with clinical correlations*. Wiley-Liss.

Dieterle, F., Schlotterbeck, G., Ross, A., Niederhauser, U., & Senn, H. (2006). Application of metabonomics in a compound ranking study in early drug development revealing drug-induced excretion of choline into urine. *Chemical Research in Toxicology*, *19*(9), 1175–1181.

Dona, A. C., Kyriakides, M., Scott, F., Shephard, E. A., Varshavi, D., Veselkov, K., & Everett, J. R. (2016). A guide to the identification of metabolites in NMR-based metabonomics/metabolomics experiments. *Computational and Structural Biotechnology Journal*, *14*, 135–153.

Droździk, M., Stefankiewicz, J., Kurzawa, R., Górnik, W., Bączkowski, T., & Kurzawski, M. (2009). Association of the MDR1 (ABCB1) gene 3435C>T polymorphism with male infertility. *Pharmacological Reports*, *61*(4), 690–696.

du Plessis, S. S., Agarwal, A., Mohanty, G., & van der Linde, M. (2015). Oxidative phosphorylation versus glycolysis: what fuel do spermatozoa use? *Asian Journal of Andrology*, *17*(2), 230–5.

Eddy, E. M., Vernon, R. B., Muller, C. H., Hahnel, A. C., & Fenderson, B. A. (1985). Immunodissection of sperm surface modifications during epididymal maturation. *American Journal of Anatomy*, *174*(3), 225–237.

Engelking, L. R. (2015). *Textbook of Veterinary Physiological Chemistry*. *Textbook of Veterinary Physiological Chemistry*. Academic Press.

Fernández-Novell, J. M., Ballester, J., Altirriba, J., Ramió-Lluch, L., Barberà, A., Gomis, R., … Rodríguez-Gil, J. E. (2011). Glucose and fructose as functional modulators of overall dog, but not boar sperm function. *Reproduction, Fertility and Development*, *23*(3), 468–480.

Ferramosca, A., & Zara, V. (2014). Review Article: Bioenergetics of mammalian sperm capacitation. *BioMed Research International*, *2014*, 1–8.

Fischer, K. A., Van Leyen, K., Lovercamp, K. W., Manandhar, G., Sutovsky, M., Feng, D., … Sutovsky, P. (2005). 15-Lipoxygenase is a component of the mammalian sperm cytoplasmic droplet. *Reproduction (Cambridge, England)*, *130*(2), 213–22.

Folgerø, T., Bertheussen, K., Lindal, S., Torbergsen, T., & Oian, P. (1993). Mitochondrial disease and reduced sperm motility. *Human Reproduction (Oxford, England)*, *8*(11), 1863–1868.

Ford, W. C., & Harrison, A. (1981). The role of oxidative phosphorylation in the generation of ATP in human spermatozoa. *Journal of Reproduction and Fertility*, *63*(1), 271–8.

Ford, W. C. L. (2006). Glycolysis and sperm motility: Does a spoonful of sugar help the flagellum go round? *Human Reproduction Update*. Oxford University Press.

Free, M. J., Schluntz, G. A., & Jaffe, R. A. (1976). Respiratory gas tensions in tissues and fluids of the male rat reproductive tract. *Biology of Reproduction*, *14*(4), 481–8.

Freitas, M. J., Vijayaraghavan, S., & Fardilha, M. (2016). Signaling mechanisms in mammalian sperm motility. *Biology of Reproduction*, *96*(1), 2–12.

Gadea, J. (2003). Review: semen extenders used in the artificial inseminarion of swine. *Spanish Journal of Agricultural Research*, *1*(2), 17.

García-Martínez, S., Sánchez Hurtado, M. A., Gutiérrez, H., Sánchez Margallo, F. M., Romar, R., Latorre, R., … López Albors, O. (2018). Mimicking physiological O2 tension in the female reproductive tract improves assisted reproduction outcomes in pig. *MHR: Basic Science of Reproductive Medicine*, *24*(5), 260–270.

Gardner, D. K. (2004). *Textbook of assisted reproductive techniques laboratory and clinical perspectives*. Taylor & Francis.

Golman, K., in 't Zandt, R., & Thaning, M. (2006). Real-time metabolic imaging. *Proceedings of the National Academy of Sciences of the United States of America*, *103*(30), 11270–5.

Grant, S. a, Long, S. E., & Parkinson, T. J. (1994). Fertilizability and structural properties of boar spermatozoa prepared by Percoll gradient centrifugation. *Journal of Reproduction and Fertility*, *100*(2), 477–83.

Gray, L. R., Tompkins, S. C., & Taylor, E. B. (2014a). Regulation of pyruvate metabolism and human disease. *Cellular and Molecular Life Sciences*, *71*(14), 2577–2604.

Gray, L. R., Tompkins, S. C., & Taylor, E. B. (2014b). Regulation of pyruvate metabolism and human disease. *Cellular and Molecular Life Sciences*.

Griesinger, C., Bennati, M., Vieth, H. M., Luchinat, C., Parigi, G., H??fer, P., … Prisner, T. F. (2012). Dynamic nuclear polarization at high magnetic fields in liquids. *Progress in Nuclear Magnetic Resonance Spectroscopy*, *64*, 4–28.

Gruetter, R., Seaquist, E. R., Kim, S., & Uğurbil, K. (1998). Localized in vivo 13C-NMR of glutamate metabolism in the human brain: Initial results at 4 Tesla. *Developmental Neuroscience*, *20*(4–5), 380–388.

Guerriero, G., Trocchia, S., Abdel-Gawad, F. K., & Ciarcia, G. (2014). Roles of reactive oxygen species in the spermatogenesis regulation. *Frontiers in Endocrinology*, *5*, 56.

Gupta, A., Mahdi, A. A., Shukla, K. K., Ahmad, M. K., Bansal, N., Sankhwar, P., & Sankhwar, S. N. (2013). Efficacy of Withania somnifera on seminal plasma metabolites of infertile males: A proton NMR study at 800 MHz. *Journal of Ethnopharmacology*, *149*(1), 208–214.

Guthrie, H. D., & Welch, G. R. (2006). Determination of intracellular reactive oxygen species and high mitochondrial membrane potential in Percoll-treated viable boar sperm using fluorescence-activated flow cytometry1. *Journal of Animal Science*, *84*(8), 2089–2100.

Hagedorn, M., McCarthy, M., Carter, V. L., & Meyers, S. A. (2012). Oxidative stress in zebrafish (Danio rerio) sperm. *PLoS ONE*, *7*(6), 2–12.

Harris, T., Gamliel, A., Sosna, J., Gomori, J. M., & Brull, R. K. (2018). Impurities of [1 - 13 C] Pyruvic acid and a method to minimize their signals for hyperpolarized pyruvate metabolism studies. *Applied Magnetic Resonance*, *49*(10), 1085–1098.

Harrow, B., & Mazur, A. (1958). *Textbook of Biochemistry*. Philadelphia: Saunders.

He, L., Bailey, J. L., & Buhr, M. M. (2001). Incorporating lipids into boar sperm decreases chilling sensitivity but not capacitation potential. *Biology of Reproduction*, *64*(1), 69–79.

Heck, D. E., Shakarjian, M., Kim, H. D., Laskin, J. D., & Vetrano, A. M. (2010). Mechanisms of oxidant generation by catalase. In *Annals of the New York Academy of Sciences* (Vol. 1203, pp. 120–125). Blackwell Publishing Inc.

Hendee, W. R., & Ritenour, E. R. (2003). *Medical Imaging Physics*. John Wiley & Sons.

Henry A.Lardy, & Phillips, P. H. (1941). The effect of certain inhibitors and activators on sperm metabolism. *Biochemical Journal*, *138*, 195–202.

Henry, O., Jolicoeur, M., & Kamen, A. (2011). Unraveling the metabolism of HEK-293 cells using lactate isotopomer analysis. *Bioprocess and Biosystems Engineering*, *34*(3), 263–273.

Henry, P. G., Adriany, G., Deelchand, D., Gruetter, R., Marjanska, M., Öz, G., … Uğurbil, K. (2006). In vivo 13C NMR spectroscopy and metabolic modeling in the brain: a practical perspective. *Magnetic Resonance Imaging*, *24*(4), 527–539.

Hereng, T. H., Elgstøen, K. B. P. P., Cederkvist, F. H., Eide, L., Jahnsen, T., Sklhegg, B. S., & Rosendal, K. R. (2011). Exogenous pyruvate accelerates glycolysis and promotes capacitation in human spermatozoa. *Human Reproduction*, *26*(12), 3249–3263.

Hernandez-Lopez, L., Umland, N., Mondragon-Ceballos, R., & Nayudu, P. L. (2005). Comparison of the effects of Percoll and PureSpermR on the common marmoset (Callithrix jacchus) semen. *Journal of Medical Primatology*, *34*(2), 86–90.

Hill, D. R., Brunner, M. E., Schmitz, D. C., Davis, C. C., Flood, J. A., Schlievert, P. M., … Osborn, T. W. (2005). In vivo assessment of human vaginal oxygen and carbon dioxide levels during and post menses. *Journal of Applied Physiology*, *99*(4), 1582–1591.

HMDB. (2010). Human Metabolome Database. Retrieved from http://www.hmdb.ca/metabolites/HMDB00619

Holt, W. V, & Harrison, R. A. P. (2002). Bicarbonate stimulation of boar sperm motility via a protein kinase A-dependent pathway: Between-cell and between-ejaculate differences are not due to deficiencies in protein kinase A activation. *Journal of Andrology*, *23*(4), 557–565.

Hore, P. J. (1989). *Nuclear Magnetic Resonance (Oxford Chemistry Primers)*. Oxford University Press.

Hoshi, K., Tsukikawa, S., & Sato, A. (1991). Importance of Ca2+, K+ and glucose in the medium for sperm penetration through the human zona pellucida. *The Tohoku Journal of Experimental Medicine*, *165*(2), 99–104.

Hu, S., Yoshihara, H. A. I., Bok, R., Zhou, J., Zhu, M., Kurhanewicz, J., & Vigneron, D. B. (2012). Use of hyperpolarized [1-13C]pyruvate and [2-13C]pyruvate to probe the effects of the anticancer agent dichloroacetate on mitochondrial metabolism in vivo in the normal rat. *Magnetic Resonance Imaging*, *30*(10), 1367–1372.

Hurd, R. E., Yen, Y. F., Chen, A., & Ardenkjaer-Larsen, J. H. (2012). Hyperpolarized 13C metabolic imaging using dissolution dynamic nuclear polarization. *Journal of Magnetic Resonance Imaging*, *36*(6), 1314–1328.

Hüttemann, M., Lee, I., Samavati, L., Yu, H., & Doan, J. W. (2007). Regulation of mitochondrial oxidative phosphorylation through cell signaling. *Biochimica et Biophysica Acta (BBA) - Molecular Cell Research*, *1773*(12), 1701–1720.

James, T. L. (2012). *Nuclear magnetic Resonance in biochemistr*. *Nuclear magnetic Resonance in biochemistr*. Elsevier.

Johnson, L. A., Weitze, K. F., Fiser, P., & Maxwell, W. M. C. (2000). Storage of boar semen. *Animal Reproduction Science*, *62*, 143–172.

Jones, A., & Bubb, W. (2000). Substrates for endogenous metabolism by mature boar spermatozoa. *Reproduction*, *119*(1), 129–135.

Josan, S., Hurd, R., Park, J. M., Yen, Y.-F., Watkins, R., Pfefferbaum, A., … Mayer, D. (2014). Dynamic metabolic imaging of hyperpolarized [2-13 C]pyruvate using spiral CSI with alternating spectral band excitation. *Magn Reson Med*, *71*(6), 2051–2058.

Kaeoket, K., Srisowanna, T., Wichaidit, U., Chanapiwat, P., & Manee-in, S. (2010). Comparative study on six different long term commercial extenders for fresh boar semen. *Thai Journal of Veterinary Medicine*, *40*(3), 257–263.

Kaldis, P., Kamp, G., Piendl, T., & Wallimann, T. (1997). Functions of creatine kinase isoenzymes in spermatozoa. In *Advances in Developmental Biology* (Vol. 5, pp. 275–312). Elsevier.

Kamp, G., Büsselmann, G., Jones, N., Wiesner, B., & Lauterwein, J. (2003). Energy metabolism and intracellular pH in boar spermatozoa. *Reproduction*, *126*(4), 517–525.

Khatun, A., Rahman, M. S., & Pang, M.-G. (2018). Clinical assessment of the male fertility. *Obstetrics & Gynecology Science*, *61*(2), 179.

Kovalski, N. N., de Lamirande, E., & Gagnon, C. (1992). Reactive oxygen species generated by human neutrophils inhibit sperm motility: protective effect of seminal plasma and scavengers. *Fertility and Sterility*, *58*(4), 809–16.

Krebs, H. (1953). The citric acid cycle. *Nobel Lecture*.

Krebs, H. A., & Johnson, W. A. (1937). Metabolism of ketonic acids in animal tissues. *The Biochemical Journal*, *31*(4), 645–60.

Krisfalusi, M., Miki, K., Magyar, P. L., & O'Brien, D. A. (2006). Multiple glycolytic enzymes are tightly bound to the fibrous sheath of mouse spermatozoa. *Biology of Reproduction*, *75*(2), 270–278.

Kruse, R., Dutta, P. C., & Morrell, J. M. (2011). Colloid centrifugation removes seminal plasma and cholesterol from boar spermatozoa. *Reproduction, Fertility and Development*, *23*(7), 858.

Kumar, R., Venkatesh, S., Kumar, M., Tanwar, M., Shasmsi, M. B., Kumar, R., … Dada, R. (2009). Oxidative stress and sperm mitochondrial DNA mutation in idiopathic oligoasthenozoospermic men. *Indian Journal of Biochemistry & Biophysics*, *46*(2), 172–7.

Kurz, L. C., Ackerman, J. J., & Drysdale, G. R. (1985). Evidence from 13C NMR for polarization of the carbonyl of oxaloacetate in the active site of citrate synthase. *Biochemistry*, *24*(2), 452–7.

Landheer, K., Sahgal, A., Myrehaug, S., Chen, A. P., Cunningham, C. H., & Graham, S. J. (2016). A rapid inversion technique for the measurement of longitudinal relaxation times of brain metabolites: application to lactate in high-grade gliomas at 3 T. *NMR in Biomedicine*, *29*(10), 1381–1390.

Lasley, J. F., & Bogart, R. (1944). Some factors affecting the resistance of ejaculated and epididymal spermatozoa of the boar to different environmental conditions. *American Journal of Physiology-Legacy Content*, *141*(5), 619–624.

Lee, S., & Lee, D. K. (2018). What is the proper way to apply the multiple comparison test? *Korean Journal of Anesthesiology*, *71*(5), 353–360

Lessley, B. A., & Garner, D. L. (1983). Isolation of motile spermatozoa by density gradient centrifugation in Percoll®. *Gamete Research*, *7*(1), 49–61.

Lewandowski, E. D., Doumen, C., White, L. T., LaNoue, K. F., Damico, L. a, & Yu, X. (1996). Multiplet structure of 13C NMR signal from glutamate and direct detection of tricarboxylic acid (TCA) cycle intermediates. *Magnetic Resonance in Medicine : Official Journal of the Society of Magnetic Resonance in Medicine / Society of Magnetic Resonance in Medicine*, *35*(2), 149–54.

Liebich, H. (1990). Functional histology. Coloured atlas and compendium of microscopical anatomy of domestic mammals.

Lloyd, S. G., Zeng, H., Wang, P. P., & Chatham, J. C. (2004). Lactate isotopomer analysis by1H NMR spectroscopy: Consideration of long-range nuclear spin-spin interactions. *Magnetic Resonance in Medicine*, *51*(6), 1279–1282.

Lopez Rodriguez, A., Van Soom, A., Arsenakis, I., & Maes, D. (2017). Boar management and semen handling factors affect the quality of boar extended semen. *Porcine Health Management*, *3*(15).

Maas, D. H., Storey, B. T., & Mastroianni, L. J. (1976). Oxygen tension in the oviduct of the rhesus monkey (Macaca mulatta). *Fertility and Sterility*, *27*(11), 1312–1317.

Macleod, J. (1943). The role of oxygen in the metabolism and motility of human spermatozoa. *American Journal of Physiology*, *138*(3), 512–518.

Malicka, J., Czaplewski, C., Groth, M., Wiczk, W., Oldziej, S., Lankiewicz, L., … Liwo, A. (2004). Use of NMR and fluorescence spectroscopy as well as theoretical conformational analysis in conformation-activity studies of cyclic enkephalin analogues. *Current Topics in Medicinal Chemistry*, *4*(1), 123–33.

Malvezzi, H., Sharma, R., Agarwal, A., Abuzenadah, A. M., & Abu-Elmagd, M. (2014). Sperm quality after density gradient centrifugation with three commercially available media: a controlled trial. *Reproductive Biology and Endocrinology*, *12*(121).

Maly, T., Debelouchina, G. G. T., Bajaj, V. V. S., Hu, K.-N., Joo, C.-G., Mak-Jurkauskas, M. L., … Griffin, R. G. (2008). Dynamic nuclear polarization at high magnetic fields. *The Journal of Chemical Physics*, *128*(5), 1–39.

Mann, T., & Lutwak-Mann, C. (2012). *Male Reproductive Function and Semen: Themes and Trends in Physiology, Biochemistry and Investigative Andrology*. Springer London.

Marco-Rius, I. (2014). Preserving hyperpolarised nuclear spin order to stufy cancer metabolism.

Marin, S., Chiang, K., Bassilian, S., Lee, W. N. P., Boros, L. G., Fernández-Novell, J. M., … Cascante, M. (2003). Metabolic strategy of boar spermatozoa revealed by a metabolomic characterization. *FEBS Letters*, *554*(3), 342–346.

Marjańska, M., Iltis, I., Shestov, A. A., Deelchand, D. K., Nelson, C., Uurbil, K., & Henry, P. G. (2010). In vivo13C spectroscopy in the rat brain using hyperpolarized [1-13C]pyruvate and [2-13C]pyruvate. *Journal of Magnetic Resonance*, *206*(2), 210–218.

Mark L. Lorschy. (2005). *Definitions of Ambient Temperature Requirements for Pigs: A Review*. *Ceramics International*.

Mastroianni, L., & jones, R. (2008). Oxygen tension within the rabbit fallopian tube. *Reproduction*, *9*(1), 99–102.

Matás, C., Sansegundo, M., Ruiz, S., García-Vázquez, F. A., Gadea, J., Romar, R., & Coy, P. (2010). Sperm treatment affects capacitation parameters and penetration ability of ejaculated and epididymal boar spermatozoa. *Theriogenology*, *74*(8), 1327–1340.

Matás, C., Vieira, L., García-Vázquez, F. A. A., Avilés-López, K., López-Úbeda, R., Carvajal, J. A. A., & Gadea, J. (2011). Effects of centrifugation through three different discontinuous Percoll gradients on boar sperm function. *Animal Reproduction Science*, *127*(1–2), 62–72.

Matzuk, M. M., Brown, C. W., & Kumar, T. R. (2001). *Transgenics in endocrinology*. Humana Press.

Mccommis, K. S., & Finck, B. N. (2016). Mitochondrial pyruvate transport: a historical perspective and future research directions. *Biochemical Journal*, *466*(3), 443–454.

McKeown, S. R. (2014). Defining normoxia, physoxia and hypoxia in tumours-implications for treatment response. *The British Journal of Radiology*, *87*(1035), 20130676.

Medrano, A., Fernández-Novell, J. M., Ramió, L., Alvarez, J., Goldberg, E., Rivera, M. M., … Rodríguez-Gil, J. E. (2006). Utilization of citrate and lactate through a lactate dehydrogenase and ATP-regulated pathway in boar spermatozoa. *Molecular Reproduction and Development*, *73*(3), 369–378.

Miki, K., Qu, W., Goulding, E. H., Willis, W. D., Bunch, D. O., Strader, L. F., … O'Brien, D. A. (2004). Glyceraldehyde 3-phosphate dehydrogenase-S, a sperm-specific glycolytic enzyme, is required for sperm motility and male fertility. *Proceedings of the National Academy of Sciences of the*

United States of America, *101*(47), 16501–6.

Mishkovsky, M., Comment, A., & Gruetter, R. (2012). In vivo detection of brain Krebs cycle intermediate by hyperpolarized magnetic resonance. *Journal of Cerebral Blood Flow and Metabolism*, *32*(12), 2108–2113.

Mo, H., & Raftery, D. (2008). Solvent signal as an NMR concentration reference. *Analytical Chemistry*, *80*(24), 9835–9839.

Mohri, H., Inaba, K., Ishijima, S., & Baba, S. A. (2012). Tubulin-dynein system in flagellar and ciliary movement. *Proceedings of the Japan Academy. Series B, Physical and Biological Sciences*, *88*(8), 397–415.

Monin, G., Lambooy, E., & Klont, R. (1995). Influence of temperature variation on the metabolism of pig muscle in situ and after excision. *Meat Science*, *40*(2), 149–158.

Morrell, J. M. J., & Wallgren, M. (2011). Colloid centrifugation of boar semen. *Reproduction in Domestic Animals*, *46*(SUPPL. 2), 18–22.

Morrell, J. M., & Wallgren, M. (2010). Androcoll ™ -P-Large selects boar spermatozoa with good membrane integrity from the sperm-rich fraction of the ejaculate. *Animal Reprod*, *7*(1), 16–20.

Mortimer, D. (2018). The functional anatomy of the human spermatozoon: relating ultrastructure and function. *MHR: Basic Science of Reproductive Medicine*.

Mukai, C., & Okuno, M. (2004). Glycolysis plays a major role for adenosine triphosphate supplementation in mouse sperm flagellar movement. *Biology of Reproduction*, *71*, 540–547.

Nallella, K. P., Sharma, R. K., Allamaneni, S. S. R., & Agarwal, A. (2005). Identification of male factor infertility using a novel semen quality score and reactive oxygen species levels. *Clinics (Sao Paulo, Brazil)*, *60*(4), 317–324.

Natali, I. (2011). Sperm preparation techniques for artificial insemination - comparison of sperm washing , swim up , and density gradient centrifugation methods. *Artificial Insemination in Farm Animals*, *7*, 115–122.

Nevo, A. C., Polge, C., & Frederick, G. (1970). Aerobic and anaerobic metabolism of boar spermatozoa in relation to their motility. *J Reprod Fertil*, *22*, 109–118.

Osinowo, O. A. (1981). Studies on leakage of enzymes from washed bull and ram spermatozoa. *J Reprod Fertil*, *62*, 549–554.

Ottosen, L. D. M., Hindkaer, J., Husth, M., Petersen, D. E., Kirk, J., & Ingerslev, H. J. (2006). Observations on intrauterine oxygen tension measured by fibre-optic microsensors. *Reproductive Biomedicine Online*, *13*(3), 380–5.

Overhauser, A. W. (1953). Phys. Rev. 89, 689 (1953) - Paramagnetic relaxation in metals. *Physical Review*.

Owen, O. E., Kalhan, S. C., & Hanson, R. W. (2002). The Key Role of Anaplerosis and Cataplerosis for Citric Acid Cycle Function. *Journal of Biological Chemistry*, *277*(34), 30409–30412.

Pacey, A. A. (2009). Sperm, human fertility and society. *Sperm Biology: An Evolutionary Perspective*,

565–597.

Paiva, C., Amaral, A., Rodriguez, M., Canyellas, N., Correig, X., Ballesc??, J. L., … Oliva, R. (2015). Identification of endogenous metabolites in human sperm cells using proton nuclear magnetic resonance (1H-NMR) spectroscopy and gas chromatography-mass spectrometry (GC-MS). *Andrology*, *3*(3), 496–505.

Panneerdoss, S., Siva, A. B., Kameshwari, D. B., Rangaraj, N., & Shivaji, S. (2012). Association of lactate, intracellular pH, and intracellular calcium during capacitation and acrosome reaction: Contribution of hamster sperm dihydrolipoamide dehydrogenase, the E3 subunit of pyruvate dehydrogenase complex. *Journal of Andrology*, *33*(4), 699–710.

Pardee, A., & Potter, V. (1948). Inhibition of succinic dehydrogenase by oxalacetate. *Journal of Biological Chemistry*, *176*, 1085–1094.

Park, J. M., Josan, S., Grafendorfer, T., Yen, Y.-F., Hurd, R. E., Spielman, D. M., & Mayer, D. (2013). Measuring mitochondrial metabolism in rat brain in vivo using MR Spectroscopy of hyperpolarized [2-13C]pyruvate. *NMR in Biomedicine*, *26*(10), 1197–1203.

Peterson, R. N., & Freund, M. (1974). Citrate formation from exogenous substrates by washed human spermatozoa. *J Reprod Fertil*, *38*, 73–79.

Piomboni, P., Focarelli, R., Stendardi, A., Ferramosca, A., & Zara, V. (2012). The role of mitochondria in energy production for human sperm motility. *International Journal of Andrology*, *35*(2), 109–124.

Posse, S., Otazo, R., Dager, S. R., & Alger, J. (2013). MR spectroscopic imaging: Principles and recent advances. *Journal of Magnetic Resonance Imaging*, *37*(6), 1301–1325.

Prendergast, F. G., & Veneziale, C. M. (1975). *Control of Fructose and Citrate Synthesis in Guinea Pig Seminal Vesicle Epithelium" The Journal Of Biological Chemistry*. *250*(2).

Quastel, J. H., & Wheatley, A. H. M. (1931). Xvi. Biological oxidations in the succinic acid series. *Biochemical Journal*, *25*(117).

Quistorff, B., & Grunnet, N. (2011, May). The isoenzyme pattern of LDH does not play a physiological role; except perhaps during fast transitions in energy metabolism. *Aging*. Impact Journals, LLC.

Reynolds, S., Calvert, S. J., Paley, M. N., & Pacey, A. A. (2017). 1H Magnetic Resonance Spectroscopy of live human sperm. *MHR: Basic Science of Reproductive Medicine*, *23*(7), 441–451.

Reynolds S, Ismail, N. F. bt, Calvert, S. J., Pacey, A. A., & Paley, M. N. J. (2017). Evidence for rapid oxidative phosphorylation and lactate fermentation in motile human sperm by hyperpolarized 13C magnetic resonance spectroscopy. *Scientific Reports*, *7*(1), 4322.

Riammer, S., Garten, A., Schaab, M., Grunewald, S., Kiess, W., Kratzsch, J., & Paasch, U. (2016). Nicotinamide phosphoribosyltransferase production in human spermatozoa is influenced by maturation stage.

Roberts, A. J., Kon, T., Knight, P. J., Sutoh, K., & Burgess, S. A. (2013). Functions and mechanics of dynein motor proteins. *Nature Reviews Molecular Cell Biology*, *14*(11), 713–726.

Rodrigues, T. B., & Cerdán, S. (2005). 13C MRS: An outstanding tool for metabolic studies. *Concepts in Magnetic Resonance Part A: Bridging Education and Research*, *27*(1), 1–16.

Rodrigues, T. B., Serrao, E. M., Kennedy, B. W. C., Hu, D.-E., Kettunen, M. I., & Brindle, K. M. (2013). Magnetic resonance imaging of tumor glycolysis using hyperpolarized 13C-labeled glucose. *Nature Medicine*, *20*(1), 93–97.

Rodriguez-gil, J. E. (2006). Mammalian sperm energy resources management and survival during conservation in refrigeration. *Reproduction in Domestic Animals*, *41*(2), 11–20.

Rodríguez-Gil, J. E., & Bonet, S. (2016). Current knowledge on boar sperm metabolism: Comparison with other mammalian species. *Theriogenology*, *85*(1), 4–11.

Ruiz-Pesini, E., Díez-Sánchez, C., López-Pérez, M. J., & Enríquez, J. A. (2007). The Role of the Mitochondrion in Sperm Function: Is There a Place for Oxidative Phosphorylation or Is This a Purely Glycolytic Process? In *Current topics in developmental biology* (Vol. 77, pp. 3–19).

Schroeder, M. A., Atherton, H. J., Ball, D. R., Cole, M. a, Heather, L. C., Griffin, J. L., … Tyler, D. J. (2009). Real-time assessment of Krebs cycle metabolism using hyperpolarized 13C magnetic resonance spectroscopy. *Faseb J.*, *23*(8), 2529–2538.

Schroeder, M. A., Clarke, K., Neubauer, S., Facc, F., & Tyler, D. J. (2012). Hyperpolarized magnetic resonance: A novel technique for the in vivo assessment of cardiovascular disease. *Circulation*, *124*(14), 1580–1594.

Selak, M. A., Armour, S. M., MacKenzie, E. D., Boulahbel, H., Watson, D. G., Mansfield, K. D., … Lee, F. S. (2005). Succinate links TCA cycle dysfunction to oncogenesis by inhibiting HIF-alpha prolyl hydroxylase. *Cancer Cell*, *7*(1), 77–85.

Shchepin, R. V, Pham, W., & Chekmenev, E. Y. (2014). Dephosphorylation and biodistribution of 1-^{13}C-phospholactate in vivo. *Journal of Labelled Compounds & Radiopharmaceuticals*, *57*(8), 517–24.

Shelby, D. R., & Foley, C. W. (1971). Influence of atmosphere and incubation temperature on the metabolism of washed boar spermatozoa. *Journal of Animal Science*, *32*(1), 103–106.

Shen, J., Petersen, K. F., Behar, K. L., Brown, P., Nixon, T. W., Mason, G. F., … Rothman, D. L. (1999). Determination of the rate of the glutamate/glutamine cycle in the human brain by in vivo 13C NMR. *Proceedings of the National Academy of Sciences*, *96*(14), 8235–8240.

Shimizu, A., Ikeguchi, M., & Sugai, S. (1994). Appropriateness of DSS and TSP as internal references for 1H NMR studies of molten globule proteins in aqueous media. *Journal of Biomolecular NMR*, *4*(6), 859–862.

Siva, A. B., Panneerdoss, S., Sailasree, P., Singh, D. K., Kameshwari, D. B., & Shivaji, S. (2014). Inhibiting sperm pyruvate dehydrogenase complex and its E3 subunit, dihydrolipoamide dehydrogenase affects fertilization in Syrian hamsters. *PLoS ONE*, *9*(5), e97916.

Smith, A. A., Corzilius, B., Barnes, A. B., Maly, T., & Griffin, R. G. (2012). Solid effect dynamic nuclear polarization and polarization pathways. *Journal of Chemical Physics*, *136*(1), 015101.

Smith, C. M., Bryła, J., & Williamson, J. R. (1974). Regulation of mitochondrial alpha-ketoglutarate metabolism by product inhibition at alpha-ketoglutarate dehydrogenase. *The Journal of Biological Chemistry*, *249*(5), 1497–1506.

Smith, E. H., Janknecht, R., & Maher, J. L. (2007). Succinate inhibition of α-ketoglutarate-dependent enzymes in a yeast model of paraganglioma. *Human Molecular Genetics*, *16*(24), 3136–3148.

Sonnewald, U., Westergaard, N., Schousboe, A., Svendsen, J. S., Unsgård, G., & Petersen, S. B. (1993). Direct demonstration by [13C]NMR spectroscopy that glutamine from astrocytes is a precursor for GABA synthesis in neurons. *Neurochemistry International*, *22*(1), 19–29.

Storey, B. T. (2008). Mammalian sperm metabolism: Oxygen and sugar, friend and foe. *International Journal of Developmental Biology*, *52*(5–6), 427–437.

Storey, B. T., & Keyhani, E. (1974). Energy metabolism of spermatozoa: III. Energy-linked uptake of calcium ion by the mitochondria of rabbit epididymal spermatozoa. *Fertility and Sterility*, *25*(11), 976–84.

Stovell, M. G., Mada, M. O., Helmy, A., Carpenter, T. A., Thelin, E. P., Yan, J.-L., … Carpenter, K. L. H. (2018). The effect of succinate on brain NADH/NAD+ redox state and high energy phosphate metabolism in acute traumatic brain injury. *Scientific Reports*, *8*(1), 11140.

Tahir Beydola, Sharma, R. K., & Agarwa, A. (2014). Chapter 29 - Sperm preparation and selection techniques. In *Medical and Surgical Management of Male Infertility by Rizk Botros RMB, Aziz Nabil, Agarwal Ashok, Jr Edmund Sabanegh* (pp. 244–251). Jaypee Brothers Medical.

Tang, M., Liu, B.-J., Wang, S.-Q., Xu, Y., Han, P., Li, P.-C., … Yin, C.-J. (2014). The role of mitochondrial aconitate (ACO2) in human sperm motility. *Systems Biology in Reproductive Medicine*, *60*(5), 251–256.

Temidayo, So., & Stefan, S. P. (2018). Diabetes mellitus and male infertility. *Asian Pacific Journal of Reproduction*, *7*(1), 6.

Tsai, C. S. (1967). Spontaneous decarboxylation of oxalacetic acid. *Canadian Journal of Chemistry*, *45*(1), 873–880.

Turner, R. M. (2003). Tales from the tail: what do we really know about sperm motility? *Journal of Andrology*, *24*(6), 790–803.

Valls-Lacalle, L., Barba, I., Miró-Casas, E., Alburquerque-Béjar, J. J., Ruiz-Meana, M., Fuertes-Agudo, M., … García-Dorado, D. (2016). Succinate dehydrogenase inhibition with malonate during reperfusion reduces infarct size by preventing mitochondrial permeability transition. *Cardiovascular Research*, *109*(3), 374–384.

VanLinden, M. R., Dölle, C., Pettersen, I. K. N., Kulikova, V. A., Niere, M., Agrimi, G., … Ziegler, M. (2015). Subcellular distribution of NAD+ between cytosol and mitochondria determines the metabolic profile of human cells. *Journal of Biological Chemistry*, *290*(46), 27644–27659.

Vyt, P., Maes, D., Quinten, C., Rijsselaere, T., Deley, W., Aarts, M., … Van Soom, A. (2008). Detailed motility evaluation of boar semen and its predictive value for reproductive performance in sows.

Vlaams Diergeneeskundig Tijdschrift, *77*(5), 291–298.

Weissleder, R. (2010). *Molecular imaging : principles and practice*. People's Medical Pub. House--USA.

Wenger, R., Kurtcuoglu, V., Scholz, C., Marti, H., & Hoogewijs, D. (2015). Frequently asked questions in hypoxia research. *Hypoxia*, *3*, 35.

Wharton, D. a. (2007). *Life at the limits: organisms in extreme environments*. *Life at the Limits: Organisms in Extreme Environments*. Cambridge University Press.

Whittington, K., & Ford, W. C. L. (1998). The effect of incubation periods under 95% oxygen on the stimulated acrosome reaction and motility of human spermatozoa. *Molecular Human Reproduction*, *4*(11), 1053–1057.

Wiedemann, N., Frazier, A. E., & Pfanner, N. (2004). The protein import machinery of mitochondria. *The Journal of Biological Chemistry*, *279*(15), 14473–6.

Wijnen, J. P., Van der Graaf, M., Scheenen, T. W. J., Klomp, D. W. J., de Galan, B. E., Idema, A. J. S., & Heerschap, A. (2010). In vivo 13C magnetic resonance spectroscopy of a human brain tumor after application of 13C-1-enriched glucose. *Magnetic Resonance Imaging*, *28*(5), 690–697.

World Health Organization. (2010). *WHO laboratory manual for the Examination and processing of human semen* (5th ed.). World Health Organisation.

Yedwab, G. A., Paz, G., Homonnai, T. Z., David, M. P., & Kraicer, P. F. (1976). The temperature, pH, and partial pressure of oxygen in the cervix and uterus of women and uterus of rats during the cycle. *Fertility and Sterility*, *27*(3), 304–309.

Zini, A., O'Bryan, M. K., Israel, L., & Schlegel, P. N. (1998). Human sperm nadh and nadph diaphorase cytochemistry: correlation with sperm motility. *Urology*, *51*(3), 464–468.